New insights into the complex regulation and function of the ASPP2 tumor suppressor: the discovery of the ΔN-ASPP2 isoform

By Kathryn Dianne Van Hook

A DISSERTATION

Presented to the Department of Cell and Developmental Biology and the Oregon Health and Science University School of Medicine in partial fulfillment of the requirement for the degree of

Doctor of Philosophy

Approved by the Oral Examination Committee

May 2013

School of Medicine
Oregon Health & Science University

CERTIFICATE OF APPROVAL

This is to certify that the Ph.D. dissertation of

Kathryn Van Hook

has been approved

[redacted]
Chair-Mathew Thayer, PhD

[redacted]
Member-Charles Lopez, MD/PhD

[redacted]
Member-Rosalie Sears, PhD

[redacted]
Member-Mu-Shui Dai, PhD

[redacted]
Member-Maureen Hoatlin, PhD

[redacted]
Member-Molly Kulesz-Martin, PhD

Table of Contents

LIST OF FIGURES……v

LIST OF TABLES……vii

LIST OF ABBREVIATIONS……viii

ACKNOWLEDGEMENTS……...xii

CHAPTER ONE: INTRODUCTION……....1

BACKGROUND AND SIGNIFICANCE……..…2

ASPP2 BACKGROUND……..4

C-MYC BACKGROUND……...21

STATEMENT OF THESIS……27

CHAPTER TWO: ΔN-ASPP2 IS A NOVEL ISOFORM OF THE ASPP2 TUMOR SUPPRESSOR THAT PROMOTES CELLULAR SURVIVAL……..…28

ABSTRACT……..29

INTRODUCTION……..…….30

RESULTS……33

DISCUSSION……...57

Table of Contents

CHAPTER THREE: *TP53BP2* IS A C-MYC TARGET GENE THAT MEDIATES C-MYC-INDUCED APOPTOSIS……..63

ABSTRACT……..64

INTRODUCTION……65

RESULTS……68

DISCUSSION……..84

CHAPTER FOUR: SUMMARY AND DISCUSSION……90

ΔN-ASPP2: NEW IMPLICATIONS FOR THE ASPP2 FAMILY……..91

EXPRESSION OF ΔN-ASPP2 IS IMPORTANT FOR NORMAL DEVELOPMENT……93

COMPLEX BINDING DYNAMICS LIKELY MEDIATE ASPP2 AND ΔN-ASPP2 FUNCTION……95

ΔN-ASPP2 AFFECTS THE LOCALIZATION OF P53 IN RESPONSE TO DAMAGE……....99

ΔN-ASPP2 ADDS COMPLEXITY TO OUR UNDERSTANDING OF THE ASPP2 FAMILY……101

THE N-TERMINUS OF ASPP2 MEDIATES TUMOR SUPPRESSIVE FUNCTIONS……..102

TP53BP2 IS A MYC TARGET GENE WITH RELEVANCE IN VARIOUS TUMOR SUPPRESSIVE PATHWAYS……106

ASPP2 HAS A MULTIFACETED ROLE IN TUMOR PREVENTION……108

Table of Contents

CHAPTER FIVE: MATERIALS AND METHODS……..111

PLASMIDS……112

ΔN-ASPP2 CLONING……113

CELL LINES, PRIMARY CELLS, AND TRANSFECTIONS……..115

MICE……116

ANTIBODIES AND CHEMICALS……..118

IMMUNOBLOTTING……119

RNA PREPARATION AND RT-PCR ANALYSIS……120

CHROMATIN IMMUNOPRECIPITATIONS AND IMMUNOPRECIPITATIONS……..122

LUCIFERASE ASSAYS……124

IMMUNOFLUORESCENCE……124

LIVE CELL IMAGING……125

CELL VIABILITY ASSAY……125

RNA-SEQ……125

5'RACE……126

APOPTOSIS ASSAY……128

APPENDIX 1: ΔN-ASPP2 METHODS DEVELOPMENT…….129

APPENDIX 2: FIGURE CONTRIBUTIONS……134

REFERENCES……135

List of Figures

CHAPTER ONE

FIGURE 1.1: SCHEMATIC OF THE ASPP2 GENE FAMILY (TRIGIANTE AND LU,2006) WITH PERMISSION)……..……6

FIGURE 1.2: GENE STRUCTURE OF TP53BP2/ASPP2……...10

FIGURE 1.3 GENE REGULATION MEDIATED BY THE MYC/MAX TRANSCRIPTIONAL NETWORK (PATEL, 2004 WITH PERMISSION)……..23

CHAPTER TWO

FIGURE 2.1. ΔN-ASPP2 IS A NOVEL N-TERMINALLY TRUNCATED ISOFORM OF ASPP2……35

FIGURE 2.2. ΔN-ASPP2 IS GENERATED FROM AN ALTERNATIVE TRANSCRIPTION START AND NOT ALTERNATIVE SPLICING……...37

FIGURE 2.3. ENDOGENOUS ΔN-ASPP2 IS EXPRESSED IN CELLS……41

FIGURE 2.4. P53 TRANSCRIPTIONAL ACTIVATION IS INHIBITED BY ΔN-ASPP2……..45

FIGURE 2.5. ΔN-ASPP2 ENHANCES CELL PROLIFERATION AND SURVIVAL……...50

FIGURE 2.6. ΔN-ASPP2 INHIBITS UV DAMAGE-INDUCED APOPTOSIS……53

FIGURE 2.7. ASPP2 IS SUPPRESSED AND ΔN-ASPP2 IS OVEREXPRESSED IN BREAST TUMORS……...56

List of Figures

CHAPTER THREE

FIGURE 3.1. TP53BP2 HAS FEATURES OF A MYC TARGET GENE AND MYC ENHANCES TRANSACTIVATION OF AN ASPP2-LUCIFERASE REPORTER……70

FIGURE 3.2. MYC INDUCES EXPRESSION OF ENDOGENOUS ASPP2…….74

FIGURE 3.3. TP53BP2 IS A DIRECT MYC TARGET……..77

FIGURE 3.4. ATTENUATION OF ASPP2 EXPRESSION LIMITS MYC-INDUCED APOPTOSIS……79

FIGURE 3.5. ASPP2 DOES NOT ACCELERATE LYMPHOMAGENESIS IN A MYC-DRIVEN TUMOR MODEL……..82

FIGURE 3.6. DIAGRAM REPRESENTING THE PROPOSED MYC-ASPP2 AXIS……89

CHAPTER FOUR

FIGURE 4.1. SCHEMATIC OF TP53BP2 GENE PRODUCTS……..92

FIGURE 4.2 ΔN-ASPP2 BINDS ASPP2 BUT NOT P53……..98

FIGURE 4.3 CHANGES IN SUBCELLULAR LOCATION OF ENDOGENOUS WILD TYPE P53 MAY BE MEDIATED BY ΔN-ASPP2……100

FIGURE 4.4. ASPP2 AND ΔN-ASPP2 HAVE A MULTIFACETED ROLE IN TUMOR SUPPRESSION……110

APPENDICES

FIGURE A1.1 ΔN-ASPP2 IS SPECIFICALLY AND QUANTITATIVELY DETECTED IN CELL LINES……..131

FIGURE A1.2 VALIDATION OF ΔN-ASPP2 KNOCKDOWN……133

List of Tables

TABLE 1.1 POTENTIAL FUNCTIONS AND PUTATIVE INTERACTING PARTNERS OF ASPP2 (ADAPTED WITH PERMISSION FROM KAMPA ET AL., 2009B)……..9

TABLE 1.2 SUMMARY OF ASPP2 EXPRESSION PATTERNS AND MUTATIONS IN HUMAN TUMORS…….20

TABLE 2.1 SUMMARY OF RNA-SEQ ANALYSIS OF ASPP2 AND ΔN-ASPP2 IN A PANEL OF BREAST TUMOR CELL LINES……..40

TABLE 5.1 ΔN-ASPP2 SEQUENCING PRIMERS……114

TABLE 5.2. GENOTYPING PRIMERS……118

TABLE 5.3. SEMI-QUANTITATIVE AND QUANTITATIVE RT-PCR PRIMERS/PROBES……121

TABLE 5.4. 5'RACE AND RT-PCR PRIMERS……127

List of Abbreviations

5’RACE	5’ rapid amplification of cDNA ends
53BP2	p53 binding protein 2
a.a.	amino acid
AKT	v-akt murine thymoma viral oncogene homolog
APCL	brain-specific adenomatous polyposis coli homolog L
APP-BP1	NEDD8-activating enzyme E1 regulatory subunit
ARF	ADP ribosylation factor
ASPP1	apoptosis-stimulating protein of p53-1
ASPP2	apoptosis-stimulating protein of p53-2
ATG5/12/16	autophagy protein 5/12/16
ATM	ataxia telangiectasia mutated
ATR	ataxia telangiectasia and Rad3 related
B-Raf	B-rapidly accelerated fibrosarcoma protein
Bax	BCL-2-associated X protein
BBP	BCL-2 binding protein
BCL-2	B cell lymphoma-2
Bcl-X_L	B cell lymphoma-extra large
bHLH-LZ	basic helix-loop-helix-leucine zipper
bp	base pair
BSA	bovine serum albumin
c-Myc	cellular Myc

List of Abbreviations

C-Raf	C-rapidly accelerated fibrosarcoma protein
cDNA	complementary DNA
ChIP	chromatin immuoprecipitation
CHK1	checkpoint kinase 1
CHK2	checkpoint kinase 2
CNS	central nervous system
Cy3	cyanine III
dCSK	*Drosophila* C-terminal Src Kinase
DLBC	diffuse large B-cell
DMEM	Dulbecco's Modified Eagle's Medium
DMSO	dimethyl sulfoxide
Dox	doxycycline
DTT	dithiothreitol
ERK1/2	extracellular receptor kinases 1 and 2
FC	follicular cell
FITC	fluorescein isothiocyanate
GAPDH	glyceraldehyde 3-phosphate dehydrogenase
GSK3	glycogen synthase kinase 3
HAT	histone acetyltransferase
HBV	hepatitis B virus
HCV	hepatitis C virus
HRP	horseradish peroxidase
iASPP	inhibitory apoptosis-stimulating protein of p53

List of Abbreviations

IgG	immunoglobulin
IP	immunoprecipitation
IRS-1	insulin receptor substrate-1
kb	kilobase
Lck	lymphocyte-specific protein tyrosine kinase
MBD1	methyl-CpG-binding domain protein 1
MDM2	Mouse double minute 2 homolog
MEK	mitogen-activated protein kinase extracellular signal-regulated kinase
Mnt	Max’s next tango
MTS	3-(4,5-dimethylthiazol-2-yl)-5-(3-carboxymethoxyphenyl)-2-(4-sulfophenyl)-2H-tetrazolium
NF-κB	nuclear factor κ-light-chain-enhancer of activated B cells
PAR-3	partitioning defective protein-3
PBS	phosphate buffer solution
PCR	polymerase chain reaction
PI3K	phosphoinositide-3-kinase
PMSF	phenylmethanesulfonylfluoride
PP1	phosphoprotein phosphatase 1
PP2A	protein phosphatase 2A
PVDF	polyvinylidene fluoride
qPCR	quantitative PCR
RAS	rat sarcoma

List of Abbreviations

RB	retinoblastoma
RFS	ROSA floxed stop
RT-PCR	reverse transcriptase PCR
S62	serine 62
SDS-PAGE	sodium dodecyl sulfate polyacrylamide gel electrophoresis
SH3	Src-homology-3 domain
siRNA	silencing RNA
std dev	standard deviation
SWI/SNF	SWItch/Sucrose NonFermentable
TAZ	tafazzin
TRRAP	transformation/transcription domain-associated protein
UTR	untranslated region
YAP	YES-associated protein

Acknowledgements

The road through graduate school has not been without its ups and downs but luckily for me it has also not been without an immense and overwhelming amount of support. First and foremost I have to give thanks to my mentor Charles Lopez. Charlie is one of the smartest, the most determined, and (importantly for me) one of the most positive people I have encountered in my academic career. He was willing to take a chance on me and for his guidance, support, knowledge, and mentorship I will always be grateful. Throughout the years Rosalie Sears and Mu-Shui Dai have gone above and beyond their roles as thesis advisors and really helped to co-mentor me through my education. Rosie is an outstanding scientist, my role model as a woman scientist following in her footsteps, and a wonderful example of how to balance work and family life. Mu-Shui is also an amazing scientist whose optimism and support has really inspired me to learn and improve everyday. To my remaining thesis advisors Mathew Thayer and Maureen Hoatlin, your guidance, ideas, time spent reading and critiquing my work, and thought-provoking discussion have been essential to this process and for that I am extremely grateful. A special thank you also to Molly Kulesz-Martin for being a member of my oral exam committee. Molly is a dedicated scientist who is committed to her role as an educator and I am grateful for her support.

I cannot express my thanks and gratitude to Zhiping Wang and Hun Joo Lee enough. They have been my day-to-day guideposts in the lab and have

endured my endless questions, failures, triumphs, laughter, tears, and everything in between with patience and understanding. They have taught me almost everything I know about bench work and I am proud to call them both my colleagues and friends. Similarly, I want to thank Casey Nold and Natalie Wilson for their enthusiasm, perseverance, and friendship. They are both well on their way to becoming accomplished professionals and I am so thankful to have had their help and support along the way. An additional thank you to Eric Fontaine, Pavana Anur, Dexi Chen, Kerstin Kampa-Schittenhelm, and Zhiyi Zhou for their assistance and support in helping me achieve this goal.

A thank you also to the ARCS Foundation and specifically to Ted Miller, Daisy Housel-Miller, and Lila Miller not only for their generous scholarship but also for their kindness and help throughout the years.

I owe special thanks to Deanne Tibbitts, not only for her Herculean efforts in helping me prepare and curate this dissertation, but also for her everlasting support and guidance throughout my entire graduate experience, from recruitment to defense. A special thank you also to my fellow Montanan, friend, and lab manager extraordinaire, Karyn Taylor. No matter if I was struggling with a problem, needed a good laugh, or wanted a sweet treat, Karyn was always there with a helping hand and smiling face. She has been my saving grace on too many occasions and I am forever grateful. To the many past and present members of the Sears and Dai labs, most notably Sarah Byers, Tiffany DeVine, Amy Farrell, Kishore Challagundla, Ellen Langer, Brittany Allen-

Acknowledgements

Petersen, Mahnaz Janghorban, and Xiaoli Zhang, thank you, thank you, thank you!

No self-respecting CDB student can get away without thanking the unparalleled Elaine Offield. Elaine is one of the kindest, most helpful, and most organized people I have ever met and her guidance through all of the requisite paperwork and requirements to achieve this goal has been irreplaceable. Thank you Elaine!

A very honorable mention to Allison Fryer, Jeanne Sutter, Melissa Wong, Dave Dawson, and John Crossen for being my advocates and cheerleaders throughout graduate school. You all believed in me and told me so--your words impacted me more than you know.

I would like to extend a special thank you to my wonderful friends--Sarah Adelhart, Ann Marie Canepa, Molly Hames, Kate Menninger, Caitlin Burgess, Julianna Papez, Nikki Honzel, Stefanie Lynch, Pam Sheffield, and Franco Pissani. I am extremely lucky to have such a fantastic and accomplished group of friends to love and support me. You have shared the highest highs and lowest lows with me and without your undying support I would not be where I am today. An additional thank you to Carol Patton, Terry and Candace Menninger and Erik and Vickie Pratt. Your love and support means the world to me and does not go unnoticed.

A special thank you to my wonderful boyfriend Jeff Lee, if not for preparing almost all of my meals for me while I wrote this dissertation, than for being a

profoundly positive addition to my life. I have been honored and touched by your patience and willingness to stand with me in this process and for that I am forever grateful. Thank you also to the Lee family, and especially Shelley Dubkin-Lee, for providing food, laughter, comfort, advice, and support during such a hectic time.

Finally to my wonderful family, Jan, Russ, Justin, and Amy Van Hook, without you not only would this goal not have been possible but I would not be the proud and confident person I am today. You never let me quit and never once expected I could fail and because of your infinite love and support I owe this achievement to you. You are my past, present, and future and I am incredibly honored to be a part of our family. Thank you, from the bottom of my heart.

Chapter One:

Introduction

Background and significance

Every year over 1.5 million people are diagnosed with cancer and more than 500,000 people succumb to the disease, making it the second-leading cause of death in the United States (American Cancer Society, 2013). Despite a sustained decline in cancer deaths in recent years, there are still key gaps in our understanding of this disease that are crucial for the development of new and more effective therapeutics (Jemal, 2013). Cancer development can be thought of as a stepwise process through which transition to malignancy requires manipulation or loss of the many checkpoints in place to prevent tumor progression. The ability of cells to induce apoptosis, a type of programmed cell death, in response to aberrant growth signals is one of these checkpoints and represents a substantial barrier for evolving tumor cells (Hanahan, 2011). A clearer understanding of how apoptotic pathways are regulated and how they become deregulated during tumor evolution is an active area of investigation, and restoration of apoptotic sensitivity in tumors remains an important goal in cancer therapy (Fesik, 2005).

Resistance to apoptotic signals is commonly achieved by deregulating or inactivating key tumor suppressor pathways. One of the most common mechanisms of inactivation is achieved by mutating the tumor suppressor p53 or by functionally inactivating the signaling pathways upstream or downstream of p53. p53 is a vital transcription factor with the ability to translate extracellular signals into biologic outcomes through its ability to initiate transcription of various

target genes. More specifically, signaling through p53 in response to genetic damage or oncogenic stress can initiate a range of cellular functions including cell cycle arrest, DNA repair, and apoptosis. The ability of p53 to initiate apoptosis is a key means through which it protects cells against tumorigenesis and important questions still remain about the precise signaling and cellular contexts required for p53-induced apoptosis (Christophorou, 2006; Efeyan and Serrano, 2007; Vousden and Prives, 2009).

p53 activity is regulated at many levels and kept low in unstressed cells due largely in part to regulation by the E3-ubiquitin ligase MDM2. In response to cellular stressors, like DNA damage or oncogenic signaling, p53 is modified and regulated by countless proteins, a full review of which is beyond the scope of this dissertation. Briefly, DNA damaging signals are transmitted to p53 through phosphorylation at a number of sites by the serine/threonine kinases ATM, ATR, CHK1, and CHK2. In the case of oncogenic signaling, p53 stability and activity are enhanced by activation of ARF, an MDM2 inhibitor. Once stabilized, p53 can activate or repress a diverse set of target genes that lead to cellular fate decisions like cell cycle arrest or apoptosis (Efeyan and Serrano, 2007). The apoptoic function of p53 is vital for its role as a tumor suppressor (Christophorou, 2006) and as a result, understanding the cell context, machinery, and interacting proteins needed to stimulate p53-mediated apoptosis is an active area of investigation. In this dissertation we will focus on the regulation of the p53-binding and apoptotic-stimulating protein, ASPP2. ASPP2 (apoptosis-stimulating protein of p53-2) is a regulator of apoptosis that cooperates with p53 and other

apoptotic proteins to promote apoptotic cell death (Naumovski and Cleary, 1996; Samuels-Lev *et al.*, 2001; Yang, 1999). Aspp2 has emerged as a tumor suppressor that can cooperate with p53 to prevent tumorigenesis *in vivo* (Kampa *et al.*, 2009a; Vives, 2006). This dissertation will explore the regulation of ASPP2 expression as well as one functional consequence of Aspp2 loss in a defined tumorigenic system. Additionally we will describe the discovery and characterization of a novel ASPP2 isoform, ΔN-ASPP2, with important regulatory potential with regards to both ASPP2 and p53.

A. ASPP2 Background

ASPP proteins: an overview of structure and function. ASPP2 (Apoptosis-stimulating protein of p53-2) is the founding member of a family of apoptosis regulating proteins that all share homology in their C-terminus. As shown in Figure 1.1, the ASPP family includes ASPP2 (also referred to as 53BP2L) and BBP (a splice isoform of ASPP2; also referred to as 53BP2S), which are both generated from the ASPP2 gene, *TP53BP2* (Naumovski and Cleary, 1996). The ASPP family also includes ASPP1 and iASPP, which are generated from separate genes on separate chromosomes (Bergamaschi, 2003; Samuels-Lev *et al.*, 2001; Yang *et al.*, 1997). ASPP2 was originally discovered as a partial clone, named 53BP2, that was found during a yeast two-hybrid screen using the DNA-binding domain of the tumor suppressor p53 as bait (Iwabuchi *et al.*, 1994). 53BP2 was later found to be a partial clone of a longer protein named BBP (BCL-

2-binding protein) for its ability to bind the anti-apoptotic protein BCL-2 (Naumovski and Cleary, 1996). It was later determined that BBP is a naturally occurring N-terminally truncated splice isoform of full-length ASPP2, the longest and most potent gene product from the *TP53BP2* locus (Samuels-Lev *et al.*, 2001).

ASPP family members all share homology in their C-terminus and contain an Ankyrin-repeat domain, SH3-domain, and a Poly-Proline rich region, which helps to further emphasize the ASPP family name (Samuels-Lev *et al.*, 2001). The proteins can be functionally subdivided with ASPP1, ASPP2, and, to a lesser extent, BBP being considered pro-apoptotic and iASPP being anti-apoptotic (Bergamaschi, 2003; Samuels-Lev *et al.*, 2001). Because the pro-apoptotic family members share homology in their N-terminus and the anti-apoptotic iASPP does not, this region is thought to contain key regulatory domains necessary for promoting apoptotic function. While the specifics of its function in apoptosis are unclear, it is known that the N-terminus of ASPP2 has an unstructured α-helical and RAS-association domain (Tidow, 2007) that is integral for RAS-mediated signaling and senescence (Wang Y., 2013; Wang, 2012b). The importance of an intact N-terminus will be explored in further detail in Chapter 2.

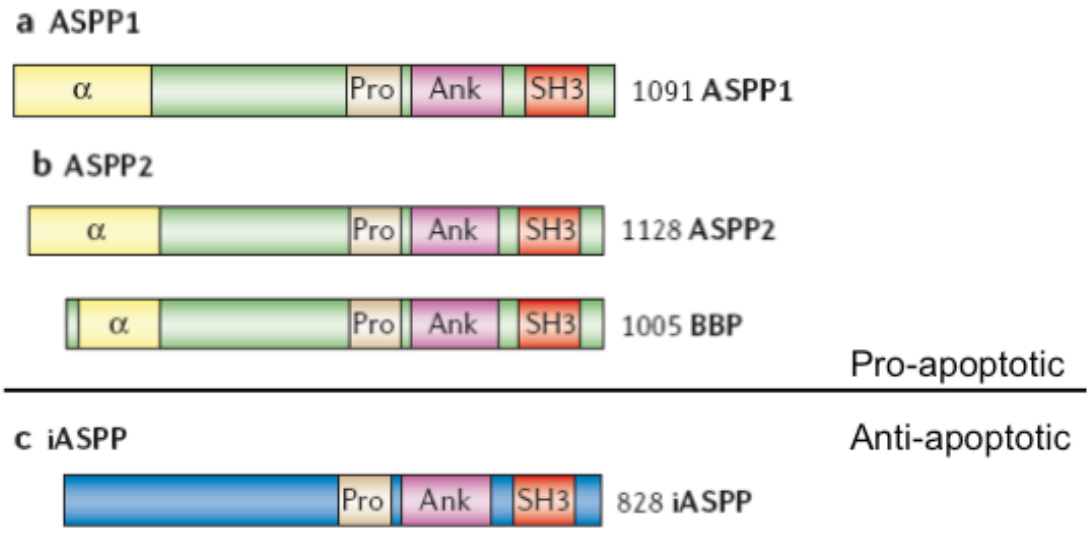

Figure 1.1: Schematic of the ASPP2 gene family (Trigiante and Lu, 2006 with permission). The functionally subdivided ASPP family of proteins share the common features of a poly-proline rich region (Pro), ankyrin repeat domain (Ank), and SH3-domain (SH3) in their C-terminus. Furthermore, the pro-apoptotic members share homology in an unstructured α-helical domain (α) in their N-terminus.

Diverse ASPP2 binding implies diverse functions. As previously mentioned, ASPP2 was originally discovered for its ability to bind to the DNA-binding domain of the tumor suppressor p53 (Iwabuchi *et al.*, 1994). The interaction of the p53 core domain and 53BP2 (a C-terminal partial clone of ASPP2) was further verified when they were co-crystallized to a resolution of 2.2 angstrom (Gorina and Pavletich, 1996). In addition, several of the more common tumor-derived hot spot mutations of p53 disrupt ASPP2-p53 binding and suggest direct regulation of p53 function (Gorina and Pavletich, 1996; Thukral *et al.*, 1994; Tidow, 2007). Interestingly, p53 cannot bind ASPP2 and DNA at the same time (Iwabuchi *et al.*, 1994), hinting at complexities in the regulation of p53 by ASPP2 that have yet to be defined.

In addition to binding p53, however, ASPP2 has been shown to bind a wide variety of other proteins. While most of the known ASPP2 binding partners interact through its C-terminal domain (Rotem-Bamberger, 2013), recent work has centered on defining associations at the N-terminus and their subsequent functional ramifications. For example, we have shown that ASPP2 associates with the signaling protein RAS through the N-terminal 126 amino acids of ASPP2 and that this association is necessary for potentiating RAS signaling and senescence (Wang, 2012b). The functional relevance of many of these interactions is still not known but they implicate ASPP2 in many p53-independent processes and in a wide array of signaling pathways. As summarized in Table 1.1, the ability of ASPP2 to bind a broad spectrum of proteins with a diverse set

of functions highlights the fact that ASPP2 has far reaching, yet poorly understood, effects within the cell.

Putative interactor	Putative function of pathway interactions	Reference(s)
	Modulates functions/pathways:	
p53 (p73/p63)	Enhances p53 transcriptional activity/Promotes p53-mediated apoptosis	Samuels-Lev 2001; Iwabuchi 1998; Bergamaschi 2004; Wang 2013
H-RAS	Potentiates RAS signaling, ERK1/2 phosphorylation, B-RAF/C-RAF dimerization, and C-RAF phosphorylation	Wang 2012; Wang 2013
BCL-2 (BCL-X_L)	Impedes cell cycle progression/Induces mitochondrial-mediated apoptosis	Naumovski 1996; Kobayashi 2005; Takahashi 2005
IRS-1	Modulates insulin signaling mediated by IRSs	Hakuno 2007
dCsk	*Drosophila* ASPP interacts with dCsk to regulate dSrc kinase	Langton 2007
APP-BP1	Inhibits neddylation pathway via interaction with APP-BP1	Chen 2003
PP1	Inhibits Protein Phosphatase 1 activity and facilitates activation of TAZ	Helps 1995; (Liu *et al.*, 2011; Skene-Arnold, 2013)
PAR-3	Facilitates establishment and maintenance of cell polarity	Cong 2010; Sottocornola 2010
ATG5	Inhibits autophagy	Wang 2012a
	Functions modulated by:	
NFκB/p65 subunit	Apoptosis inhibited by NFκB pathway	Yang 1999; Takahashi 2005
HCV core protein	Apoptosis inhibited by HCV core protein	Cao 2004
Ddx42p	Apoptosis/cell growth suppression inhibited by DEAD box protein Ddx42p	Uhlmann-Schiffler 2009
DDA3	Stimulation of p53-mediated BAX activation inhibited by DDA3	Sun 2008
	Undefined functional association:	
YAP	Phosphorylation by c-Yes inhibits interaction with YAP (a p73 co-activator)	Espanel 2001
APCL	Intracellular localization modulated by APCL	Nakagawa 2000
14-3-3s	Associates with 14-3-s during interphase	Meek 2004

TABLE 1.1 POTENTIAL FUNCTIONS AND PUTATIVE INTERACTING PARTNERS OF ASPP2 (adapted from Kampa *et al*., 2009b with permission).

The *TP53BP2* locus is inherently complex. ASPP2 is encoded by the 66 kb gene *TP53BP2* located on the minus strand of chromosome 1q42.1 (Yang *et al.*, 1997). Both *ASPP2* and *BBP* transcripts originate from *TP53BP2* (*Aspp2* in mice) through alternative splicing (Takahashi *et al.*, 2004). Removal of exon 3, which harbors a premature stop codon, generates the *ASPP2* transcript and ultimately ASPP2 (also known as 53BP2L), a proposed 1,134 amino acid protein with a predicted size of approximately 135 kDa (Samuels-Lev *et al.*, 2001). The *BBP* transcript is generated in one of two ways. First, retention of exon 3, and thus the premature stop codon, can cause translation to initiate in exon 6 as opposed to exon 1 (Takahashi *et al.*, 2004). Additionally, splicing can cause the removal of both exons 2 and 3, resulting in a frame shift that creates a premature stop codon in exon 4, again causing translation to initiate in exon 6 (Figure 2.2A). Both transcripts give rise to the N-terminally truncated BBP (53BP2S), which lacks the first 126 amino acids as compared to ASPP2, is 1,005 amino acids in length, and has a predicted size of approximately 115 kD (Figure 1.2; Naumovski and Cleary, 1996).

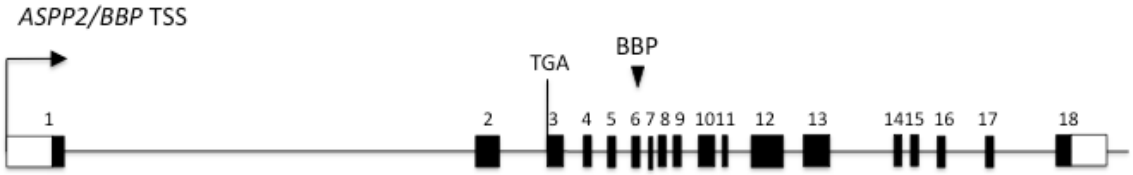

Figure 1.2: Gene structure of *TP53BP2/ASPP2.* Both *ASPP2* (*53BP2L*) and *BBP* (*53BP2S*) are generated from the *TP53BP2* locus. ASPP2 translation initiates in exon 1 while BBP translation utilizes an ATG in exon 6 due to a premature stop codon located in exon 3. Black triangle=BBP translation start site; TSS=transcription start site; TGA=stop codon.

ASPP2 expression is regulated on many levels.

Transcriptional Regulation

Current knowledge about the regulation of ASPP2 expression is limited, but several findings suggest that it is complex and occurs at multiple levels. Studies show that epigenetic changes, such as methylation at the *TP53BP2* promoter, can inhibit ASPP2 expression (Liu, 2005; Sarraf and Stancheva, 2004). In HeLa cells, stable transcriptional repression of *TP53BP2* occurs through histone 3-lysine 9 (H3-K9) methylation of the promoter by a complex formed by the methyl CpG binding protein MBD1 and the methylase SETDB1 (Sarraf and Stancheva, 2004). Additionally, the *TP53BP2* promoter was shown to be hypermethylated in a subset of tumor cell lines when compared to normal fibroblasts, indicating that abnormal methylation may be involved in down-regulating *TP53BP2* gene expression during tumorigenesis (Liu, 2005).

TP53BP2 has also been identified as an E2F gene target (Chen, 2005; Dynlacht, 2005; Fogal *et al.*, 2005; Hershko *et al.*, 2005), connecting it to the RB/E2F tumor suppression pathway. The E2F family of transcription factors transactivates many genes that are important for cell cycle progression as well as genes involved in apoptosis, thus allowing proliferation while also sensitizing cells to apoptotic signals (Sherr, 2002). Identification of *TP53BP2* as an E2F target gene provides a link between two important tumor suppressor pathways and strengthens the argument that ASPP2 plays an important role in preventing tumorigenesis. Interestingly, although mutation of all known E2F binding sites in

an *TP53BP2* promoter-luciferase reporter shows loss of E2F-induced transcriptional stimulation, transactivation of this mutated promoter is still significantly higher than empty vector controls when exposed to serum (Chen, 2005), indicating that other serum-stimulated, non-E2F-mediated pathways may also regulate ASPP2 expression. In Chapter 3 I will present data demonstrating that the oncoprotein c-MYC regulates *TP53BP2* transcription and discuss the possible functional consequences of this regulation.

Protein Regulation

ASPP2 protein expression responds to various types of cellular stimuli. Serum, UV irradiation, the DNA-damaging drugs idarubicin and doxorubicin, as well as the proteasome inhibitor bortezomib all induce expression of ASPP2 protein (Lopez, 2000; Lossos *et al.*, 2002; Samuels-Lev *et al.*, 2001; Zhu, 2005), but very little is known about the upstream pathways involved in these reponses. Additionally, ASPP2 protein degradation is posttranslationally controlled by ubiquitin-mediated proteolysis (Zhu, 2005).

Cellular Localization

ASPP2 localizes to several subcellular compartments, which may be cell type or context dependent. ASPP2 contains a nuclear localization signal within its ankyrin repeat domain (amino acid residues 795-894) that, when expressed alone or as a fusion with other proteins, localizes to the nucleus (Sachedev 1998 ;Yang 1999). Despite this signal however, full-length ASPP2 is

predominantly located in the cytoplasm and near the plasma membrane as a result of its association with the small GTPase protein RAS (Iwabuchi *et al.*, 1998; Naumovski and Cleary, 1996; Wang Y., 2013; Wang, 2012b). Additionally, ASPP2 can transiently localize to the mitochondria and enhance apoptosis, though the mechanism remains unclear (Kobayashi, 2005).

Tissue Distribution

The distribution of protein expression throughout a panel of tissues is often a helpful tool for understanding a protein's function. ASPP2 appears to be ubiquitously expressed in most tissues but its expression levels vary. Northern blot analysis, using a probe near the 3' end of the transcript, shows elevated levels of *ASPP2* mRNA in several human tissues including heart, testis, and peripheral blood leukocytes (Yang 1999). Moreover, whole mount *in situ* hybridization of mice at embryonic day 9.5, using probes that target both the 5'-end and 3'-end of the transcript, shows that *ASPP2* is strongly expressed in the central nervous system-- specifically the brain, spinal cord, and optic cup (Sottocornola *et al.*, 2010).

ASPP2 promotes apoptosis. Before ASPP2 was known to be the full-length gene product from the *TP53BP2* locus, Yang and colleagues showed that overexpression of BBP in cells induces apoptosis (Yang 1999). In 2000, Lopez *et al.* demonstrated that ASPP2 was UV-damage inducible and that loss of the endogenous protein promotes cell survival in response to damage, thus implicating it in the damage response pathway (Ao *et al.*, 2001). In 2001, a

seminal study by Samuels-Lev *et al*. showed that full-length ASPP2 promotes apoptosis and does so, at least in part, through a p53-mediated mechanism, which supported and clarified earlier results showing the ASPP2 binds the tumor suppressor p53 in its core domain (Gorina and Pavletich, 1996; Iwabuchi *et al.*, 1994). They postulated that ASPP2 enhances apoptosis by promoting preferential binding and transactivation of p53 on its pro-apoptotic target genes (e.g. *Bax, PIG3, Puma*) and not cell cycle arrest genes (e.g. $p21^{WAF}$*, mdm-2*; (Samuels-Lev *et al.*, 2001). These findings give insight into a possible mechanism of how ASPP2 may cooperate with p53 to promote apoptosis and define ASPP2 as a key regulator of p53 function.

While primarily studied as a p53-interacting protein, ASPP2 is known to bind and affect a variety of other proteins, several of which are involved in apoptotic pathways (Table 1.1). For example, ASPP2 binds and modulates the apoptotic activity of the p53 family members p63 and p73, demonstrating p53-independent roles as well (Bergamaschi 2004). Additionally, ASPP2 binds the pro-survival proteins BCL-2 and NF-κB/p65 and expression of either BCL-2 or NF-κB can suppress ASPP2-mediated apoptosis (Takahashi *et al.*, 2005; Yang, 1999). Additionally, ASPP2 can stimulate apoptosis by localizing to the mitochondria to promote depression of the mitochondrial transmembrane potential, though the details of the precise mechanisms involved remain unclear (Kobayashi, 2005). Taken together, these findings clearly demonstrate that ASPP2 promotes apoptosis, but also underscores the need to clarify precisely how and under what cellular contexts it functions to promote cell death.

ASPP2 has clear functions beyond apoptosis.

Cell cycle

Several studies have demonstrated a role for ASPP2 in the cell cycle. The ASPP2 splice isoform BBP can block cell cycle progression by inducing accumulation of cells in G_2/M (Naumovski and Cleary, 1996). Additionally, Aspp2 appears to play a role in the G_0/G_1 cell cycle checkpoint in response to γ-irradiation, as murine thymocytes that lack one copy of *Aspp2* do not arrest at G_0/G_1 as efficiently as their wild type counterparts (Kampa *et al.*, 2009a). Indeed, a role for ASPP2 in cell cycle regulation is suggested by its physical and functional association with p53, a master tumor suppressor with defined roles in cell cycle checkpoint control (Efeyan and Serrano, 2007).

Senescence

RAS is a widely studied small GTPase that controls an intracellular signaling cascade that is responsible for a variety of cellular outcomes, including senescence (Collado, 2010). Senescence, a type of irreversible cell cycle arrest, is considered an intrinsic protective response against malignant transformation. Because of the presence of a predicted RAS-association domain in the N-terminus of ASPP2, a series of studies have looked at whether ASPP2 plays a role in this complex signaling pathway. ASPP2 was shown to be a mediator of RAS-induced senescence by demonstrating that loss of ASPP2 in multiple primary cell types attenuated activated RAS-induced senescence (Wang *et al.*, 2010; Wang, 2012b). Additionally, ASPP2 binds directly to RAS at the plasma

membrane through the first 126 N-terminal residues making this interaction entirely separate from its C-terminal p53-binding ability. Furthermore, ASPP2 potentiates RAS signaling as shown by phosphorylation of the downstream mediator ERK1/2, enhanced dimerization of the protein kinases B-RAF/C-RAF, and increased phosphorylation of C-RAF (Wang, 2012b). Additional data suggests that RAS-induced senescence may be mediated by ASPP2 through its ability to inhibit RAS from inducing accumulation of the cell cycle regulatory protein cyclin D1 within the nucleus (Wang *et al.*, 2010). Together these findings define a clear role for ASPP2 in senescence and broaden our understanding of one mechanism through which it may act as a tumor suppressor *in vivo.*

Cell polarity and development

In an effort to more clearly understand the role of ASPP2 *in vivo* two different groups have genetically targeted *Aspp2* in mouse models to examine the outcome of its depletion. While the differences in the two targeting strategies appear to have created some disparities (see Chapter 2), both *Aspp2*$^{-/-}$ animal models show profound developmental defects (Kampa *et al.*, 2009a; Vives, 2006). Vives *et al.* found that mice were born runted and with cranial, retinal, and heart abnormalities while Kampa *et al.* were unable to recover any *Aspp2*$^{-/-}$ animals even as early as embryonic day 6.5. Further analysis determined that Aspp2 has a vital role in the development of the central nervous system (CNS), more specifically that it plays a role in the establishment and maintenance of neural progenitor cells (Sottocornola *et al.*, 2010).

Further investigation into the mechanism behind the CNS defects revealed that animals lacking *Aspp2* were deficient in their ability to establish and maintain the integrity of tight junctions, an important cell-cell connection needed to regulate epithelial cell polarity. Loss of Aspp2 expression correlates with a loss of tight junction integrity and an impaired ability to maintain apical domains in polarized cells in culture and *in vivo* (Cong, 2010; Sottocornola *et al.*, 2010). Interestingly, Aspp2 was shown to co-localize with, bind to, and regulate the organization of the PAR-3 polarity complex at apical junctions within the brain (Cong, 2010).

Autophagy

Autophagy is a regulated cellular process through which a cell catabolizes organelles and macromolecules. It is a complex process that can be initiated as a means of recycling cellular components during nutrient deprivation or to promote cell death, depending on the cell type and context. This dual role in both survival and cell death makes it important for both the pathogenesis and treatment of cancer (Kundu, 2008). Recently, studies have shown that certain types of cancer are dependent upon autophagy for survival and tumor growth and that inhibition of autophagy can result in tumor regression and upregulation of protective pathways like senescence (Wang, 2012a; Yang, 2011). Interestingly, ASPP2 has been shown to inhibit autophagy. Specifically, the N-terminus of ASPP2 is proposed to share structural similarity with the essential autophagic protein ATG16 and thus competes with it for binding partners. This competition inhibits

autophagy by inhibiting the necessary ATG16/ATG12/ATG5 complex and, as a result, enhances RAS-induced senescence (Wang, 2012a). This notion that levels of autophagy, and by extension ASPP2, can regulate a cell's response to oncogenic RAS is very interesting and opens up new avenues of investigation for improved cancer therapeutics.

ASPP2 is a bona fide tumor suppressor repressed in human cancer. Given that ASPP2 plays a role in promoting apoptosis, and that it does so by cooperating with pathways that are often deregulated in human cancer, many studies have focused on examining ASPP2 (or lack thereof) during cancer progression (Table 1.2). Two separate animal studies have shown that loss of one copy of *Aspp2* leads to an increase in spontaneous tumor formation. *Aspp2*$^{+/-}$ mice were also shown to be more sensitive to tumorigenesis induced by ionizing radiation as compared to their wild type littermates (Kampa *et al.*, 2009a; Vives, 2006). In accordance with these data, several studies report that low levels of *ASPP2* mRNA are seen in invasive and metastatic breast cancer patient samples (Bergamaschi, 2003; Cobleigh *et al.*, 2005; Hedenfalk *et al.*, 2001; Samuels-Lev *et al.*, 2001; Sgroi, 1999) as well as in various other tumor types and a number of human cancer cell lines (Liu, 2010; Liu, 2005; Lossos *et al.*, 2002; Meng, 2013; Mori *et al.*, 2000; Pomeroy *et al.*, 2002; Zhao *et al.*, 2010). A full summary of ASPP2 expression in human tumors is shown in Table 1.2. Decreased levels of *ASPP2* mRNA correlates with poor prognosis in some non-Hodgkin's lymphomas (Lossos *et al.*, 2002) and shorter recurrence-free survival in breast cancer patients (Cobleigh *et al.*, 2005). Moreover, *ASPP2* mRNA levels

strongly correlate with sensitivity to genotoxic stress (Mori *et al.*, 2000), suggesting that ASPP2 may play a role in sensitizing tumor cells to apoptotic stimuli thus protecting them from malignant transformation. Furthermore, loss of *Aspp2* in mice leads to the development of retinal dysplastic rosettes, similar to those seen in human neuronal tumors and BBP inhibits RAS/E1A-mediated transformation in rat embryonic fibroblasts (Iwabuchi *et al.*, 1998; Sottocornola *et al.*, 2010).

There remains a great deal of work to be done in order to understand the genetic mechanisms surrounding loss of *ASPP2* expression during tumor development. However, we do know that while mutations in *TP53BP2* are rare, they have been reported in gastric cancers with high microsatellite instability and that single nucleotide polymorphisms in the gene have been found associated with gastric cancer susceptibility (Ju *et al.*, 2005; Mori *et al.*, 2000; Park *et al.*, 2010). Additionally, epigenetic silencing of the *TP53BP2* promoter by methylation is frequently observed in human cancer (Liu, 2005; Sarraf and Stancheva, 2004; Zhao *et al.*, 2010). These data, taken together with the mechanistic and functional data showing that ASPP2 enhances apoptosis, regulates senescence, and possibly regulates cell cycle checkpoints and autophagy, strongly suggest that ASPP2 is a tumor suppressor that is vital for protection against malignant transformation. Indeed, loss of ASPP2 expression in cancer may afford a selective advantage by conferring evolving tumor cells with a degree of apoptotic or senescent resistance.

Tumor type	Notes	Reference(s)
Breast	Reduced levels of *ASPP2* expression seen in both invasive and metastatic breast tumor tissue (Sgroi 1999) and *ASPP2* downregulation may be favored in tumor cells expressing wild type but not mutant p53 (Samuels-Lev 2001).	Sgroi, 1999; Samuels-Lev, 2001; Cobleigh, 2005; Bergamaschi, 2003; Hedenfalk, 2001
Non-Hodgkin's Lymphoma specifically diffuse large B-cell (DLBC), follicular center (FC), and Burkitt's lymphoma	*ASPP2* expression higher in DLBC lymphomas as compared to FC. Variability of *ASPP2* expression in DLBC lymphoma was much greater than that seen in FC. *ASPP2* expression inversely proportional to serum lactate dehydrogenase levels. Levels of *ASPP2* expression are extremely low or undetectable in cell lines derived from Burkitt's lymphoma.	Lossos, 2002
Gastric cancer	Single nucleotide polymorphisms within *TP53BP2* show significant correlation with gastric cancer susceptibility (Ju 2005). ASPP2 expression lower in gastric cancer and precancerous lesions as compared to benign gastric disease group (Meng 2013). ASPP2 frameshift mutations are detected in gastic cancers with high microsatellite instability (Park 2010).	Ju, 2005; Meng, 2013; Park, 2010
Hepatitis B virus positive-hepatocellular carcinoma	Downregulation of ASPP2 (and ASPP1) as a result of promoter hypermethylation is observed in human patient samples of HBV-positive hepatocelluar carcinoma as compared to surrounding non-tumor tissue.	Zhao, 2010
Endometrial endometrioid adenocarcinoma	Lower expression of ASPP2 seen in endometrial endometrioid adenocarcinoma as compared to normal endometrial tissue.	Liu, 2010
Embryonic tumors of the central nervous system	Low expression seen in desmoplastic samples as compared to normal brain.	Pomeroy, 2002

TABLE 1.2. SUMMARY OF ASPP2 EXPRESSION PATTERNS AND MUTATIONS IN HUMAN TUMORS.

B. c-MYC Background

c-MYC is a master transcription factor. c-MYC is the most widely studied member of a family of basic helix-loop-helix-leucine zipper (bHLH-LZ) transcription factors. It controls a wide variety of cellular processes, including proliferation, differentiation, metabolism, and apoptosis, by mediating the transcription of a diverse set of target genes (Cowling, 2006). MYC is also one of the most commonly overexpressed proteins in cancer due in part to its ability to promote proliferation (Meyer and Penn, 2008; Nesbit, 1999). Structurally, MYC is comprised of a C-terminal DNA-binding domain (bHLH-LZ) and an N-terminal transactivation domain, which mediate interactions with transcriptional cofactors and play an important role in regulating protein stability (Meyer and Penn, 2008). Along with its obligate binding partner MAX, the MYC:MAX heterodimer activates gene transcription by binding specific DNA sequences (CACGTG) called E-box regulatory elements within the promoters of target genes (Blackwell, 1990; Blackwood, 1991; Prendergast, 1991). MYC recruits and binds to a variety of chromatin remodeling co-factors, such as histone acetyltransferases (HATs) and TRRAP (transformation/transcription domain-associated protein) that facilitate the modification and opening of chromatin to allow gene activation (Cowling, 2006; McMahon, 1998). Partnering of MYC with MAX and subsequent gene activation is opposed by competition for MAX binding by both the MNT and the MAD family of transcriptional repressors (Hurlin, 2006). MAD:MAX and MNT:MAX heterodimers also bind to E-box regulatory elements within their target promoters and, in a process converse to MYC:MAX, promote gene repression

by recruiting transcriptional co-repressors such as SIN3A (Ayer DE, 1995; Hurlin, 2006). In this way, the availability of competing transcription factors can act as a level of control to ensure that MYC transcription is occurring at the correct time and under appropriate cell conditions.

While most commonly known to activate transcription, MYC has also been linked to gene repression through its ability to bind the transcription factor MIZ-1. Interestingly, one of the mechanisms of MIZ-1-mediated repression does not appear to rely upon E-box regulatory sequences but rather on initiator (INR) elements in the promoters of target genes (Cowling, 2006; Patel, 2007).

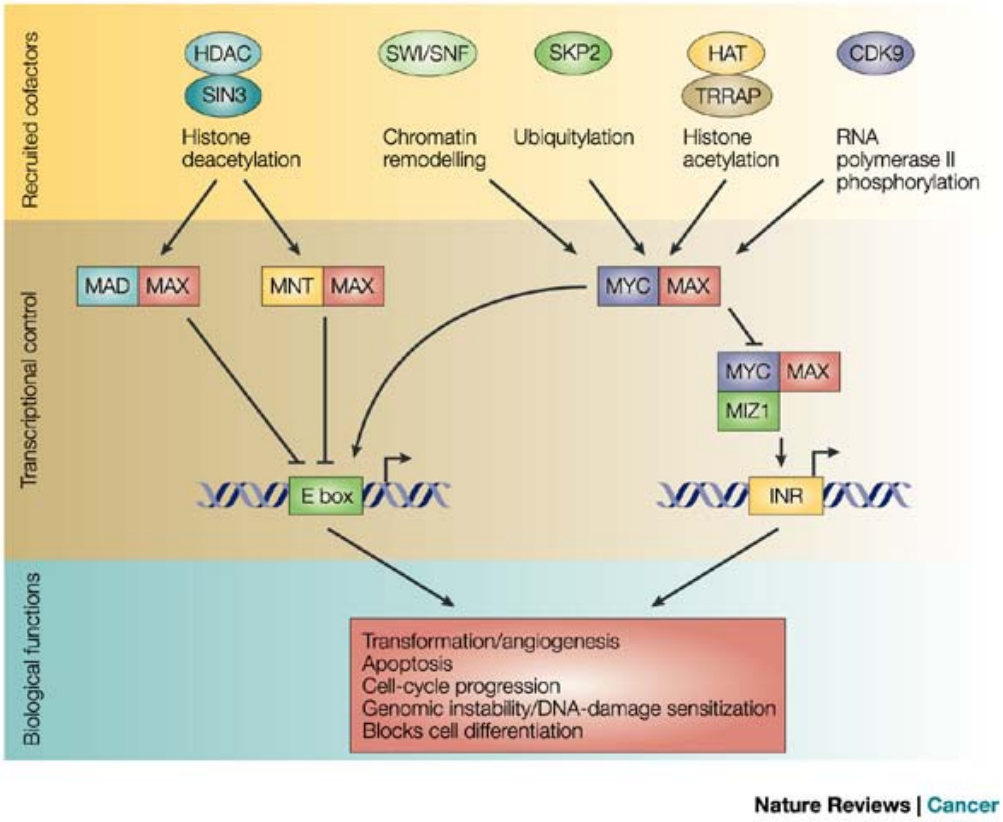

Figure 1.3 Gene regulation mediated by the MYC/MAX transcriptional network (Patel, 2004 with permission). MYC heterodimerizes with MAX to bind E-box regulatory elements within target gene promoters to initiate transcription. The opening of chromatin is aided in part through remodeling proteins such as SWI/SNF and TRRAP. MYC:MAX further promotes transcription by recruiting and facilitating the phosphorylation of RNA polymerase II. MYC is capable of gene repression through its interaction with MIZ-1 and their association with initiator (INR) elements within target gene promoters. MNT and MAD family proteins compete with MYC for MAX binding and represses target genes, also through binding to E-box motifs. Under normal cycling conditions MYC:MAX transcription promotes proliferation, apoptosis, and blocks differentiation. In its pathogenic state, such as is seen in cancer, MYC promotes transformation and angiogenesis making it a powerful oncogene.

MYC functions in normal cell proliferation and apoptosis.

MYC is frequently elevated in human cancer (Nesbit, 1999), which highlights the importance of keeping c-MYC expression tightly controlled so its function is restricted to the appropriate cellular context.

At the gene level, *MYC* expression is controlled by a bevy of transcription factors, including β-catenin/TCF4 and the activating E2F proteins (Wierstra, 2008). As a serum-responsive and proliferation-promoting protein, MYC is produced in response to mitogenic signals aimed at advancing cell division. At rest, a cell contains low levels of MYC and upon mitogenic stimulation its expression rapidly increases to promote transcription of the early response genes needed for cell cycle entry and progression (Sears, 1999). Indeed, expression of MYC in the absence of growth stimulation is sufficient for entry into the cell cycle (Eilers, 1991). MYC facilitates transition of cells from G_1 into S phase by direct activation of the important cell cycle regulators cyclin D2 and cyclin E, and E2F(1-3) while simultaneously repressing cyclin inhibitors such as p21 (Bouchard, 1999; Fernandez *et al.*, 2003; Leone *et al.*, 2001; Sears *et al.*, 1997; Seoane *et al.*, 2002; Wu, 2003). As proliferative signaling diminish, so does MYC expression and activity, thus temporally limiting its function to ensure cell division proceeds under the correct conditions. Conversely, as MYC expression wanes, expression of the repressive MNT and MAD family of proteins increases, thus increasing competition for MAX and further limiting MYC activity (Hurlin, 2006).

We know that deregulation of MYC is a common mechanism for evolving

tumor cells to drive cell cycle progression. However, like many oncoproteins, it also sensitizes cells to apoptosis when MYC expression levels exceed a critical threshold, thus protecting the cell from aberrant MYC activity (Evan, 1992; Murphy *et al.*, 2008; Nilsson, 2003). It is proposed then that the selective advantage afforded to cells with deregulated or elevated levels of MYC is kept in check by its ability to limit proliferation by inducing apoptosis (Evan, 1992; Nilsson, 2003). Evan *et al.* first conclusively demonstrated this surprising discovery by showing that when Rat1 fibroblasts are cultured in low serum they rapidly undergo apoptosis in a MYC-dependent manner (Evan, 1992). This apoptotic response can be initiated through both p53-dependent and independent mechanisms. MYC activation of the tumor suppressor ARF promotes stabilization of p53 by inhibiting its inhibitor MDM2 leading to p53 activation and induction of apoptosis (Zindy *et al.*, 1998). The BCL-2 family of proteins strongly influences apoptosis by governing mitochondrial membrane permeability and MYC has been implicated in activating the pro-apototic function of several of these proteins, specifically BAK and BAX (Jiang, 2007; Juin, 2002). Also, MYC repression of MIZ-1 allows for the induction of apoptosis by reducing expression of the anti-apoptotic protein BCL-2 (Patel, 2007). Fundamental questions remain, however, about the direct mechanisms involved in executing MYC-induced apoptosis and the cell context required to trigger this important cell death response. The ability of c-MYC to induce apoptosis puts selective pressure on evolving tumor cells to deregulate this apoptotic response and not surprisingly, deregulation of apoptotic machinery is one of the most common

cooperating mutations found in tumors with elevated MYC (Nilsson, 2003). In Chapter 3 I will provide evidence to suggest that direct upregulation of ASPP2 is one pathway through which MYC may enhance apoptosis in response to oncogenic or environmental stress.

In addition to sensitizing cells to apoptosis and positively regulating genes needed for cell cycle progression, MYC also targets genes that promote cell growth by way of ribosome biogenesis, inhibit terminal differentiation, promote stem cell self renewal, and enable anchorage-independent migration (Dang, 2012). With such a wide array of functions it is easy to imagine how deregulation of this one protein has such a strong impact on promoting tumorigenesis.

Statement of thesis

Evidence is clear that ASPP2 is a tumor suppressor that plays a role in protecting against malignant transformation. What is not known, is precisely how the gene products from the *TP53BP2* locus are regulated and how this regulation translates into meaningful action within the cell. Given ASPP2's role as a pro-apoptotic tumor suppressor and the established complexity at the *TP53BP2* locus, I hypothesized that multiple pathways must regulate ASPP2 expression and that ASPP2 function may be impacted by previously unknown protein isoforms. In Chapter 2, I focus on the discovery and characterization of a novel isoform from the *TP53BP2* locus and how it might play a role in promoting tumorigenesis. In Chapter 3, I concentrate on my examination of *TP53BP2* as a MYC target gene and the extent to which this regulation affects the established role for ASPP2 as a tumor suppressor.

Chapter Two:

ΔN-ASPP2 is a Novel Isoform of the ASPP2 Tumor Suppressor that Promotes Cellular Survival

ΔN-ASPP2 is a Novel Isoform of the ASPP2 Tumor Suppressor that Promotes Cell Survival

Abstract

Apoptosis-Stimulating Protein of p53 2 (ASPP2 aka 53BP2L) is a tumor suppressor that works, at least in part, through enhancing p53-dependent apoptosis. Full-length ASPP2 is necessary for potent stimulation of p53-dependent apoptosis, though the precise mechanisms and cell contexts that enable this function remain to be clarified. The complexity of the *TP53BP2* allele led us to investigate whether additional ASPP2 isoforms might contribute to the modulation of ASPP2 and/or p53 function. We now describe a new isoform, ΔN-ASPP2, generated from an internal transcription start site that encodes an N-terminally truncated protein missing a predicted 254 amino acids. Here we report that ΔN-ASPP2 suppresses p53 target gene transactivation, promoter occupancy, and endogenous p53 target gene expression in response to DNA damage. Additionally, ΔN-ASPP2 promotes proliferation, resistance to genotoxic stress-induced growth inhibition, and apoptosis. We have also found that *ΔN-ASPP2* expression is increased in human breast tumors as compared to adjacent normal breast tissue; in contrast, full-length *ASPP2* expression is suppressed in the majority of these breast tumors. Together, our results provide insight into how this new ASPP2 isoform may play an important role in regulating the ASPP2-p53 axis.

Introduction

The p53 pathway is a critical and central player in the regulation of both cellular stress response and tumor suppression. Defects in the p53 axis result in subsequent defects in downstream tumor suppressive pathways such as cell cycle arrest, apoptosis, and senescence (Meek, 2009; Pietsch *et al.*, 2008). Not surprisingly, p53 is known to be one of the most highly mutated genes in human cancer. However, in some cancers (such as breast) the frequency of p53 mutations is relatively low (~20%) as compared to other cancers (Gasco *et al.*, 2002). Thus, functional inactivation of the p53 pathway must occur by mechanisms besides p53 mutation. Precisely how the p53 pathway is functionally inactivated remains complex and incompletely understood.

ASPP2 is the founding member of a family of p53-binding proteins that share homology in their C-terminus. The C-terminal ankryin-repeat and SH3 domains of ASPP2 bind the p53 core domain (Gorina and Pavletich, 1996; Iwabuchi *et al.*, 1994) and modulate p53 function (Bergamaschi, 2003; Iwabuchi *et al.*, 1994; Kampa *et al.*, 2009b; Samuels-Lev *et al.*, 2001). The full-length 1,134 amino acid (a.a.) ASPP2 (aka 53BP2L), and to a lesser extent the 1,005 a.a. splice variant BBP (aka 53BP2S) (Naumovski and Cleary, 1996; Takahashi *et al.*, 2004) stimulate p53-mediated transcription, inhibit cell growth, promote apoptosis, and inhibit RAS/E1A-mediated transformation of rat embryonic fibroblasts (Lopez, 2000; Naumovski and Cleary, 1994; Naumovski and Cleary, 1996; Samuels-Lev *et al.*, 2001; Yang, 1999). ASPP2 selectively stimulates p53

(and p73/p63)-transactivation of target genes (Bergamaschi *et al.*, 2004; Samuels-Lev *et al.*, 2001) but also mediates p53-independent functions to inhibit cell growth (Wang, 2012b). Importantly, targeting of the *TP53BP2* allele in mouse models demonstrates that Aspp2 is a bonafide tumor suppressor (Kampa *et al.*, 2009a; Vives, 2006). Indeed, clinical studies also demonstrate reduced ASPP2 expression in human tumors and correlation with poor clinical outcome (Lossos *et al.*, 2002; Samuels-Lev *et al.*, 2001; Zhao *et al.*, 2010). Not surprisingly given its complex functions, ASPP2 expression is complex and controlled by both transcriptional and post-translational mechanisms (Chen, 2005; Kampa *et al.*, 2009b; Lopez, 2000; Zhu, 2005). Moreover, the *TP53BP2* locus is an 18 exon gene spanning over 50 kB, which suggests that additional mechanisms may further regulate ASPP2 expression. Despite these findings, little is known about the mechanisms controlling ASPP2 expression and function or how its loss may impact tumorigenesis and resistance to therapy.

The ASPP2 N-terminus contains important structural and functional domains (Tidow, 2007). The originally described partial clone known as 53BP2 (encoding an artificial 528 a.a. protein that is missing the N-terminal 600 a.a.) has dominant-negative activity against ASPP2 and p53 (Samuels-Lev *et al.*, 2001). Interestingly, the natural occurring N-terminally truncated ASPP2 splice isoform BBP (missing the first 123 a.a.) has attenuated function compared to full-length ASPP2 including decreased apoptosis and growth-inhibitory functions (Samuels-Lev *et al.*, 2001). Indeed, there are many examples of protein isoforms having distinct and important functions that differ from their full-length products (such as

the complex isoforms of the p53, p63, and p73 families) (Fujita *et al.*, 2009; Samuels-Lev *et al.*, 2001). Despite our understanding that the *TP53BP2* locus is complex and that an intact N-terminus is needed for ASPP2's full growth inhibitory and tumor suppressor function, little is known about naturally occurring ASPP2 N-terminally truncated isoforms or their functions.

In this report, we describe a new ASPP2 isoform that we have named ΔN-ASPP2. We demonstrate that ΔN-ASPP2: (i) is derived from an alternative transcription start site within intron 6 of *TP53BP2*, (ii) encodes an N-terminally truncated ASPP2 protein, (iii) antagonizes p53 transactivation and p53 promoter occupancy after cellular stress, (iv) promotes cell proliferation and suppresses cytotoxic damage-induced growth inhibition and apoptosis, and (v) is overexpressed in human breast tumors as compared to adjacent normal breast tissue, while full-length ASPP2 expression is suppressed in these tumor samples. Together our data provide novel insight into the regulation of ASPP2 function and identify a dominant-negative ASPP2 isoform that may ultimately play an important role in human cancer and provide a new target for therapy.

Results

ΔN-ASPP2 is a novel N-terminally truncated isoform of ASPP2. Since the *TP53BP2* locus is structurally complex (Kampa *et al.*, 2009a) we wished to explore if novel *TP53BP2* gene products were generated that could provide insight into the complexity of ASPP2 function (Kampa *et al.*, 2009b). We utilized 5'-RACE with GeneRacer® (Invitrogen) to detect mature capped *ASPP2* mRNA transcripts in human, mouse, and rat cDNA libraries (Figure 2.1). In addition to the expected known full-length *ASPP2* transcript (Samuels-Lev *et al.*, 2001), we identified and sequence-verified a novel *ASPP2* mRNA generated from an internal transcription start site (TSS) within intron 6 in mouse/human or intron 7 in rat (Figure 2.1A). We named the new isoform ΔN-ASPP2 since the predicted ATG in exon 8 would generate an N-terminal truncated 880 a.a. protein. ΔN-ASPP2 is not a splice isoform of the full-length *ASPP2* transcript, since exon 1-initiatied RT-PCR only detects *ASPP2* and *BBP* mRNA in human (Figure 2.2A) and mouse cDNA libraries (Figure 2.2B). Upon sequence verification we discovered that a newly described *BBP* transcript [as opposed to the known transcript described in (Takahashi *et al.*, 2004)], can be generated by splicing out both exons 2 and 3. The resulting exon 1-4 splicing causes a frameshift, which reveals a premature stop codon in exon 4, consequently promoting translation initiation in exon 6 (Figure 2.2A).

Sequencing of the 5'-RACE products identified a unique 5'-untranslated region (containing a portion of intron 6/7 of full-length *ASPP2*) in the mature *ΔN-ASPP2* mRNA but not in the mature *ASPP2* and *BBP* mRNAs. To further verify

the identity of ΔN-ASPP2, the TSS in rat *ΔN-ASPP2* was additionally mapped using RT-PCR with a reverse exon 9 primer coupled with a series of forward primers derived from intron 7 through exon 8 (Figure 2.1B, bottom panel). The same primer sets were used on genomic DNA from the same source (Figure 2.1B, top panel). As expected, we amplified all fragments (f1-6) in genomic DNA. However RT-PCR was only able to amplify f1 and f2 from the cDNA library, which is consistent with the TSS identified by 5'RACE. The genomic sequence was further analyzed using the promoter prediction software Promoter 2.0 (Knudsen, 1999) and revealed a high scoring TSS (score 1.071) that is within 380 base pairs of our experimentally determined ΔN-ASPP2 TSS. The open reading frame of ΔN-ASPP2 is predicted to truncate the 254 N-terminal amino acids compared with full-length ASPP2 (Figure 2.1C).

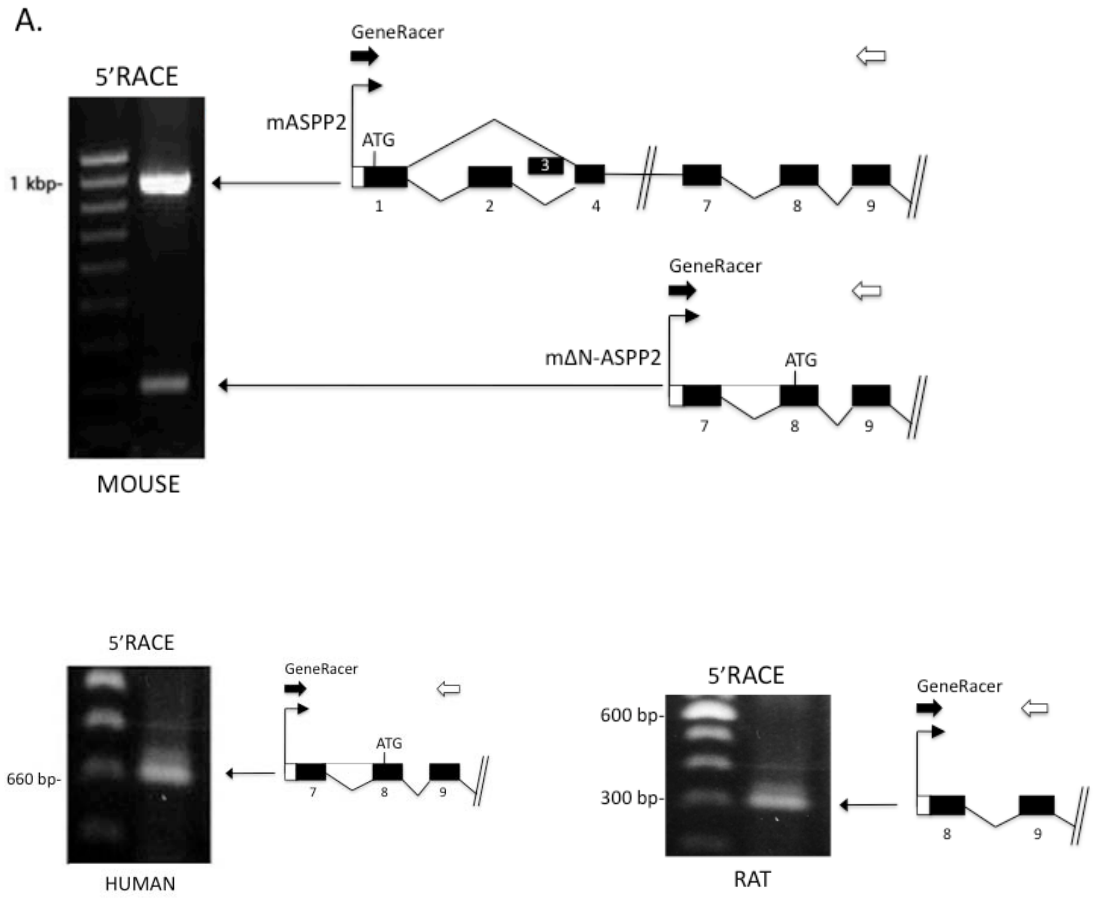

Figure 2.1. ΔN-ASPP2 is a novel N-terminally truncated isoform of ASPP2. (A) Mouse, human, and rat 5'RACE products generated from a GeneRacer® forward primer (black arrow) and an *ASPP2*-specific reverse primer (white arrow).

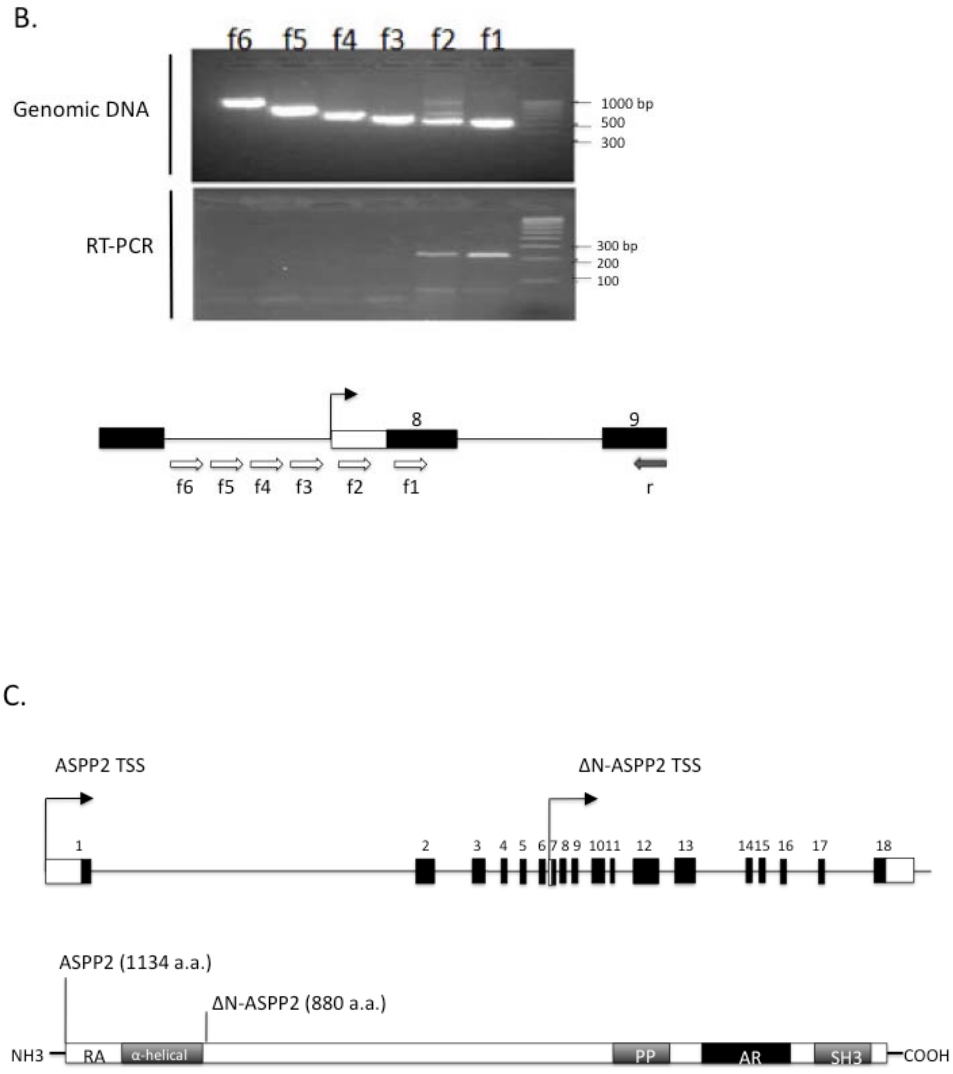

Figure 2.1. ΔN-ASPP2 is a novel N-terminally truncated isoform of ASPP2. (B) Gel mapping of ΔN-ASPP2 transcription start site within intron 7. Rat genomic DNA or a brain cDNA library was amplified using the indicated forward primers (white arrows) and an exon 9 reverse primer (black arrow) and run on a 1% agarose gel. (C) Diagram of *TP53BP2* gene structure with *ASPP2* and *ΔN-ASPP2* TSS indicated (*top*) and putative protein structure (*bottom*). Black boxes=open reading frame; white-boxes=untranslated regions; TSS=transcription start site; RA=RAS-association domain; PP=poly proline region; AR=ankyrin repeats; SH3=Sarc homology-3 domain.

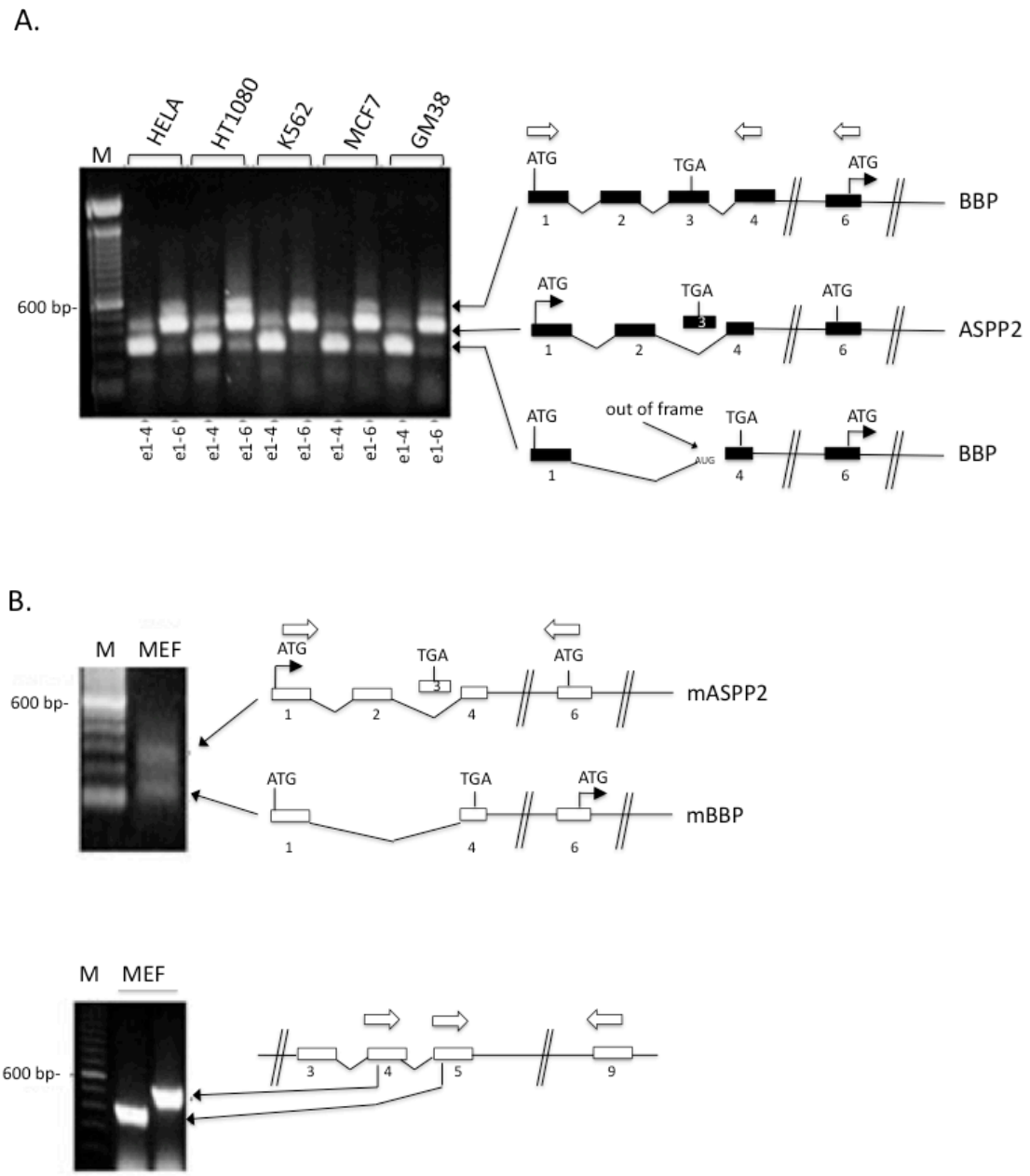

Figure 2.2. ΔN-ASPP2 is generated from an alternative transcription start and not alternative splicing. cDNA was prepared from total RNA for both human cell lines and mouse embryonic fibroblasts. (A and B; *top panel*) Sequenced PCR products verify that only *ASPP2* and *BBP* transcripts are generated from exon 1-initiated transcription in human cell lines and MEFs. e1-4 indicates exon 1 forward/exon 4 reverse amplicon and e1-6 indicates exon 1 forward/exon 6 reverse amplicon. All 3 PCR products, corresponding to 3 distinct transcripts, migrate faster in e1-4 reactions due to smaller amplicon size. (B; *bottom panel*) Sequenced PCR products verify that only one transcript is generated from an exon-4 or exon-5 initiated amplification. White arrows indicate primers used.

Endogenous ΔN-ASPP2 is expressed in cells. To confirm that the newly identified *ΔN-ASPP2* TSS (Figure 2.1) generated an intact *ΔN-ASPP2* mRNA and protein, we first cloned and sequenced the entire ΔN-ASPP2 cDNA using a 5'-UTR-specific forward primer and 3'UTR-specific reverse primer (Figure 2.3A). We did not detect mutations in the open reading frame (ORF) shared with ASPP2. To demonstrate that the ΔN-ASPP2 cDNA could generate an ASPP2-immunoreactive protein, we engineered the ΔN-ASPP2 cDNA, including the unique 5' UTR, into an expression vector and transfected the construct into cells (Figure 2.3B). Using a C-terminal specific ASPP2 antibody on lysates prepared from transfected cells, we found an ASPP2-immunoreactive protein of ~125 kD, which migrated faster than the ~165 kD full-length ASPP2 (Figure 2.3B). It is known that ASPP2 migrates anomalously slow (~165 kD as compared to predicted ~135 kD) in SDS-PAGE due to its poly-proline rich domain (Samuels-Lev *et al.*, 2001). This domain is conserved in ΔN-ASPP2 (Figure 2.1C), which would similarly account for ΔN-ASPP2 migrating more slowly than predicted (~125 kD as compared to predicted ~90 kD). To confirm that the ~125 kD endogenous band is ΔN-ASPP2, we used ASPP2 N-terminal and C-terminal-specific antibodies to epitope-map endogenous ΔN-ASPP2 protein in human cancer cell lines. As expected, an endogenous ASPP2-immunoreactive band of the expected ~125 kD size of ΔN-ASPP2 was only recognized by the C-terminal (a.a. 691-1128), but not the N-terminal (a.a. 50-150), epitope-specific antibody (Figure 2.3C, left panel verses right panel). Likewise, the ΔN-ASPP2 expression vector generated a protein with a similar epitope-specific pattern (Figure 2.3D).

Finally, adding additional support that ΔN-ASPP2 is naturally-occurring, in conjunction with our collaborators in Paul Spellman's lab we obtained data from an unbiased whole transcriptome sequencing (RNA-seq) database created from a panel of breast cancer cell lines and detected the presence of the 5'UTR sequence that is unique to ΔN-ASPP2 in some human tumor cell lines, including HCC202, DU4475, SUM159PT, and 21MT1 (Table 2.1).

We previously targeted exons 10-17 of the *Aspp2* allele in a mouse model (Kampa *et al.*, 2009a). Since this targeting construct is predicted to disrupt the transcription of both *Aspp2* and *ΔN-Aspp2* mRNA (Figure 2.1C), we examined *Aspp2*$^{+/exon10-17}$ mouse embryonic fibroblasts (MEFs) and found decreased mouse *ΔN-Aspp2* mRNA levels (Figure 2.3E, right panel) and decreased C-terminal mouse Aspp2-immunoreactive ~125 kD protein (Figure 2.3E, left panel) compared to *Aspp2*$^{+/+}$ MEFs. Together, these results confirm the existence of a new N-terminally truncated ASPP2 isoform.

Cell line	Subtype	ASPP2	ΔN-ASPP2
21MT1	Basal	+	+
MCF7	Luminal	+	--
AU565	Luminal	+	--
BT20	Basal	+	--
SUM159PT	Claudin low	+	+
HCC202	Luminal	+	+
DU4475	Basal	+	+
CAMA1	Luminal	+	--
SKBR3	Luminal	+	--
BT474AZ	Luminal	+	--
HCC2218	Luminal	+	--
UACC812	Luminal	+	--
SUM190PT	Luminal	+	--
T47D	Luminal	+	--
ZR75B	Luminal	+	--
LY2	Luminal	+	--
MCF12A	Non-malignant	+	--
MDA-MB-453	Luminal	+	--

Table 2.1 Summary of RNA-seq analysis of ASPP2 and ΔN-ASPP2 in a panel of breast tumor cell lines. (+) denotes the presence of the *ASPP2*-specific or *ΔN-ASPP2*-specific search query while (--) denotes no detection.

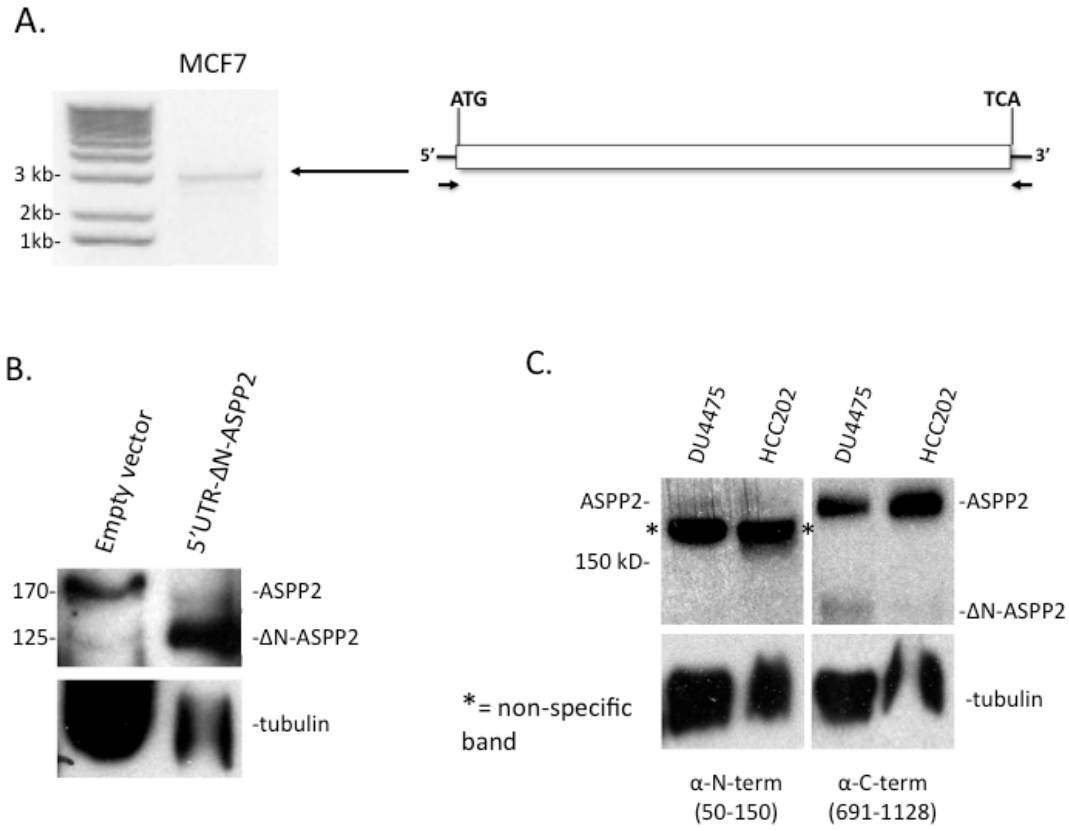

Figure 2.3. Endogenous ΔN-ASPP2 is expressed in cells. (A) *Left:* Agarose gel showing ΔN-ASPP2 cloning product generated from amplification of an MCF7 human cDNA library constructed from total RNA. *Right*: Schematic of the sequence amplified using the indicated 5'UTR-specific forward primer and 3'UTR-specific reverser primer. (B) Immunoblot of ectopically expressed full-length ΔN-ASPP2 clone and empty vector transfected lysate from H1299 cells. Lysates were probed with a C-terminally-derived ASPP2-immunoreactive antibody (ASPP2a from Sigma) (C) *Left panels:* Immunoblot epitope-mapping of lysates prepared from breast cancer cell lines and probed for endogenous ASPP2 and ΔN-ASPP2 with both a C-terminally-derived (*right panel*; ASPP2b antibody) and N-terminally-derived (*left panel*; ASPP2c antibody) ASPP2-immunoreactive antibodies were used at a concentration of 1:500.

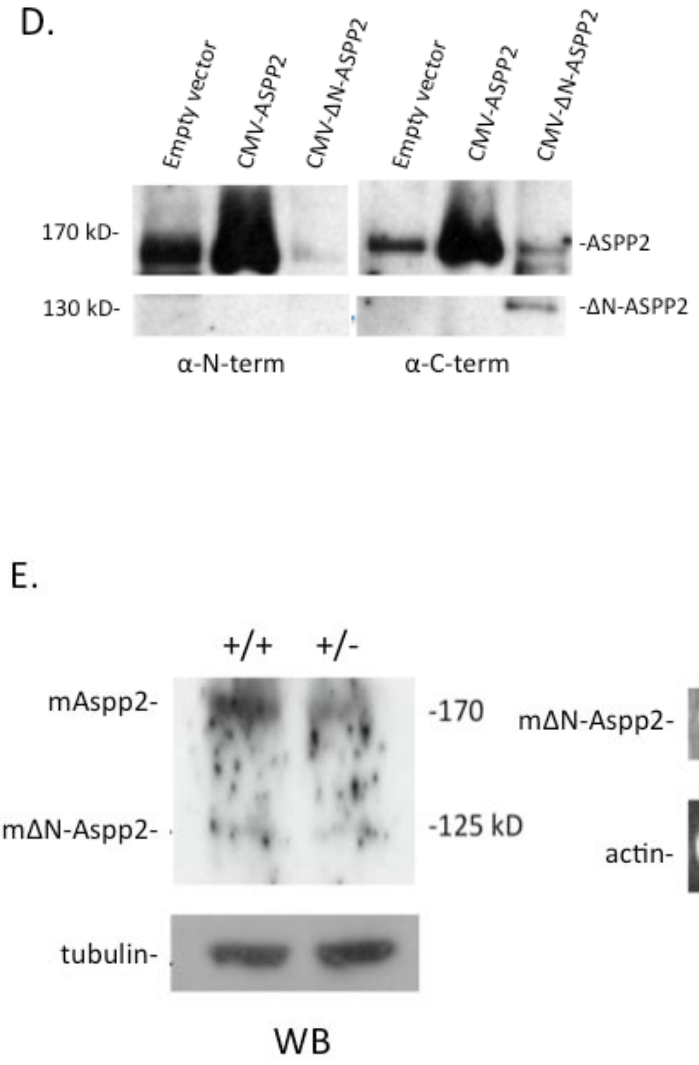

Figure 2.3. Endogenous ΔN-ASPP2 is expressed in cells. (D) Immunoblot epitope-mapping of ectopic ΔN-ASPP2, full-length ASPP2, or an equivalent concentration of empty vector control transfected into U2OS cells and probed with an N-terminally (*left*; ASPP2c) or C-terminally (*right*; ASPP2a) derived ASPP2 antibodies at a concentration of 1:500. The membrane was serially probed by quenching HRP signal with 3% hydrogen peroxide between antibodies. (E) *Left panel:* Immunoblot showing endogenous Aspp2 and ΔN-Aspp2 in wild type and *Aspp2*-heterozygous MEFs using a C-terminally-derived ASPP2 antibody (ASPP2d). *Right panel:* Semi-quantitative RT-PCR of *mΔN-Aspp2* and *mAspp2* transcripts in cDNA generated from *Aspp2*$^{+/+}$ and *Aspp2*$^{+/-}$ MEFs.

p53 transcriptional activation is inhibited by ΔN-ASPP2. Our discovery of the new N-terminally truncated ASPP2 isoform, ΔN-ASPP2 (Figs. 2.1 and 2.3), suggests that it may harbor unique function(s), since the N-terminally truncated ASPP2 splice isoform BBP has a reduced ability to enhance p53-mediated apoptosis, and the partial transcript 53BP2 (encoding an artificial N-terminally truncated protein) is dominant-negative against p53 and ASPP2 (Samuels-Lev *et al.*, 2001; Takahashi *et al.*, 2004). We therefore explored whether ΔN-ASPP2 could oppose p53 function by quantifying how its expression modulated exogenous p53 transactivation. Using a *p21*-luciferase reporter in the p53 null H1299 cell line (Figure 2.4) we found, as expected, that p53 alone stimulated the luciferase construct while ΔN-ASPP2 alone did not (Figure 2.4A). However, ΔN-ASPP2 inhibited p53 transactivation of the *p21*-luciferase reporter in a dose-dependent manner (Figure 2.4A). We next tested whether ΔN-ASPP2 could inhibit endogenous wild-type p53 transactivation function using a *p21*-luciferase reporter in the isogenic paired HCT116p53$^{+/+}$ and HCT116p53$^{-/-}$ cell lines (Bunz *et al.*, 1998). As expected, transfection of a *p21*-luciferase reporter into HCT116p53$^{+/+}$ cells resulted in a >5-fold increase in activity as compared to HCT116p53$^{-/-}$ cells (Figure 2.4B, third verses first column). Expression of ΔN-ASPP2 alone in HCT116p53$^{-/-}$ cells did not alter *p21*-luciferase reporter activity (Figure 2.4B, second versus first column). However when ΔN-ASPP2 was expressed in HCT116p53$^{+/+}$ cells, inhibition was also dose-dependent and there was a 50% reduction in p53 stimulation of the *p21* reporter (Figure 2.4B, fourth and fifth columns versus third).

To provide mechanistic insight into how ΔN-ASPP2 attenuates p53 transactivation, we performed quantitative chromatin immunoprecipitation (qChIP) of endogenous wild-type p53 using a U2OS osteosarcoma cell line with tetracycline-inducible FLAG-ASPP2 or FLAG-ΔN-ASPP2 (Figure 2.4C, boxed inset). As expected (Samuels-Lev *et al.*, 2001), cisplatin-induced cell damage combined with expression of full-length ASPP2 increased endogenous wild-type p53 protein >4-fold at the *Bax* promoter as compared to control (Figure 2.4C top panel). In contrast, expression of ΔN-ASPP2 did not increase endogenous wild-type p53 at the *Bax* promoter (Figure 2.4C, top panel). However, ΔN-ASPP2 expression reduced endogenous p53 occupancy at the *p21* promoter after cisplatin treatment (Figure 2C bottom panel) as compared to cells expressing full-length ASPP2 (Figure 2.4C bottom panel). Consistent with these results, we found that ΔN-ASPP2 expression inhibited doxorubicin-induced expression of endogenous *p21* mRNA by qRT-PCR in HCT116p53$^{+/+}$ cells (Figure 2.4D). Together, these results demonstrate that ΔN-ASPP2 and ASPP2 have opposing effects on p53 target gene activation and promoter occupancy.

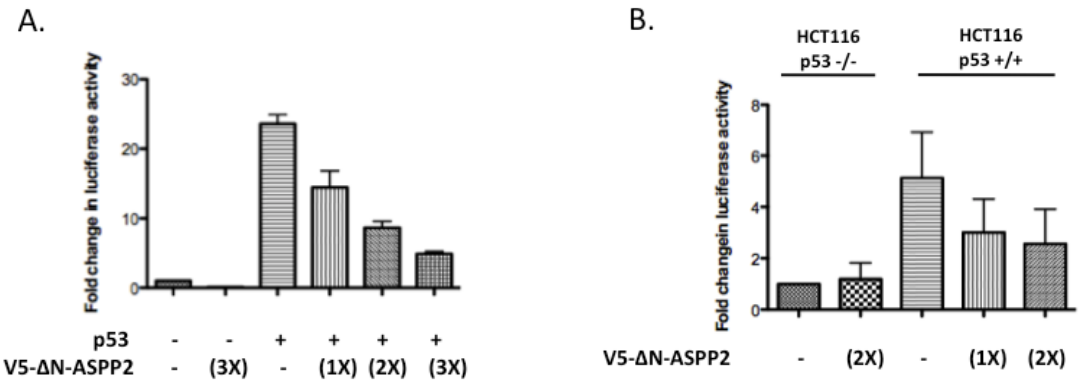

Figure 2.4. p53 transcriptional activation is inhibited by ΔN-ASPP2. (A) Luciferase activity on a *p21*-reporter in H1299 cells transfected with equivalent amounts of p53, ΔN-ASPP2, and/or empty vector along with β-galactosidase. Values were normalized to β-galactosidase activity and fold change is compared to *p21*-reporter alone. Error bars represent the standard error of the mean of 3 biological replicates. (B) Luciferase activity on a *p21*-reporter in the p53 wild type and null isogenic HCT116 cell lines transfected with increasing amounts of V5-ΔN-ASPP2. Values were normalized to β-galactosidase activity and fold change is compared to *p21*-reporter alone. Error bars represent the standard error of the mean of 3 biologic replicates.

C.

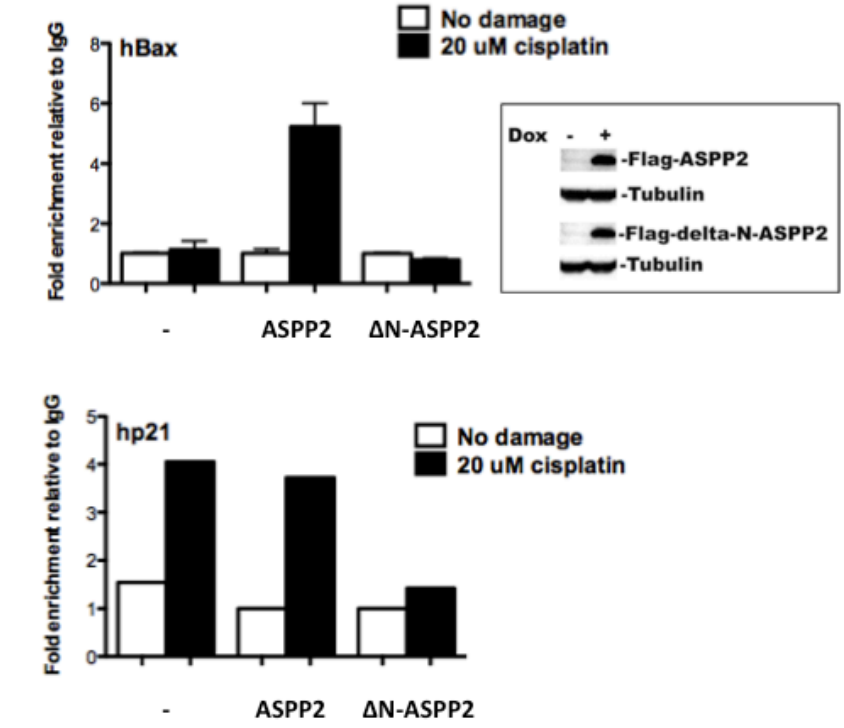

D.

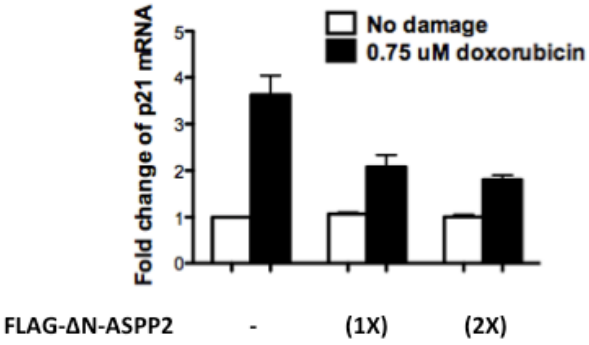

Figure 2.4. p53 transcriptional activation is inhibited by ΔN-ASPP2. (C) Chromatin immunoprecipitation for endogenous wild type p53 using lysates prepared from doxycycline induced or uninduced U2OS-tr-FLAG-ΔN-ASPP2 or tr-FLAG-ASPP2 following exposure to 20 μM cisplatin for 4 hours. Quantitative PCR showing *Bax* promoter binding (*upper*) and *p21* promoter binding (*lower*). Samples were normalized to % input and equivalently processed mouse immunoglobulin control IP. Error bars represent the standard error of the mean of 2 biologic replicates. (*Inset*) Immunoblot using equivalent amounts of lysate

prepared from U2OS tetracycline-responsive FLAG-ΔN-ASPP2 or FLAG-ASPP2 cell lines. (D) Quantification of *p21* mRNA in HCT116 p53 wild type cells after transfection with increasing amounts of FLAG-ΔN-ASPP2 and following damage with 0.75 μM doxorubicin for 4 hours. Values normalized to *GAPDH* and fold change relative to mock transfected samples with no damage.

ΔN-ASPP2 enhances cell proliferation and survival. To further explore our findings that ΔN-ASPP2 inhibits the p53 pathway and opposes ASPP2 function (Figure 2.4), we quantified cell proliferation in the conditionally expressing ΔN-ASPP2 and ASPP2 U2OS cell lines. Using a live cell imaging system (IncuCyte^{TM}) that measures cell confluence, we found an increase in cell confluence following induction of ΔN-ASPP2 as compared to un-induced cells when measured at 18 hours (Figure 2.5A, 29.0% verses 16.3% confluence). However, cells expressing full-length ASPP2 showed a reduced level of confluence versus un-induced cells (Figure 2.5A, 20.1% confluence verses 33.6%), indicating that while ASPP2 appears to suppress proliferation, ΔN-ASPP2 enhances it. Additionally, when cells conditionally expressing ΔN-ASPP2 were treated with cisplatin, we found they were more resistant to the growth-inhibitory effects of cisplatin than un-induced cells (Figure 2.5B, top panel). Conversely, we noted an increase in growth inhibition in cells expressing full-length ASPP2 at these doses and time points as compared to un-induced cells (Figure 2.5B, bottom panel), again suggesting that ASPP2 and ΔN-ASPP2 have opposing effects on proliferation.

Since expression of ASPP2 affects cell viability, we next asked what effect expression of ΔN-ASPP2 would have on cell viability. Using a colorimetric MTS assay we found that expressing ΔN-ASPP2 resulted in more viable cells after 24 hours as compared to un-induced cells (Figure 2.5C left panel, first and second columns), which is consistent with our finding that ΔN-ASPP2 promotes cell survival (Figure 2.5B). Additionally, when cells expressing ΔN-ASPP2 were

exposed to cisplatin for 24 hours, cell viability was not decreased at 5μM, and only a modest decrease was seen at 25 μM (Figure 2.5C, *left panel*, third versus second columns and fourth versus second columns). In stark contrast and as expected, expression of full-length ASPP2 showed a marked inhibition of cell viability alone and in combination with cisplatin (Figure 2.5C, *right panel*). Together these data demonstrate a novel biological function of ΔN-ASPP2 to promote cell proliferation and viability, which is in contrast to ASPP2 function (Lopez, 2000; Samuels-Lev *et al.*, 2001).

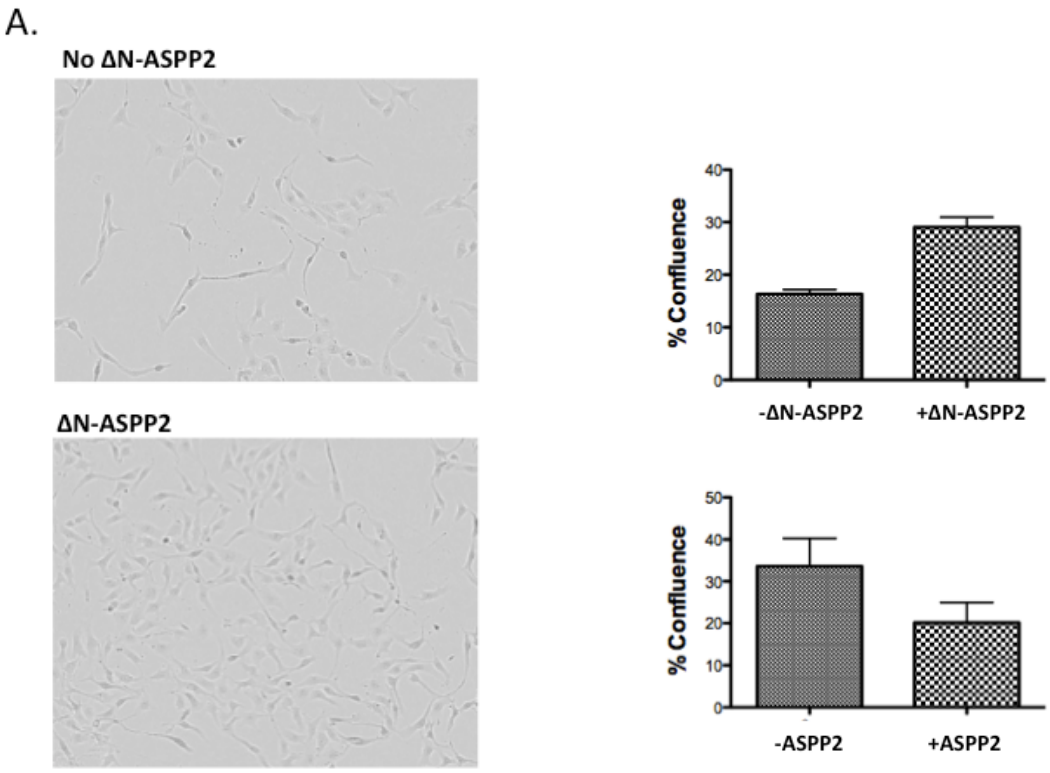

Figure 2.5. ΔN-ASPP2 enhances cell proliferation and survival. (A) *Left:* Representative pictures showing U2OS cell confluence with and without FLAG-ΔN-ASPP2 expression for 18 hours. *Right*: Histogram representing the percent confluence, as determined by Incucyte confluence algorithm, for U2OS cells with and without FLAG-ΔN-ASPP2 (*top)* or FLAG-ASPP2 expression (*bottom*) for 18 hours. Error bars represent the standard error of the mean of 3 biological replicates.

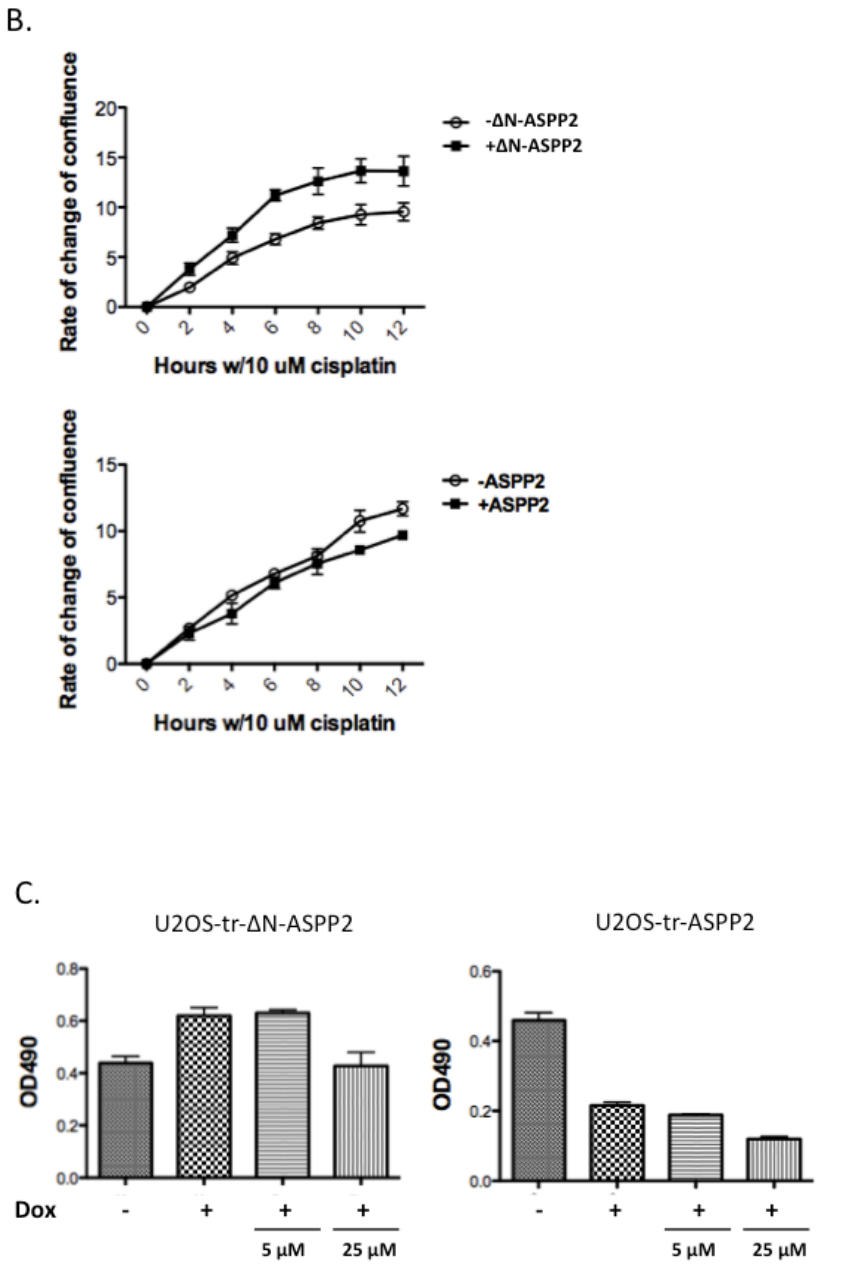

Figure 2.5. ΔN-ASPP2 enhances cell proliferation and survival. (B) Scatter plot showing the relative differences in the rate of confluence change for U2OS cells with or without FLAG-ΔN-ASPP2 expression (*top*) and with or without FLAG-ASPP2 expression (*bottom*) following exposure to 10 μM cisplatin for the indicated time points. (C) MTS viability assay for U2OS cells with or without FLAG-ΔN-ASPP2 expression (*left*) and with or without FLAG-ASPP2 expression (*right*) following exposure to cisplatin for 24 hours. Error bars represent the standard error of the mean of 3 biological replicates.

ΔN-ASPP2 inhibits damage-induced apoptosis. Since the ASPP2 N-terminus is important for full growth suppressive and pro-apoptotic functions including UV-induced apoptosis (Kampa *et al.*, 2009a; Samuels-Lev *et al.*, 2001), we reasoned that ΔN-ASPP2 would inhibit apoptosis and promote survival pathways after cell damage. To explore this, U2OS cells were transfected with either a FLAG-ΔN-ASPP2 expression vector or a control vector and irradiated with 40 J/m^2 UVC. Apoptotic cells were then quantified 18 hours later by Annexin-V staining and flow cytometry. We found that ΔN-ASPP2 significantly inhibited UV-induced apoptosis compared to control transfected cells (Figure 2.6A). These findings are in contrast to our prior findings that full length ASPP2 promotes UV-induced apoptosis (Lopez, 2000; Samuels-Lev *et al.*, 2001). Since ΔN-ASPP2 inhibited p53 transactivation of target genes (Figure 2.4), we determined whether ΔN-ASPP2 altered the induction of endogenous p53 after UV-irradiation. However, we observed equivalent induction of p53 with or without ΔN-ASPP2 after UV-irradiation (Figure 2.6B). Together, these results demonstrate that ΔN-ASPP2 inhibits damage-induced apoptosis without altering damaged-induced endogenous p53 levels.

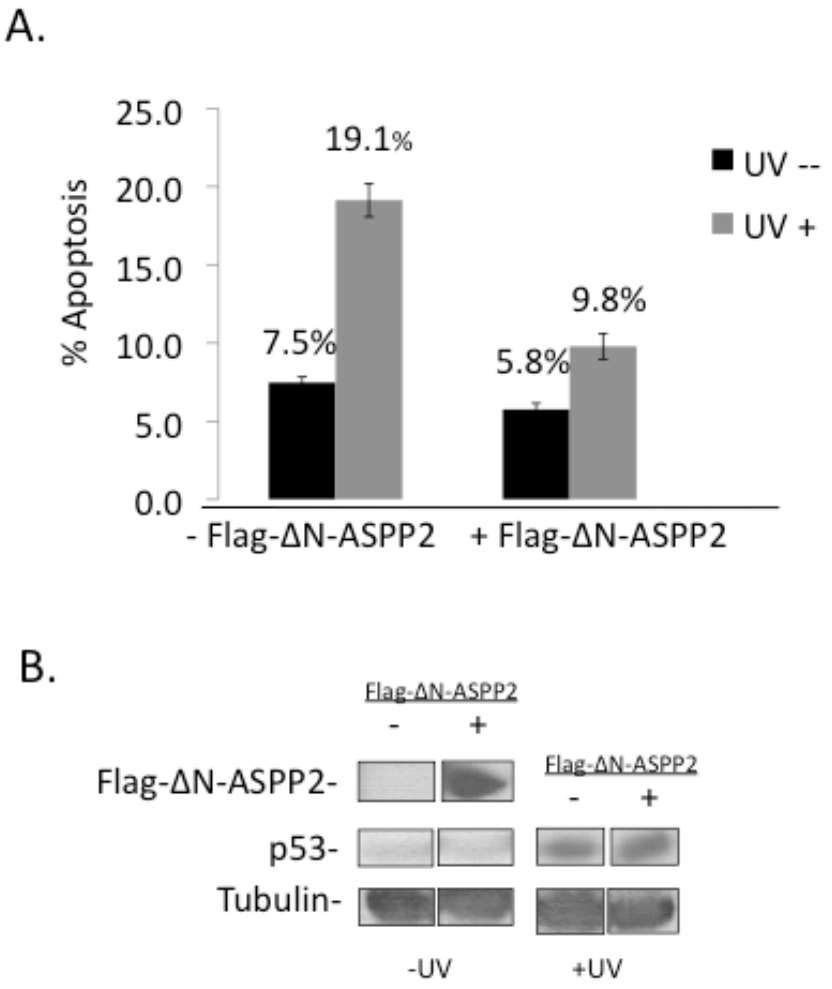

Figure 2.6. ΔN-ASPP2 inhibits UV damage-induced apoptosis. (A) Percent Annexin V positive cells (represented as % apoptosis) in U2OS cells transfected with equivalent amounts of empty vector or FLAG-ΔN-ASPP2 and following exposure (or not) to 40 J/m^2 UV for 24 hours. Cells were harvested and stained as described in *Methods* and analyzed by flow cytometry for Annexin V positivity. Error bars represent the standard error of the mean of 3 biological replicates. (B) Immunoblot using equivalent amounts of lysate prepared from U2OS cells showing FLAG-ΔN-ASPP2 and p53 expression before and after UV exposure described in (A).

ASPP2 is suppressed and ΔN-ASPP2 is overexpressed in breast tumors. Mouse models targeting Aspp2 reveal it can function as a tumor suppressor (Kampa *et al.*, 2009a; Vives, 2006) and numerous studies show that *ASPP2* mRNA levels are suppressed in human breast cancer and other tumor types (Lossos *et al.*, 2004; Meng, 2013; Samuels-Lev *et al.*, 2001; Sgroi, 1999). Since our data demonstrates that ΔN-ASPP2 promotes cell growth and cell survival (Figure 2.4 and 2.5), we asked whether ΔN-ASPP2 was aberrantly over-expressed in human cancer. We measured *ΔN-ASPP2* expression in matched breast tumor and adjacent normal breast tissue collected during mastectomies. Using 5'UTR-specific forward primers to specifically detect *ΔN-ASPP2* but not *ASPP2* we found that *ΔN-ASPP2* expression was elevated as compared to adjacent normal tissue (Figure 2.7A). Conversely, full-length *ASPP2* mRNA expression determined by an *ASPP2*-specific exon 1-2 junction probe, was suppressed in many of these breast cancer specimens when compared to matched normal tissue (Figure 2.7B), which is consistent with previous reports (Bergamaschi, 2003; Cobleigh *et al.*, 2005; Lossos *et al.*, 2002; Samuels-Lev *et al.*, 2001; Sgroi, 1999). Relative *ASPP2* and *ΔN-ASPP2* expression across normal tissues did not exhibit wide variation and so does not account for differences across tumors (*ΔN-ASPP2/GAPDH* mean=0.034 (0.019-0.054), std. dev.=0.011; *ASPP2/GAPDH* mean=0.812 (0.61-0.9), std. dev.=0.069). Coupled with our findings that ΔN-ASPP2 inhibits cell death and promotes cell proliferation (Figures 2.4-2.6), our finding that ΔN-ASPP2 is overexpressed in

human breast cancers suggests that ΔN-ASPP2 may play an important role in human tumorigenesis.

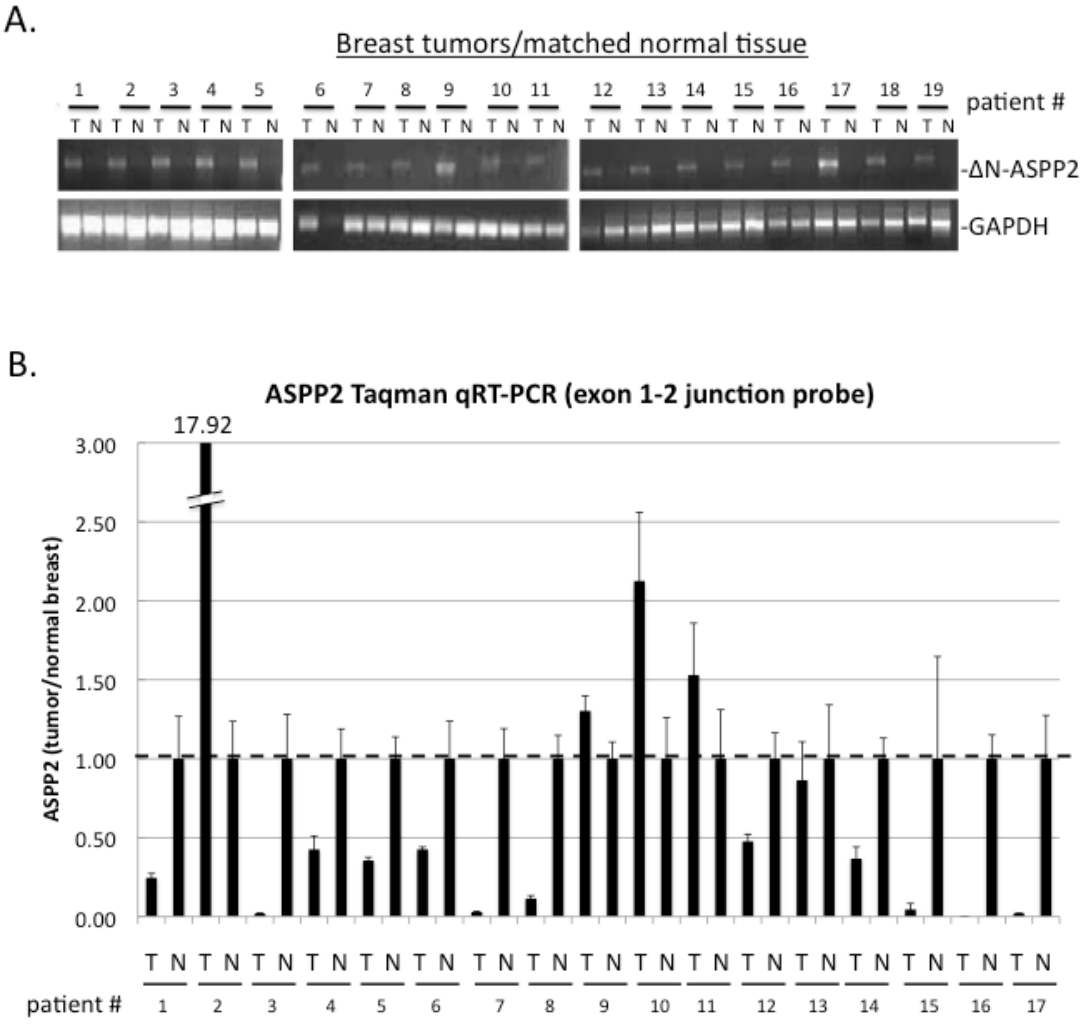

Figure 2.7. ASPP2 is suppressed and ΔN-ASPP2 is overexpressed in breast tumors. (A) Semi-quantitative RT-PCR of *ΔN-ASPP2* expression in breast tumor (T) and adjacent normal tissue (N) collected during mastectomies. (B) Quantitative RT-PCR of full-length *ASPP2* in breast tumor (T) and adjacent normal (N). *ΔN-ASPP2* and *ASPP2* expression in tumors is relative to matched normal tissue and normalized to *GAPDH*. Dotted line (ASPP2 data) set as reference to show fold change.

Discussion

Despite mouse models demonstrating that Aspp2 can function as a tumor suppressor (Kampa *et al.*, 2009a; Vives, 2006), the precise mechanisms of this important function remain unclear. Moreover, regulation of ASPP2 expression adds yet another level of complexity that must be considered when examining ASPP2 function(s). Our discovery of a new and potentially oncogenic ASPP2 isoform provides significant insight into understanding the complex regulation and function of ASPP2. Using multiple methodologies, we have demonstrated that a novel capped transcript, that we have named ΔN-ASPP2, is generated from the *TP53BP2* locus from an alternative transcription start site (Figure 2.1A) and that it is not a splice isoform of previously described transcripts (Figure 2.2; Takahashi *et al.,* 2004. Moreover, *ΔN-ASPP2* mRNA and protein expression can be detected in both human and mouse tissues (Figure 2.3B, C and E), although the precise tissue types and/or differences in developmental expression remain to be explored.

Our data suggest that ΔN-ASPP2 antagonizes the growth-inhibitory functions of ASPP2 and promotes cell survival (Figures 2.5 and 2.6). This is consistent with prior reports demonstrating that N-terminally truncated isoforms of ASPP2 have reduced growth-inhibitory and pro-apoptotic functions (Samuels-Lev *et al.*, 2001). Indeed, our results also lead us to speculate that ΔN-ASPP2 might harbor dominant-negative function against the ASPP2-p53 pathway as has been demonstrated by the partial clone 53BP2 encoding an N-terminally truncated protein (Samuels-Lev *et al.*, 2001). The existence of the ΔN-ASPP2

isoform might contribute to observed differences reported between *Aspp2* targeted mouse models (Kampa *et al.*, 2009a; Vives, 2006). Both targeting strategies demonstrate that *Aspp2* is a haplo-insufficient tumor suppressor (Kampa *et al.*, 2009a; Vives, 2006). However exon 3-targeted mice (*Aspp2*$^{\Delta exon3/\Delta exon3}$) die shortly after birth, while exon 10-17 targeted mice (*Aspp2*$^{\Delta exon10\text{-}17/\Delta exon10\text{-}17}$) are not detected even as early as embryonic day 6.5. This developmental variation suggests that there are distinct differences created by the different targeting strategies. Our results demonstrating that ΔN-Aspp2 is generated from a downstream TSS (Figure 2.1C) suggest that the *Aspp2*$^{+/\Delta exon10\text{-}17}$ targeting strategy disrupts the coding sequence for both full-length Aspp2 and ΔN-Aspp2. The *Aspp2*$^{+/\Delta exon3}$ targeting strategy (Vives, 2006) however would be predicted to not disrupt the coding sequence for ΔN-Aspp2. Consistent with this notion, *Aspp2*$^{\Delta exon3/\Delta exon3}$ MEFs continue to express the Bbp/53BP2S splice isoform (Wang Y., 2013) generated by exon 3 splicing (Takahashi *et al.*, 2004) or exon 2/3 splicing (Figure 2.2A).

In addition to these developmental differences, *Aspp2*$^{+/\Delta exon3}$*;p53*$^{+/-}$ mice genetically cooperate with p53 as evidenced by accelerated tumor formation in a p53 haplo-insufficient background (Vives, 2006). In contrast, *Aspp2*$^{+/\Delta exon10\text{-}17}$*;p53*$^{+/-}$ mice do not cooperate with p53 to accelerate tumors(Kampa *et al.*, 2009a). Our data suggesting that ΔN-ASPP2 antagonizes ASPP2-p53 function is consistent with this observation. If *Aspp2*$^{+/\Delta exon3}$ mice leave ΔN-Aspp2 intact, its dominant-negative activity could further inhibit p53 to accelerate tumors in a *p53*$^{+/-}$ context. However targeting both *Aspp2* and *ΔN-Aspp2* in *Aspp2*$^{+/\Delta exon10\text{-}17}$

mice would attenuate ΔN-Aspp2 dominant-negative function, and thus mask genetic cooperation between Aspp2 and p53--resulting in no accelerated tumors in a $p53^{+/-}$ context. Additionally, mounting evidence suggests an important role for Aspp2 in development and cell polarity *in vivo* (Cong, 2010; Kampa et al., 2009a; Sottocornola et al., 2010; Vives, 2006). Given the severe developmental defects of $Aspp2^{\Delta exon10\text{-}17/\Delta exon10\text{-}17}$ embryos, our findings emphasize the need for clearer understanding of the temporal and tissue-specific regulation of ASPP2 and all of the known isoforms, including ΔN-ASPP2.

Characterization of the ASPP family of proteins has added to our understanding of p53 regulation and function and here we gain interesting insight into how ΔN-ASPP2 may contribute. Our findings that ΔN-ASPP2 can promote cell proliferation (Figure 2.5A), inhibit the growth suppressive effects of cisplatin (Figure 2.5B, 2.5C) and inhibit UV-induced apoptosis (Figure 2.6), are in direct contrast to known ASPP2 functions (Lopez, 2000; Samuels-Lev *et al.*, 2001) and underscores the added complexities which control the ASPP2-p53 pathway. Although the exact mechanisms of how ASPP2 and ΔN-ASPP2 regulate p53 remain unclear, ASPP2 promotes apoptosis in part through its ability to enhance p53 transactivation—making it tempting to speculate that the pro-survival functions of ΔN-ASPP2 might be in part due to inhibiting p53 transcription (Samuels-Lev *et al.*, 2001; Wang Y., 2013) Indeed, we found that ΔN-ASPP2 can inhibit endogenous p53 transactivation of a *p21*-luciferase reporter (Figure 2.4A) as well as inhibit damage-induced activation of the endogenous p53 target gene p21 (Figure 2.4D). Importantly, we confirmed that ΔN-ASPP2 could directly

inhibit endogenous p53 promoter occupancy on the endogenous p53 targets *p21* and *Bax* in response to cell damage. Intriguingly, full-length ASPP2 has been reported to promote p53 transactivation preferentially on pro-apoptotic targets genes (Samuels-Lev *et al.*, 2001). Our discovery that ΔN-ASPP2 can inhibit p53 transactivation on both pro-apoptotic and cell cycle arrest target genes, suggests that ΔN-ASPP2 may be functioning as a more non-selective dominant-negative against p53 transactivation.

It remains to be mechanistically determined how ΔN-ASPP2 modulates p53 occupancy on target gene promoters. However, ASPP2 is well known for its ability to directly bind p53 (Gorina and Pavletich, 1996; Iwabuchi *et al.*, 1994) and the structural identity between ASPP2 and ΔN-ASPP2 at the C-terminal p53 binding domain predicts that ΔN-ASPP2 may also bind p53. Thus, it is tempting to speculate that ΔN-ASPP2 inhibits p53 function by direct interaction to prevent it from binding to p53 target gene promoters. Alternatively, ΔN-ASPP2 may compete with ASPP2 (or ASPP1) for p53 binding and thus inhibit ASPP2/1 stimulation of p53 transactivation (Samuels-Lev *et al.*, 2001). Interestingly, ASPP2 is hypothesized to participate in an intermolecular interaction via its proline rich region and SH3-domains (Rotem *et al.*, 2008; Rotem-Bamberger, 2013), both of which are conserved in ΔN-ASPP2. Thus it is also possible that ΔN-ASPP2 may directly bind and inhibit full-length ASPP2 function. It remains formally possible that ΔN-ASPP2 could bind other co-factors that may ultimately indirectly inhibit p53 function. The extent to which different cellular contexts (e.g. cell damage) can affect the mechanism(s) that influence ΔN-ASPP2 function also

remains unclear. Nevertheless, our findings open the door for further study of these complex regulatory networks controlled by ΔN-ASPP2 and ASPP2.

Prior studies show that ASPP2 expression is suppressed in breast cancer when compared to adjacent normal tissue (Cobleigh *et al.*, 2005; Samuels-Lev *et al.*, 2001; Sgroi, 1999). While informative, these studies were limited by their inability to distinguish full-length *ASPP2* expression from that of the *BBP* or *ΔN-ASPP2* transcripts. We analyzed a series of breast cancer patient samples and matched normal tissue and similarly found decreased full-length *ASPP2* expression using *ASPP2*-specific qPCR, enabling us to specifically show a reduction in *ASPP2* expression in tumor tissue for the first time (Figure 2.7B). Conversely, we found that *ΔN-ASPP2* was overexpressed in these same breast cancer samples as compared to adjacent normal tissue (Figure 2.7A). These findings, taken together with evidence that ΔN-ASPP2 negatively regulates p53 transactivation, promotes cell proliferation, inhibits damage-induced growth suppression and apoptosis, provide an intriguing hypothesis that aberrant ΔN-ASPP2 expression might promote tumor development and/or resistance to therapy. However, transgenic mouse models will be required to definitively confirm the oncogenic potential of ΔN-Aspp2 *in vivo*.

Our discovery of a new isoform of ASPP2 is significant because it sheds new light on both prior and ongoing ASPP2 studies. Here we have interrogated the function of ΔN-ASPP2 relative to known p53 mediated pathways. However, mounting evidence demonstrates important p53-independent ASPP2 functions beyond cell survival and apoptosis (Cong, 2010; Wang, 2013; Wang, 2012a;

Wang, 2012b) and, based on our data presented in this chapter, it is likely that ΔN-ASPP2 will play an important role in these pathways as well. Although the precise mechanisms and functions of ΔN-ASPP2 remain to be elucidated, our findings that ΔN-ASPP2 is overexpressed in human cancers, promotes resistance to cell damage and enhances cell survival, makes it a potential target to be exploited for cancer therapy.

Chapter Three:

TP53BP2 is a c-MYC Target Gene that Mediates c-MYC-induced Apoptosis

Abstract

Apoptosis-Stimulating Protein of p53 2 (ASPP2 aka 53BP2L) is a pro-apoptotic tumor suppressor that is downregulated in many types of cancer. Transcription of *TP53BP2* is controlled by the activating members of the E2F family of transcription factors, but little else is known about the upstream pathways or cellular contexts that regulate ASPP2 expression. C-MYC is a well-studied oncogenic transcription factor with the ability to promote cellular proliferation, while also engaging apoptotic targets to protect cells against cell cycle deregulation. This process is known to occur through both p53-dependent and independent mechanisms, but the exact mechanisms of how MYC induces apoptosis remain unclear. Here we show that *TP53BP2* is a direct MYC target gene with the ability to mediate the apoptotic function of MYC. The *TP53BP2* promoter was found to contain several MYC binding sites, and both *ASPP2*-luciferase reporter and endogenous ASPP2 expression were enhanced upon MYC expression. Moreover, MYC was found to bind a MYC-specific regulatory element in the *TP53BP2* promoter suggesting direct transcriptional regulation. Interestingly, attenuation of ASPP2 expression inhibited MYC-induced apoptotic cell death in response to low serum. These results identify *TP53BP2* as a transcriptional target of MYC and suggest a role for ASPP2 as a novel downstream mediator of MYC function.

Introduction

Apoptosis-stimulating protein of p53 2 (ASPP2) is a pro-apoptotic protein that has been shown to enhance the ability of the tumor suppressor p53 to initiate apoptosis (Samuels-Lev *et al.*, 2001). Additionally, ASPP2 interacts with and affects the function of several other apoptotic proteins, such as BCL-2 and NF-κB (Naumovski and Cleary, 1996; Takahashi *et al.*, 2005). Studies of animal models have demonstrated that targeted deletion of the *Aspp2* gene leads to an increase in both spontaneous and irradiation-induced tumor formation as well as apoptotic defects in response to γ-irradiation, strongly suggesting that Aspp2 is a tumor suppressor (Kampa *et al.*, 2009a; Vives, 2006). This is further supported by studies showing reduced levels of *ASPP2* mRNA in a variety of cancer types including breast cancer, non-Hodgkin's lymphoma, and non-small cell lung cancer (Li, 2012; Lossos *et al.*, 2002; Samuels-Lev *et al.*, 2001; Sgroi, 1999). Although mutations in the human ASPP2 gene, *TP53BP2I,* are rare, it is subject to epigenetic silencing in a variety of tumor types (Liu, 2005; Sarraf and Stancheva, 2004); therefore highlighting the importance of a clearer understanding of the upstream pathways responsible for its expression. We have previously shown that *TP53BP2* is transcriptionally regulated by the activating members of the E2F family of transcription factors (Chen, 2005). This finding is significant because it provides information on the cellular pathways used by these known oncogenes to also sensitize cells to apoptotic stimuli. Despite these

findings, little else is know about the upstream pathways leading to ASPP2 expression or the role it plays in promoting apoptosis.

Like E2F, MYC is a transcription factor that plays a crucial role in cellular processes such as proliferation, differentiation, and apoptosis (Dang, 2012). As a transcriptional activator MYC functions by binding E-box regulatory elements (CACGTG) within target gene promoters to promote transcription (Blackwell, 1990). While MYC is known to also transcriptionally suppress certain genes this process is not believed to require E-box regulatory elements (Cowling, 2006). Tight regulation normally keeps MYC levels low in quiescent cells, but approximately 70% of human tumors have elevated levels of MYC, suggesting that deregulation of MYC expression is an important step in cellular transformation (Dang, 2012). Interestingly, overexpression of MYC is also known to activate several apoptotic pathways as a means of protection against the proliferative advantage afforded these cells (Evan, 1992; Juin, 2002; Zindy *et al.*, 1998). It is not surprising then that mutations that deactivate these protective pathways are the most common cooperating mutations in tumors with deregulated MYC (Nilsson, 2003). Understanding how cells with oncogenic potential, such as those that overexpress MYC, circumvent this apoptotic pathway, and specifically the downstream pathways involved in this process, will have valuable therapeutic consequences.

Here we describe a role for ASPP2 in MYC-mediated apoptosis by placing it downstream of MYC transactivation. We demonstrate that MYC can stimulate an *ASPP2*-luciferase reporter construct and upregulate both ASPP2 protein and

mRNA. Moreover, we show that MYC regulation of ASPP2 expression is likely direct by demonstrating an enrichment of MYC at E-box regulatory elements within the *TP53BP2* promoter using chromatin immunoprecipitation. We further functionally validate these findings by demonstrating that attenuation of ASPP2 expression inhibits MYC-mediated apoptosis. Intriguingly, we show that attenuated Aspp2 expression does not accelerate lymphomagenesis in a MYC-driven tumor model, suggesting complex regulation of MYC-induced apoptosis *in vivo*. Together these results define *TP53BP2* as a MYC target gene and ASPP2 as a downstream mediator of MYC-induced apoptosis.

Results

The *TP53BP2* promoter has features of a MYC target gene and is responsive to MYC transactivation. We have previously demonstrated that the ASPP2 gene, *TP53BP2*, is controlled by the activating E2F proteins (E2F1-3), thus implicating ASPP2 in oncogene-mediated sensitization to apoptosis (Chen, 2005; Dynlacht, 2005; Fogal *et al.*, 2005; Hershko *et al.*, 2005). We noted, however, that while mutation of single E2F binding sites can cause de-repression of an *TP53BP2* promoter-luciferase construct, mutation of all four known E2F binding sites in this reporter does not fully abolish promoter transactivation in response to serum. These results indicate that non-E2F-mediated pathways are also likely regulating ASPP2 expression. Like E2F, the oncogenic transcription factor MYC has been shown to promote proliferation together with apoptosis, leading us to hypothesize that it may control *TP53BP2* as well. Examination of the previously defined promoter region of *TP53BP2* (Chen, 2005) reveals one canonical and three non-canonical MYC binding sites (E-boxes), lending support to our prediction that *TP53BP2* is directly regulated by MYC (Figure 3.1A and B).

In order to address the extent to which MYC can promote transactivation of *TP53BP2* we transfected increasing amounts of V5-tagged MYC (V5-MYC) into U2OS osteosarcoma cells in combination with either an *E2F2*-luciferase reporter (as a positive control) or an *ASPP2*-luciferase reporter containing all four putative MYC binding sites (-1530→+276; Figure 3.1B). Twelve hours after transfection, cells were starved in medium containing 0.2% serum for 30 hours,

to decrease influence from other serum-stimulated transcription factors, before assaying for luciferase activity. As expected, MYC enhanced luciferase activation of its known target, *E2F2*. Additionally, MYC expression also enhanced expression of the *ASPP2*-luciferase reporter in a dose dependent manner (Figure 3.1C). To further narrow the focus of luciferase activation of *TP53BP2* to MYC activity, we used a human embryonic kidney cell line, 293T, that was engineered to stably express tetracycline-inducible HA-tagged MYC (293T-tr-HA-MYC; Figure 3.1D). Cells were transfected with either an *ASPP2*-luciferase reporter containing the four putative E-boxes (-1530→+276) or a reporter with a gross deletion that removes three of the four predicted MYC binding motifs (-1080→+276). Again, induction of HA-MYC expression promoted enhanced luciferase activity as compared to uninduced samples on the full *ASPP2* reporter (Figure 3.1E). Conversely, the E-box-deficient *ASPP2*-luciferase reporter was not stimulated to the same magnitude under these same conditions (Figure 3.1E). Moreover, the higher baseline luciferase activity seen with the deletion reporter is likely a result of the de-repression seen after the removal of other repressive elements in the gross deletion (Li, 1994). Taken together these data suggest that the *TP53BP2* promoter is regulated by MYC through E-box regulatory elements.

A.

-1560 AATTCTTTTTTTTTTTTTTCAGATGGAGTTTCACTCTCGTTGCCCAGGCTGAAGTGCAGTG
-1500 GGGTGATCTCTGCTCATTGCAACCTCCGCTTCCCAGGTTCAAGAGATTCTCCTGCCTCAG
-1440 CCTCCCGAGTAGCTGGCATTACAGGCATGCGCCACCATGCCCGGCTAATTTTTATATTTT
-1380 TAGTAGAGACAAGGGTTTCACCACGTGGCCAGGCTGGTCTCGAACTCCTGACCTCAGGTG
-1320 ATCTGCCCGCCTCGGCCTCCCAAAGTGCTGGGATTACAGGCGTGAGCCACTGCGCCCGGG
-1260 CGAGAACGTTAAATTCTAGTTGAATTAACCGTAATTTAGTATTTCCAGATACAGTATCTG
-1200 GGATGGTGCAATAGGGAGTTCGATGGAGATTCTGGTAAGGGATATGGTGGGCTAAGAAAG
-1140 AATTGTCTGTTCTTGATACTAGATAAACCCAGGGGATTTACCCCACTTCAGGTTCTAGAA
-1080 TCATGTATAAAGGCAGAGAAAAGTGATTCTGAGTGAACTTGCACTGACAACTTACTAGAA
-1020 CAAAGCTTCCTGGAGTTAGGGTTCCCGCAGTATGTGTCTCTCTGGAAGGTGGAATAAAAG
-960 CCTGAACCCGCTCTGCTACTCTTTGGAAGGCAGCCCTGCCATTTCCCTAGGCCTTGGCCT
-900 CCCTCCCTGGAAAAGGATGGTATCCACCGGCTCCCCGTATCGGAGGCTGTTTGCAGGGTG
-840 TTCCCAGCACCCCCCAGGGAAGCTCCTCAGAATGCTGCCTGACACATTTTTACAAAATTT
-780 ATTTTTATTGTGGTAAAACATACACAACATAAAAGTTATCCCTTTATCCAGTTTGCGGTG
-720 TACGTTTGTTAACCTTACAGCAAGTAACACATGAGTTTTAAATTAGAATTTGGACAACGG
-660 CAAATGAGATGAAAGGCGAACAATCCGAAAGCCGGATCACTGAGGAGCTCTGGGAACGCG
-600 CCGCGAGCTGAAGCCACACGGGGAACTCCATTTTGTCGGGACAGGGTCGGTCCTGGCCGC
-540 CTCCAGGGAGTCGGGTAGTTTCCGCGGCGTGGCCCGGGCCTCCCCTGAAGTCCGTCCGCC
-480 TCTCTCCGCCTGGCCCAGCGGCGCGGCCGCCGGAGGACTCTGTCCACGCGCCCAACGTCG
-420 GGCGCCCTGTTCTGAAGGCAAAGGGTCCCCTGCCTCGCACGACTCGGAGCCGCCGAGGAG
-360 GTGACGGCGGCAGCCCTGGGGCGGCTCGGTGCCATTCACTACCATCCTGTTTTCCTGAGG
-300 CGCGGCCTTCCAATTGCCCCGGCTCCGCTAGGAGGCGCGCGCTCCAGCCGCTCCGCCGCG
-240 CGGCCCCGACCGCACTTCAGTCCGGGGCGAAGAAAGAAAAGGCGGCCGGCTCCCGCCGCT
-180 CCCCGTCTACCCAGCCGGGCCCGCGCAGGCGCGCGCAGCTCCCGTTCCCGCGGCCGCCCC
-120 TCCCCCAGGCCGCCGGGCGCGCCGCGGGCGGGGTCGGCGCGGGGGGCGGAGCCGGCACGG
-60 GCTCGGCTGGGGCCCGACCCGGGATTAGTTGGTTTCGGAGCGGAGGAGGGAGCCCCGACC
+1 GTCACGAGCGTCGAAGAGACAAAGCCGCGTCAGGGGGCCCGGCCGGGGCGGGGGAGCCCG
+61 GGGCTTGTTGGTGCCCCAGCCCGCGCGGAGGGCCCTTCGGACCCGCGCGCCGCCGCTGCC
+121 GCCGCCGCCGCCTCGCAACAGGTCCGGGCGGCCTCGCTCTCCGCTCCCCTCCCCCGCATC
+181 CGCGACCCTCCGGGGCACCTCAGCTCGGCCGGGGCCGCAGTCTGGCCACCCGCTTCCATG
+241 CGGTTCGGGTCCAAGATGATGCCGGTAAGTGGGCGAGCGGCCAGGGCGTCGGGCCCGGAA
+301 GTGTGCGGGGTCGCGTGCCGGGGGCTGGTCCGCGCCCTCGGGCGCGTCGGGGAAGGAGCC
+361 TGGGGGCCGCAGCCCGCGCGGAGGGGCCGGGGCTTTCCGAGCTTCGAGCGGGTTTCAGGA
+421 AGGGGAGGCTCCATCCTCTGGGCTCTGCGCCCACAGCCGTCGTGGGGGCGCGGCGAGACC
+481 CTAACCTCGAGGCGGGTTCCTCCAGCTGCTCCGGAGTCAGGCGAGCCGCCCGCGAGCCCA
+541 GCAGCCACTCAAACTTTTCGTCTTTCACTGGGTCTTGACTTTTTTGCAGTTCTTGAAGGT

Figure 3.1. *TP53BP2* has features of a MYC target gene and MYC enhances transactivation of an *ASPP2*-luciferase reporter. (A) Genomic sequence directly upstream of the *TP53BP2* gene. Canonical MYC binding site is shown in red, non-canonical MYC binding sites are shown in pink, and E2F binding sites are shown in blue. Exon 1 is shown in green.

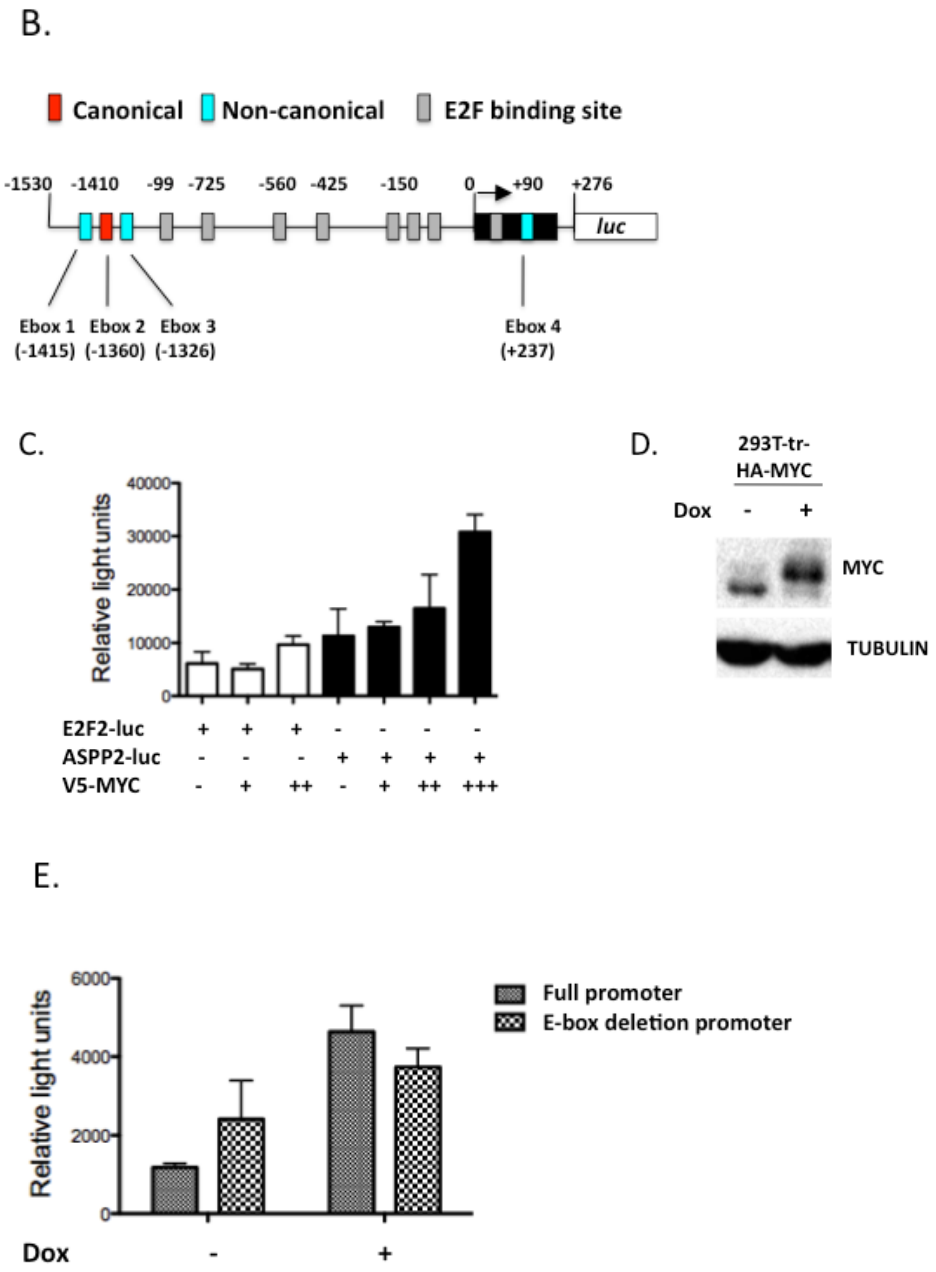

Figure 3.1. *TP53BP2* has features of a MYC target gene and MYC enhances transactivation of an *ASPP2*-luciferase reporter. (B) Diagram of the *ASPP2*-luciferase construct used and the locations of putative MYC binding sites. (C) Luciferase activity of the *E2F2* and *ASPP2*-reporter constructs in U2OS cells following transfection with V5-MYC and normalization to β-galactosidase activity. Cells were transfected with reporter constructs, V5-MYC, equivalent amounts of empty vector, and β-galactosidase. ~12 hours later medium was changed to 0.2% serum for 30 hours. Cells were then harvested and assayed for luciferase

and β-galactosidase activity as described in *Methods*. (D) Immunoblot showing expression of HA-MYC in 293T-tr-HA-MYC cells after induction with doxycycline for 4 hours. Y69 MYC antibody was used at a dilution of 1:1000. (E) Luciferase activity from 293T-tr-HA-MYC cells starved in 0.2% serum medium for 30 hours with and without induction of Myc for 12 hours by doxycycline (1 μg/mL) on the *ASPP2*-reporter construct (-1530→+276) and an E-box deletion mutant *ASPP2*-reporter (-1080→+276).

MYC promotes expression of endogenous ASPP2. Given that MYC stimulates an *ASPP2*-luciferase reporter, we asked whether MYC would stimulate endogenous ASPP2 expression. To test this we again utilized the 293T-tr-HA-MYC cell line. Because both ASPP2 and MYC are serum responsive proteins (Blanchard, 1985; Chen, 2005), cells were starved for 24 hours prior to MYC induction and maintained in starvation media throughout the experiment to decrease endogenous background levels of both ASPP2 and MYC. Induction of MYC led to an increase in both ASPP2 protein (Figure 3.2A) and mRNA (Figure 3.2B), suggesting that the endogenous *TP53BP2* promoter is MYC responsive.

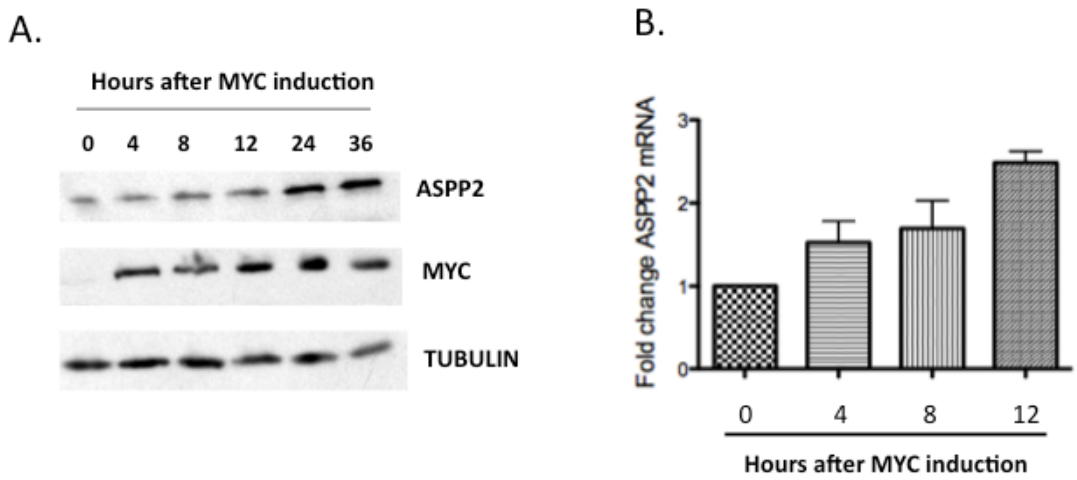

Figure 3.2. MYC induces expression of endogenous ASPP2. (A) Immunoblot from 293T-tr-HA-MYC cells showing changes in ASPP2 protein levels following 24 hours of starvation in 0.2% serum and after induction of MYC for the indicated periods of time. ASPP2a antibody was used at a concentration of 1:1000. (B) Quantitative RT-PCR showing changes in *ASPP2* mRNA under the same conditions as in (A). Error bars represent the standard error of the mean of 2 biological replicates.

MYC directly binds an E-box-containing *TP53BP2* promoter region. We have shown that *TP53BP2* is an E2F(1-3) target (Chen, 2005) and it has been previously shown that the activating E2Fs are direct targets of MYC transcription (Fernandez *et al.*, 2003; Leone *et al.*, 2001; Sears *et al.*, 1997) making it possible that ASPP2 response to MYC expression is indirect. However, given that the *TP53BP2* promoter contains putative MYC binding sites (Figure 3.1A) and is responsive to MYC in a luciferase reporter assay (Figure 3.2) we wanted to test the ability of MYC to bind directly to the *TP53BP2* promoter in its native chromatin state. To do this we transfected H1299 cells with V5-MYC and assessed the amount of E-box-containing *TP53BP2* promoter bound to MYC following chromatin immunoprecipitation (ChIP) with a V5-antibody. The region of the *TP53BP2* promoter containing the canonical E-box was enriched in samples where V5-MYC is being expressed and immunoprecipitated but not in samples that contain mouse IgG as a non-specific control antibody (Figure 3.3A). This enrichment is specific because control primers designed 3 kb upstream of the *TP53BP2* promoter do not display the same binding pattern (Figure 3.3A). To further illustrate the ability of MYC to bind the *TP53BP2* promoter we performed a ChIP with 293T-tr-HA-MYC cells and assessed the binding quantitatively. We found a greater than 15-fold enrichment of MYC binding to the *TP53BP2* promoter as compared to uninduced samples (Figure 3.3B). Importantly, the known MYC target *rDNA* (Gomez-Roman, 2003) showed enrichment upon MYC induction as well, while again the control region did not (Figure 3.3B). We further demonstrated that endogenous MYC bound to the *TP53BP2* promoter after

performing ChIP with a MYC antibody in H1299 cells (Figure 3.3C). Together these data provide evidence that MYC binds directly to the *TP53BP2* promoter through predicted E-box regulatory elements.

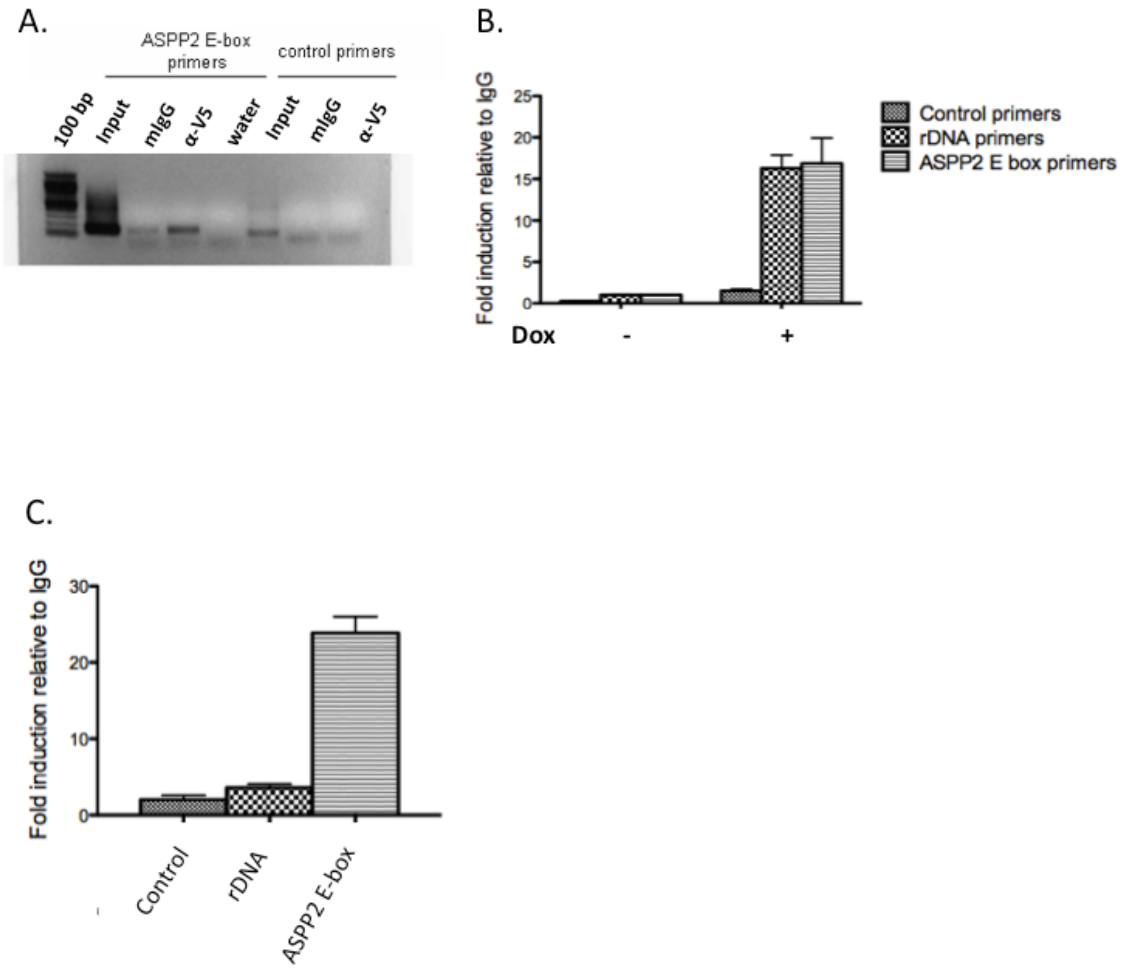

Figure 3.3. *TP53BP2* is a direct MYC target. (A) Chromatin immunoprecipitation showing enrichment of an E-box-containing region of the *TP53BP2* promoter bound to MYC following immunoprecipitation with an α-V5 or an equivalent amount of α-mouse IgG antibody in H1299 cells transfected with V5-MYC. Control primers in a non-specific upstream location do not show enrichment. Water lane is a PCR control (B) Quantitative ChIP from 293T-tr-HA-MYC cells showing changes in MYC binding to both the *TP53BP2* and *rRNA* promoters following MYC induction for 8 hours and IP. Enrichment of the control promoter region is not seen. Values are normalized to % input and non-specific α-mouse IgG IP. Error bars represent technical replicates. (C) Quantitative ChIP from H1299 cells demonstrating binding of endogenous MYC to the *rDNA* and *TP53BP2* promoter but not an upstream control region. Values are normalized to % input and non-specific mouse IgG IP. Error bars represent technical replicates.

Loss of ASPP2 inhibits MYC-induced apoptosis. Since ASPP2 inhibits cell growth and promotes apoptosis (Lopez, 2000; Samuels-Lev *et al.*, 2001) and MYC binds directly to the *TP53BP2* promoter (Figure 3.3) and induces its expression (Figure 3.2), we reasoned that ASPP2 may play a role downstream of MYC to help promote apoptosis. To test whether attenuation of ASPP2 expression can limit MYC-induced apoptosis, 293T-tr-HA-MYC inducible cells were first transfected with either scrambled siRNA or *ASPP2*-specific siRNA. Since studies have shown that MYC expression in low serum conditions can trigger cell death (Evan, 1992), media was changed twenty-four hours after transfection to 0.1% serum. Cells were harvested and assessed for apoptosis by staining with fluorescently labeled annexin V and propidium iodide and analyzed by flow cytometry. As expected, enforced expression of MYC under low serum conditions greatly increased apoptosis (Figure 3.4). Note also that inducing MYC produced a concomitant increase in ASPP2 protein level. Notably, attenuation of ASPP2 expression reduced the amount of apoptosis seen in response to MYC induction (Figure 3.4). These findings, coupled with the ability of MYC to bind directly to the *TP53BP2* promoter (Figure 3.3) provide support that *TP53BP2* is a MYC target gene that may have a functional role in promoting apoptosis.

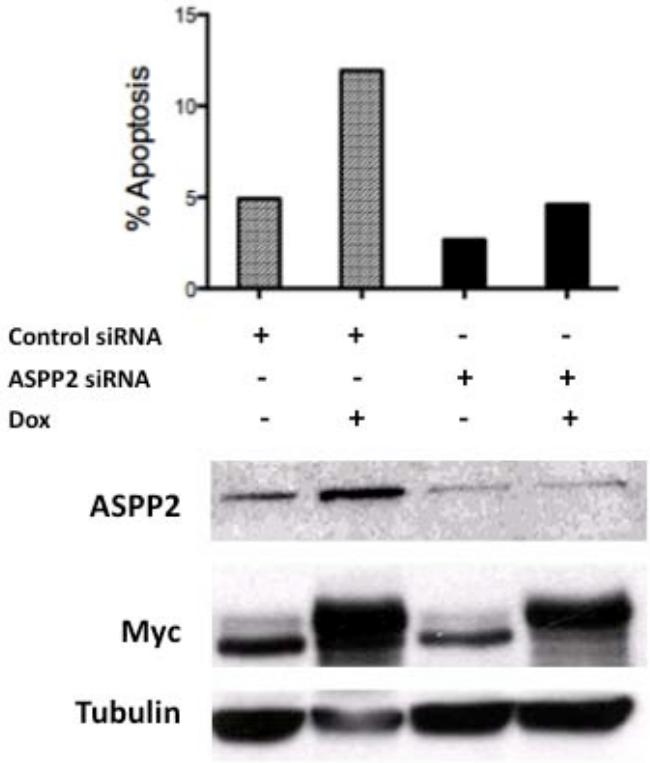

Figure 3.4. Attenuation of ASPP2 expression limits MYC-induced apoptosis. *Top panel*: Percent Annexin V positive cells (represented as % apoptosis) in 292T-tr-HA-MYC cells following transfection with either control or *ASPP2* siRNA as indicated and induction of MYC with doxycycline (1 µg/mL) in 0.1% serum containing medium for 24 hours. Cells were harvested and stained as described in *Methods* and analyzed by flow cytometry for Annexin V positivity. *Bottom panel*: Immunoblot of lysates collected from cells processed as described in *top panel*. ASPP2a antibody was used at a concentration of 1:1000.

***Aspp2* haploinsufficiency does not accelerate lymphomagenesis in a Myc-driven tumor model.** To take the functional observations of our newly described MYC-ASPP2 axis a step further and add physiological relevance to our findings, we tested whether *Aspp2* haploinsufficiency could affect the pathogenesis of Myc-induced lymphoma *in vivo.* To do this we utilized a unique mouse model [denoted RFS-c-Myc, (Wang, 2011)] in which a gene for HA-tagged Myc has been knocked into the *ROSA26* locus, resulting in a low and ubiquitous level of Myc expression. However, the Myc gene is preceded by a stop codon flanked by two loxP sites, which prevents expression of HA-tagged Myc in the absence of Cre recombinase. Tissue-specific expression of Cre then results in excision of loxP sites and the stop codon, and ultimately expression of Myc in the tissue of interest. To induce Myc expression in T cells, we crossed RFS-c-Myc mice with mice carrying the transgene *Lck*-Cre, in which Cre expression is driven by the T cell-specific *Lck* promoter (Link, 2012). Given that these animals express a temporally deregulated but low level of Myc in T cells and are found to be no more susceptible to spontaneous tumor formation than control animals (Sarah Byers; data not shown, we hypothesized that the cells' protective ability to promote apoptosis may still be intact. Given that *Aspp2*$^{+/-}$ thymocytes exhibit apoptotic defects following λ-irradiation (Kampa *et al.*, 2009a) we further reasoned that crossing RFS-c-Myc/*Lck*-Cre mice into an *Aspp2* haploinsufficient background would generate an apoptotic defect that would promote lymphomagenesis. We successfully generated these animals (RFS-c-Myc/*Lck*-Cre/Aspp2$^{+/-}$; Figure 3.5B), and monitored them, along with littermate controls, for

spontaneous tumor formation. Interestingly, we found that an *Aspp2*$^{+/-}$ background does not accelerate lymphoma formation in deregulated Myc-expressing animals as compared to RFS-c-Myc/*Lck*-Cre/Aspp2$^{+/+}$ or RFS-c-Myc/*Aspp2*$^{+/+}$ and RFS-c-Myc/*Aspp2*$^{+/+}$ controls lacking *Lck*-Cre expression (Figure 3.5C). Though negative, these data are consistent with our previous finding that *Aspp2* haploinsufficiency does not accelerate lymphomagenesis in the EμSR-tTA/tet-o-*MYC* mouse model, in which a much higher level of Myc drives the development of T cell lymphoma (Felsher and Bishop, 1999; Kampa *et al.*, 2009a). Taken together these data suggest that the subtle apoptotic deficiencies seen with *Aspp2* haploinsufficiency are not sufficient to impact Myc-driven tumors in these models. Furthermore, they underscore the limitations of what we currently know about the oncogenic context under which apoptosis is activated and the specific mediators needed to execute these programs.

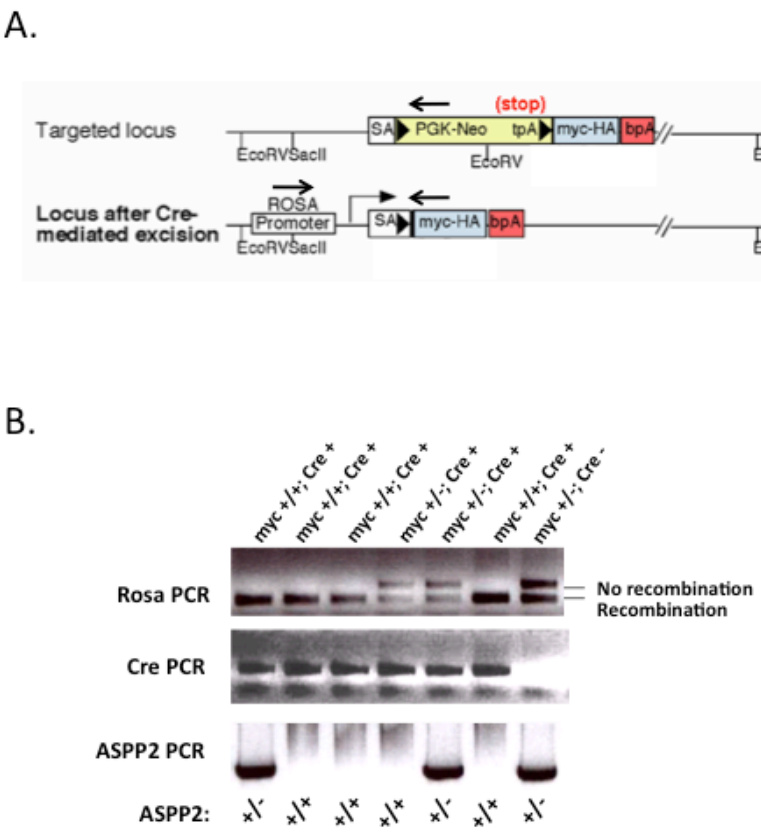

Figure 3.5. *Aspp2* does not accelerate lymphomagenesis in a Myc-driven tumor model. (A) Schematic of the knock-in strategy and primer locations for the RFS-c-Myc transgenic mice (Wang, 2011). Black arrows indicate the location of the RFS genotyping primers. Black triangles=loxP sites; tpA=transcription stop site. Crossing RFS-c-Myc mice with *Lck*-Cre mice generates T cell-specific Myc-expressing animals. (B) Representative genotyping of RFS-c-Myc/*Lck*-Cre/*ASPP2* mice. Recombination at the *ROSA26* locus was assessed with a published 3-primer system illustrated by black arrows in panel A (Wang, 2011). *Lck*-Cre status was assessed with primer in *Methods*. *Aspp2* status was assessed using primers located within the neomycin gene of the previously described targeting construct (Kampa *et al.*, 2009a).

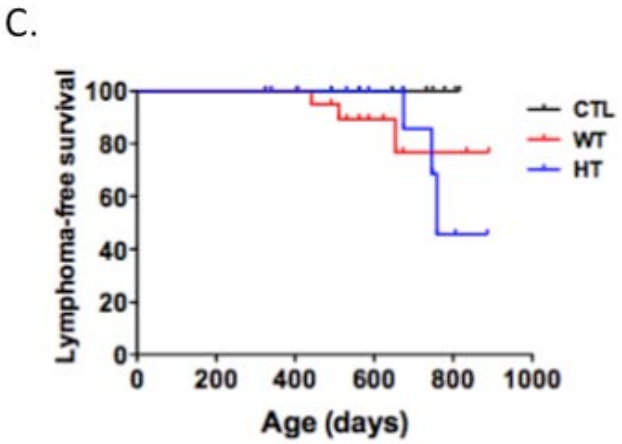

Figure 3.5. *Aspp2* does not accelerate lymphomagenesis in a Myc-driven tumor model. (C) Kaplan-Meier lymphoma-free survival curve of RFS-c-Myc/*Lck*-Cre/*Aspp2*$^{+/+}$ (WT; n=28), RFS-c-Myc/*Lck*-Cre/*Aspp2*$^{+/-}$ (HT; n=23), and RFS-c-Myc/*Aspp2*$^{+/+}$ and RFS-c-Myc/*Aspp2*$^{+/-}$ control mice (CTL; n=13)

Discussion

The details about the cellular context required to induce apoptosis in cancer cells is incompletely understood and remains a barrier to therapeutic intervention. Overcoming this limitation requires a better understanding of the upstream signaling and cellular contexts that induce expression of apoptotic regulators, like ASPP2. Using a variety of molecular techniques we have shown that ASPP2 expression is controlled by the oncogenic transcription factor MYC and have provided evidence that increasing ASPP2 expression is one mechanism through which MYC induces apoptosis. These results are significant because they establish a new connection between MYC and the diverse signaling pathways that ASPP2 is involved in regulating, including apoptosis, senescence, and autophagy (Samuels-Lev *et al.*, 2001; Wang, 2012a; Wang, 2012b).

Here we report that *TP53BP2* is a direct MYC target gene. First, we have found that the *TP53BP2* promoter contains three non-canonical and one canonical E-box binding motif (Figure 3.1A and B), sites that are known to be bound by MYC for the purpose of positively regulating transcription (Blackwell, 1990). Second, an *ASPP2*-luciferase reporter containing these E-box motifs is stimulated by expression of MYC (Figure 3.1C and E). Importantly, when three of the MYC binding sites are deleted, the ability of MYC to stimulate the luciferase reporter is reduced (Figure 3.1E), suggesting that specific MYC-responsive binding or regulatory elements are located within the *TP53BP2* proximal promoter. A higher level of baseline luciferase activity is observed in the E-box

deleted *TP53BP2* construct, suggesting repressive elements located in this region. While we cannot rule out the possibility of repression by other transcription factors (e.g. E2F family members) it remains possible that repression of *TP53BP2* may occur at E-boxes through MAX:MNT or MAX:MAD heterodimers (Patel, 2004). Next, we demonstrate that this transactivation translates to endogenous expression by showing that induction of MYC increases endogenous ASPP2 expression at both the protein and transcript level (Figure 3.2). Finally, we show that both overexpressed and endogenous MYC bind directly and specifically to an E-box-containing region of the *TP53BP2* promoter in its native chromatin state. Taken together these data strongly suggest that ASPP2 expression can be directly controlled by MYC through regulatory elements in its promoter.

While exciting, these data do not fully explore the extent to which cellular context or interplay with other transcription factors contributes to controlling ASPP2 expression. We have previously shown that ASPP2 is similarly regulated by the activating members of the E2F family of transcription factors (Chen, 2005). *E2F1, E2F2,* and *E2F3* are also MYC target genes (Fernandez *et al.*, 2003; Leone *et al.*, 2001; Sears *et al.*, 1997), making it possible that transcription at *TP53BP2* is being controlled by an indirect circuit involving MYC and the E2F family. E2F transcription factors have distinct functions and expression of E2F1 is of particular importance for MYC-induced apoptosis (Leone *et al.*, 2001). Though a precise role for E2F1 in MYC-induced apoptosis remains untested, our work

showing regulation of *TP53BP2* by E2F1 provides a novel link between MYC, ASPP2, and the induction of apoptosis.

An interesting possibility might be that these transcription factors do not compete for binding but rather cooperate to facilitate ASPP2 expression. Indeed, MYC is required for full binding of E2F1 to *E2F* promoters (Leung *et al.*, 2008). These data suggest that MYC binding to E-box regulatory elements in *E2F* promoters aids in opening up chromatin by promoting histone 4 acetylation prior to E2F1 binding (Leung *et al.*, 2008). In this way, E2F1 transcription can only proceed once MYC activity has accumulated, thus implicating MYC as a 'permissive' factor that primes target promoters for activation by other transcription factors (Frank, 2001; Leung *et al.*, 2008). This type of regulation has not been shown for apoptotic targets, but our findings that both E2F(1-3) and MYC bind *TP53BP2* open up the intriguing possibility that MYC activity may control E2F1 transcription of *TP53BP2* in a similar manner in order to restrict apoptosis to the appropriate cellular context.

In addition to establishing *TP53BP2* as a MYC target gene we have evidence to suggest that ASPP2 can promote MYC-induced apoptosis (Figure 3.4). While modest, these results open the door to many new and exciting questions about how MYC promotes apoptosis and the mechanisms used by evolving tumor cells to evade this level of tumor suppression. Our results do not, however, directly address whether ASPP2 is facilitating MYC-induced apoptosis in a p53-dependent or independent manner. Interestingly however, our results showing that ASPP2 knockdown inhibits MYC-induced apoptosis (Figure 3.4)

were performed in the 293T cell line, in which p53 is inactivated by the transforming viral large T antigen. ASPP2 has been implicated in both p53-dependent and independent apoptotic pathways and these results open up the possibility that ASPP2 may cooperate with p63 or p73 to promote apoptosis in this system (Bergamaschi *et al.*, 2004).

We have previously established that *Aspp2* haploinsufficiency does not accelerate lymphomagenesis in the EμSR-tTA/tet-o-*MYC* mouse model where MYC expression is driven to very high levels by the tetracycline-activating protein under the control of the immunoglobulin heavy chain enhancer (Felsher and Bishop, 1999; Kampa *et al.*, 2009a). Here we extend these studies by examining the effect of *Aspp2* haploinsufficiency in the RFS-c-Myc mouse model where Myc expression is deregulated, but protein levels are more physiologic (Wang, 2011). RFS-c-Myc/*Lck-Cre* mice are not prone to tumor formation (Sarah Byers; data not shown), making this an ideal model to study the possibly subtle effects of *Aspp2* haploinsufficiency. Here we provide evidence that RFS-c-Myc/*Lck-Cre/Aspp2*$^{+/-}$ animals are not more prone to lymphomagenesis as compared to their *Aspp2*$^{+/+}$ littermates, suggesting that loss of only one copy of *Aspp2* is too slight a defect to spur Myc-driven tumor formation in this model. The apoptotic-deficiency provided by *Aspp2* heterozygosity in this model could be underpowered suggesting that loss of both *Aspp2* alleles may be more efficient at promoting accelerated lymphomagenesis. It remains possible also that Myc can induce apoptosis through other Aspp2-independent mechanisms in this system, thus compensating for *Aspp2* knockdown. Either way, our results

highlight the need for a better understanding of the contexts required to stimulate apoptosis in a pathogenic state, such as deregulated Myc.

Like the E2F transcription factors, MYC transactivates many genes that are important for both cell cycle progression and apoptosis thereby coupling entry into the cell cycle with sensitization to apoptotic stimuli. By engaging apoptotic targets, such as *TP53BP2*, MYC effectively lowers the apoptotic threshold ensuring that proliferation is controlled (Figure 3.6). In tumors where apoptotic pathways have been functionally inactivated, however, there is no longer a protective feedback mechanism to guard against the proliferative advantage of overexpressed or deregulated MYC. Interestingly, expression of ASPP2 is lost in a variety of human tumors including Burkitt's lymphoma, a malignancy driven by elevated levels of MYC due to translocation (Lossos *et al.*, 2002). Additionally, loss of ASPP2 is due, at least in part, to epigenetic silencing of its promoter (Liu, 2005; Sarraf and Stancheva, 2004) leading us to speculate that this silencing may block MYC transactivation of *TP53BP2*, thus limiting the apoptotic potential of the cell and leaving proliferation unchecked (Figure 3.6). Studies, like those shown in this chapter, aimed at understanding the uncoupling of proliferation and apoptosis in tumor cells are significant because being able to restore and/or exploit the machinery needed to initiate cell death in cancer cells has far reaching therapeutic consequences.

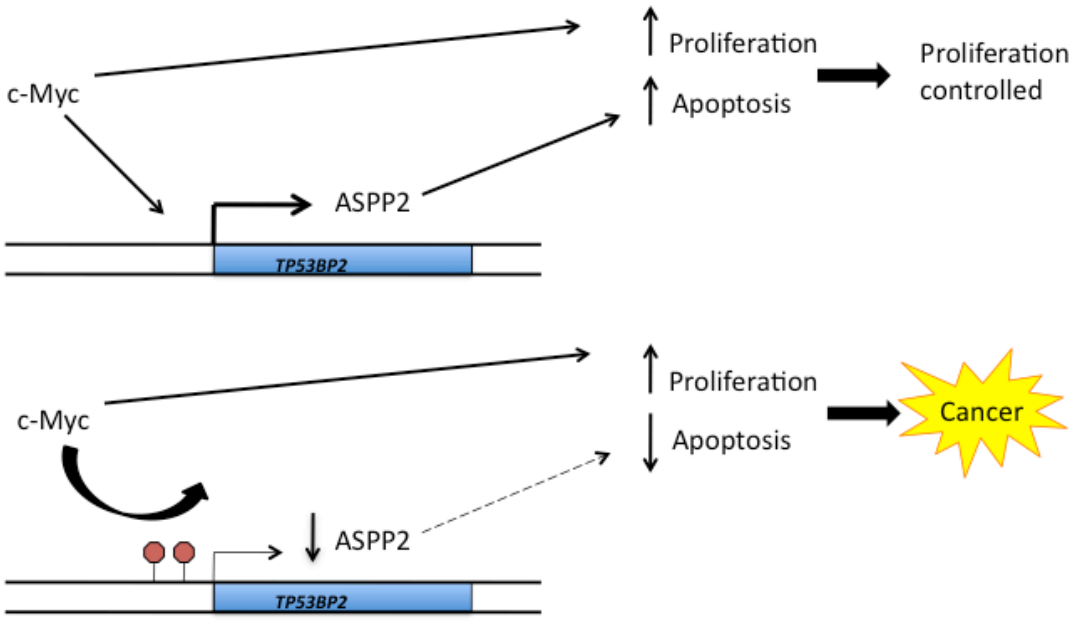

Figure 3.6. Diagram representing the proposed MYC-ASPP2 axis. (A) Diagram of our working hypothesis that *TP53BP2* is a direct target of MYC transcription and is a downstream mediator of MYC-induced apoptosis. In normal proliferating cells (*top panel*) MYC can concurrently drive proliferation while remaining sensitized to apoptotic stimuli, thus allowing for controlled proliferation. In a cancer cell where ASPP2 expression is limited, possibly through repressive chromatin markings (*bottom panel*), MYC-driven proliferation is uncoupled from apoptosis leading to unchecked proliferation and tumor progression.

Chapter Four:

Summary and Discussion

Summary and Discussion

The central goal of this dissertation was to gain insight into the complex pathways that regulate ASPP2 expression and to explore the structure and function of a previously unidentified ASPP2 isoform. In Chapter 2 we presented our discovery of a new member of the ASPP family, ΔN-ASPP2, that has clear functions that are distinct from ASPP2. In doing so we have changed the landscape of the ASPP family and how it is interpreted. In Chapter 3 we described a new level of transcriptional regulation for the ASPP2 gene, *TP53BP2,* by characterizing it as a target gene for the proto-oncogene MYC and laid the foundation for exploring its role in the context of MYC-induced apoptosis. Here we discuss the possible implications of both findings.

ΔN-ASPP2: New implications for the ASPP2 family

Our contribution to the ASPP family, ΔN-ASPP2, is an N-terminally truncated isoform of ASPP2 that is generated from an internal alternative transcription start site and is missing the first 256 amino acids as compared to full-length ASPP2 (also referred to also 53BP2L; Figure 4.1). Like the previously described ASPP2 isoform BBP (also referred to as 53BP2S; Naumovski and Cleary, 1996) , this N-terminal truncation profoundly affects its function, and here we report that ΔN-ASPP2 promotes cell proliferation, enhances cell survival following damage, and inhibits apoptosis (Chapter 2). This discovery has added to and consequently

changed what we know and how we think about both ASPP2 and the other ASPP family members and requires that we reevaluate previously published reports on ASPP2. It is becoming increasingly obvious that ASPP2 cannot be studied in isolation and that understanding the regulation and cell context behind expression of each isoform will be needed to appreciate their contributions to cellular function and pathogenesis both together and separately.

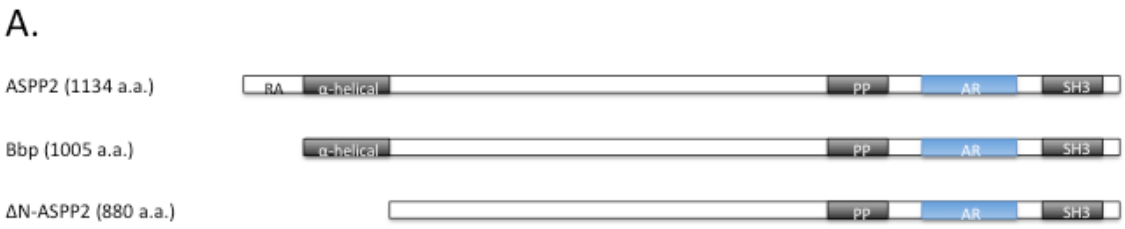

Figure 4.1. Schematic of *TP53BP2* gene products. Diagram showing the various protein products originating from *TP53BP2*. ASPP2 is the longest and most apoptotically active member. BBP is 126 amino acids shorter than ASPP2 and is functionally distinct with regards to stimulation of both apoptosis and senescence. ΔN-ASPP2 is 256 amino acids shorter than ASPP2 and promotes cell survival and proliferation. RA=RAS-association domain; PP=poly-proline domain; AR=ankyrin repeat domain.

Summary and Discussion

Expression of ΔN-ASPP2 is important for normal development

As discussed in Chapter 2, the existence of ΔN-ASPP2 may help to explain some of the differences that have been observed between the two existing *Aspp2* knock-out mouse models (Kampa *et al.*, 2009a; Vives, 2006). While both models clearly demonstrate that Aspp2 is a haploinsufficient tumor suppressor, the developmental differences also provide a basis for speculation on how ΔN-Aspp2 functions. The exon 3 knockout (*Aspp2*$^{\Delta exon3/\Delta exon3}$), generated by Vives *et al.*, presented with cranial and heart defects and died before weaning (Vives, 2006). Based on our understanding of *Aspp2* gene structure (Figure 2.1C) these animals are predicted to have lost Aspp2 but retain expression of Bbp (Wang, 2013) and ΔN-Aspp2. We generated an *Aspp2* exon 10-17 targeted mouse (*Aspp2*$^{\Delta exon10\text{-}17/\Delta exon10\text{-}17}$), depleted of Aspp2, Bbp, and ΔN-Aspp2 (Kampa *et al.*, 2009a). Homozygote animals were never recovered in this model, presumably due to a catastrophic developmental defect, as we were not able to identify homozygote embryos (Kampa *et al.*, 2009a). These results are consistent with whole mount *in situ* hybridization results from *Aspp2*$^{+/+}$ mice using both 5' and 3' probes (to detect all known transcripts), which shows expression beginning at embryonic day 9.5 (Sottocornola *et al.*, 2010).

So how is continued expression of ΔN-ASPP2 affecting development in these mice? While that has yet to be rigorously tested, we do know that *Aspp2*$^{\Delta exon3/\Delta exon3}$ embryos have an expanded pool of neural progenitor cells, due in part to a shortening of the cell cycle (Sottocornola *et al.*, 2010). This may be

explained by our data showing that ΔN-ASPP2 promotes proliferation (Figure 2.5). Depletion of ASPP2 without a concomitant depletion of ΔN-ASPP2 may shift the isoform ratio out of balance, making it easier for ΔN-ASPP2 to exert dominant negative effects against p53 and its ability to promote cell cycle arrest. The fact that *Aspp2*$^{\Delta exon3/\Delta exon3}$ animals survive through gestation, as compared to *Aspp2*$^{\Delta exon10\text{-}17/\Delta exon10\text{-}17}$ embryos, may suggest a level of functional redundancy between Aspp2 and ΔN-Aspp2 that has yet to be explored. Given that Aspp2 plays a vital role in the establishment and maintenance of cellular contacts that are needed for normal development (Cong, 2010; Sottocornola *et al.*, 2010) it will be interesting to study the extent to which ΔN-Aspp2 is necessary in the same systems.

Perhaps an important role for ΔN-ASPP2 during development can help to explain the variability in detecting it in different, possibly more differentiated, cell types. Indeed, detection of ΔN-ASPP2 can be difficult and possibly restricted to a specific cell type and/or context. One hypothesis could be that expression of ΔN-ASPP2 is important during development to promote cell proliferation, cell survival, and tissue growth but that its importance decreases (and oncogenic potential increases) as cells differentiate. In this way, it would be advantageous for cells to limit ΔN-ASPP2 expression to specific developmental stages and turn down/off expression, perhaps indefinitely, once cells have differentiated. It will be interesting to determine the protein half-life of ΔN-ASPP2 and compare it to full-length ASPP2 (~60-80 min; Zhu, 2005) as it remains possible that the ASPP2 N-terminus harbors a stabilizing or de-stabilizing regulatory element that ΔN-

ASPP2 lacks. The regulation of ΔN-ASPP2 expression may not be limited to protein stability however. A complete examination of ΔN-ASPP2 expression will involve interrogating the transcriptional regulation of ΔN-ASPP2 (see pg 81), the stability of the *ΔN-ASPP2* transcript, differences in the efficiency of protein synthesis between ΔN-ASPP2 and ASPP2, and any post-translational modifications that may affect ΔN-ASPP2 stability. No matter the outcomes, the results of these experiments will be helpful and add to our understanding of ΔN-ASPP2 function.

Complex binding dynamics likely mediate ASPP2 and ΔN-ASPP2 function

In Chapter 2 we presented data demonstrating that ΔN-ASPP2 promotes proliferation, increases survival in response to genotoxic stress (Figure 2.5), inhibits apoptosis (Figure 2.6), and is overexpressed in primary breast cancer as compared to adjacent normal tissue (Figure 2.7), leading us to speculate that it may promote tumor growth or initiation. We anticipate, as with ASPP2, that some of these effects are due, at least in part, through an ability to regulate p53. ΔN-ASPP2 can inhibit promoter occupancy of p53 at both the *Bax* and *p21* promoters (Figure 2.4C) but our mechanistic understanding of how this occurs remains incomplete. We do know that ASPP2 binds to p53 in its core domain (Gorina and Pavletich, 1996; Iwabuchi *et al.*, 1994) and that the domains necessary for this interaction are presumably preserved in ΔN-ASPP2, making it possible that ΔN-ASPP2 may directly bind and inhibit p53 transactivation.

Interestingly, however, ΔN-ASPP2 does not appear to bind p53 under standard cell culture conditions (Figure 4.2A). These results, while surprising, suggest a level of regulation or a cell context that we have not yet uncovered. While not apparent in unstressed cells, perhaps certain types of cellular stress can promote the association of ΔN-ASPP2 and p53. Indeed, the ability of ASPP2 to enhance p53 binding to its targets is stimulated by cisplatin, indicating the opposite might be true for ΔN-ASPP2 (Figure 2.4C).

It is also important to consider that ΔN-ASPP2 may also be regulated by predicted intramolecular associations with itself or intermolecular associations with ASPP2 and/or BBP. Structural studies using ASPP2-derived peptides predict an intramolecular interaction between the intrinsically unstructured poly proline domain and SH3 domain (Rotem *et al.*, 2007; Rotem-Bamberger, 2013). Again, since both of these domains are predicted to be preserved in ΔN-ASPP2, we expected that ASPP2 and ΔN-ASPP2 may interact and regulate one another. We tested this interaction through co-immunoprecipitation using differentially tagged ASPP2 and ΔN-ASPP2 expression vectors (Figure 4.2B and C). Reciprocal pull-downs of either FLAG-ASPP2 or FLAG-ΔN-ASPP2 verify that intermolecular binding and regulation are a possibility. Interestingly, binding/regulation of ASPP2 to itself (or ΔN-ASPP2) may also affect the interaction with, and thus the function of, p53 (Rotem-Bamberger, 2013). While we do not yet know the physiological relevance of these interactions or whether they are direct, mediated through a complex of proteins, or whether they are

context dependent, they open up the interesting possibility of a direct regulatory network between ASPP2, ΔN-ASPP2, and p53.

Adding another level of complexity to the ASPP2 family is an observation made by our colleagues at the University of Tubingen, Germany who have recently identified several tumor-derived C-terminally truncated isoforms of ASPP2 that arise as a result of alternative splicing. The isoforms, dubbed ASPP2κ and ASPP2μ, are transcribed from an mRNA missing exon 17 which results in a frameshift and encodes a unique C-terminal peptide and a premature stop codon as compared to full-length ASPP2 (Kampa-Schittenhelm, 2013). The resulting protein is endogenously expressed in acute myeloid leukemia and appears to have lost a portion of its p53-DNA binding domain, making it tempting to speculate about its capacity to bind p53, ASPP2, ΔN-ASPP2, or other C-terminal binding partners (Table 1.1) and about what that may mean for disease pathogenesis. Though further studies are needed to understand how this isoform functions in a disease state, these findings underscore the inherent complexity of this gene family and the need for a clearer insight into how they cooperate to promote/prevent disease progression.

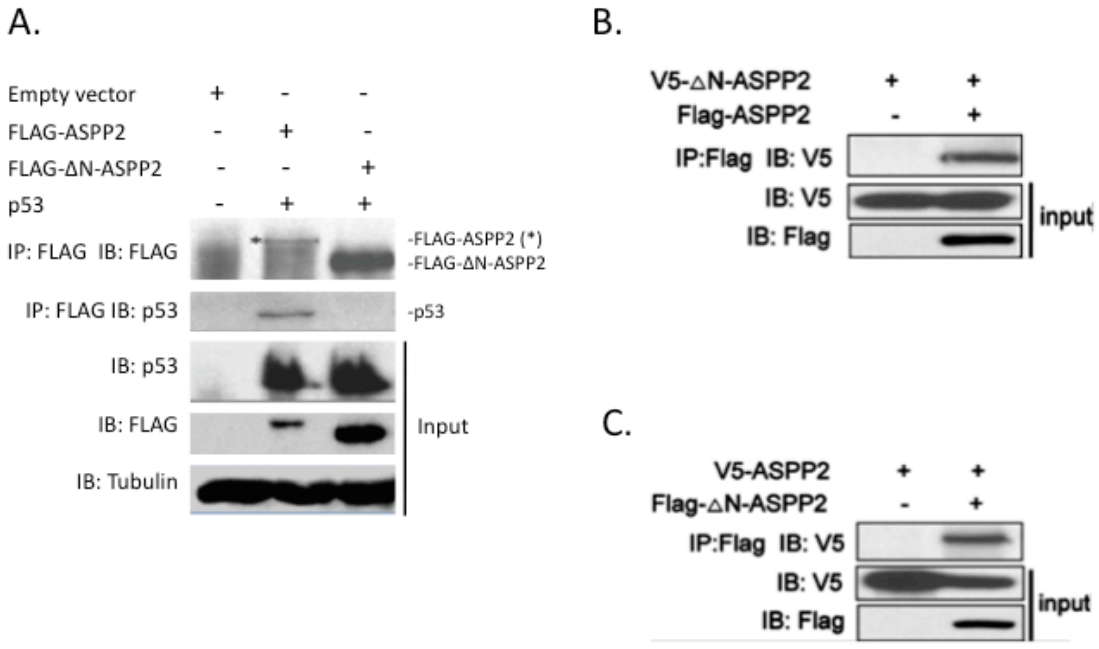

Figure 4.2 ΔN-ASPP2 binds ASPP2 but not p53. (A) H1299 cells were transfected with the indicated plasmids and lysates were immunoprecipitated (IP) with α-FLAG. 10% of lysate was run for inputs and samples were immunoblotted (IB) with the indicated antibodies. (B and C) 293T cells were transfected with the indicated plasmids and lysates were immunoprecipitated with α-FLAG. Total input was run in parallel and samples were immunoblotted with the indicated antibodies.

Summary and Discussion

ΔN-ASPP2 affects the localization of p53 in response to damage

In discussing the binding capacity of ASPP2, ΔN-ASPP2, and p53 it is also important to consider their cellular locations. ASPP2 is known to be primarily cytoplasmic and very often localized to the plasma membrane due to its association with both RAS and PAR-3 (Cong, 2010; Wang, 2013; Wang, 2012b). To assess the location of ΔN-ASPP2, HCT116 $p53^{+/+}$ cells were transfected with FLAG-ΔN-ASPP2 and stained and analyzed by immunofluorescence. As seen in Figure 4.3 (*top*) ΔN-ASPP2 appears to localize primarily to the cytoplasm with some possible punctate staining within the nucleus. Endogenous p53, as expected, is concentrated within the nucleus. Interestingly, after exposure to cisplatin for 4 hours, FLAG-ΔN-ASPP2 remains cytoplasmic but the staining for p53 shifts dramatically from nuclear to cytoplasmic (Figure 4.3 *bottom*). This shift is made even more compelling when it is compared to an untransfected cell in the same field that shows, as predicted, an increase in p53 staining within the nucleus. This suggests that ΔN-ASPP2 can alter the location of p53 even in the presence of cell damage. There are many possible explanations for this shift. Perhaps ΔN-ASPP2 has sequestered p53 in the cytoplasm in a complex made possible by the cellular stress conditions. It is also possible that ΔN-ASPP2 may inhibit nuclear import of p53 or promote nuclear export through yet undiscovered mechanisms. Regardless of the mechanism, these results hint at how ΔN-ASPP2 may inhibit p53 transactivation (Figure 2.4) and, by extension, apoptosis and/or cell cycle arrest (Figure 2.5 and 2.6).

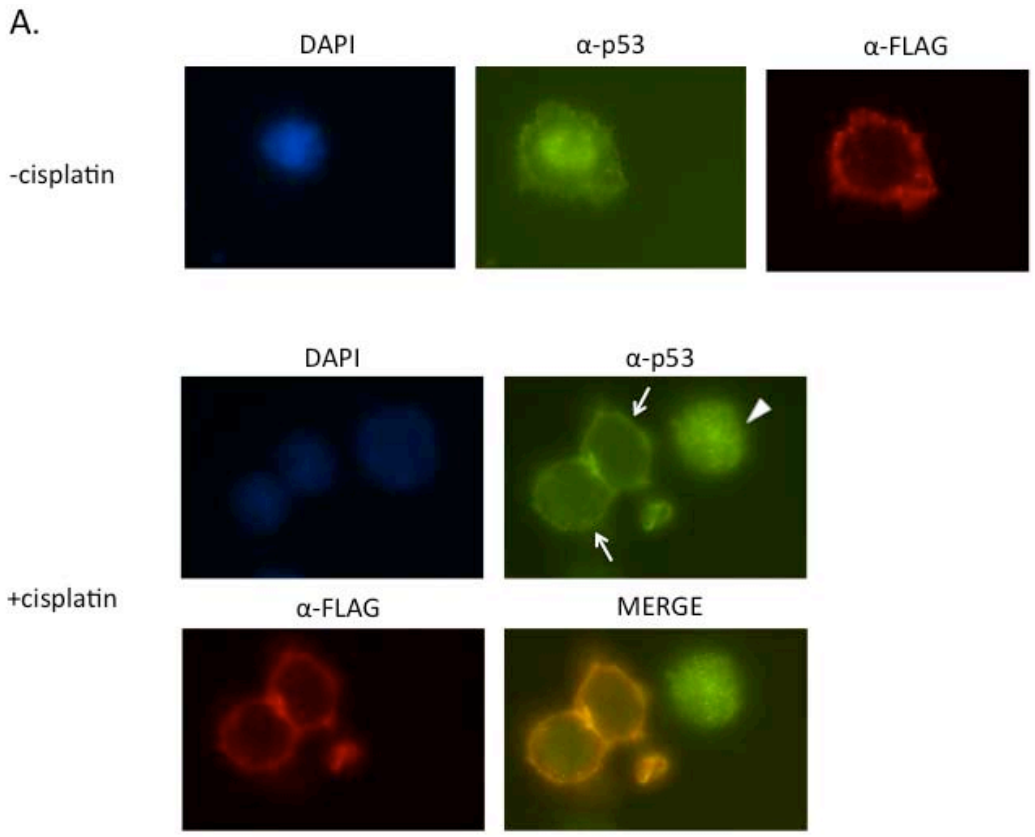

Figure 4.3 Changes in subcellular location of endogenous wild type p53 may be mediated by ΔN-ASPP2. (A) FLAG-ΔN-ASPP2 was transfected into HCT116 cells and exposed to 20 μM cisplatin for 4 hours. Cells were fixed, blocked, and incubated with α-FLAG and α-p53 as described in *Methods*. White arrows indicate FLAG-ΔN-ASPP2-transfected cells with cytoplasmic p53 staining. White triangle indicates untransfected cell with nuclear p53 staining.

Summary and Discussion

ΔN-ASPP2 adds complexity to the our understanding of the ASPP2 family

The literature is replete with examples of protein isoforms that exert dominant negative effects on other splice variants from the same gene. The p53/p63/p73 gene families all contain a dizzying array of both C-terminally and N-terminally distinct isoforms that appear to have widely varying functions. p73, for example, has seven C-terminal isoforms and 5 N-terminal isoforms, making for a possible 35 different combinations from the same gene. While studies have yet to fully elucidate the differences of the p53/p63/p73 isoforms, truncations at the N-terminus in each gene family are generally noted as having dominant negative effects against longer gene products (Allocati, 2012; Khoury and Bourdon, 2010). MYC also has been described as having several N-terminally distinct isoforms that arise from alternative translation initiation sites. One isoform, MycS (a protein lacking the first 100 N-terminal amino acids as compared to full-length MYC) can promote proliferation but not apoptosis in *Drosophila melanogaster,* illustrating a distinct and important functional difference (Benasayag, 2005). These findings, while incompletely understood, again emphasize the importance of protein isoform dynamics and the functional consequences of changes in protein structure.

Given the inherent complexity within the ASPP2 family as a result of the various isoforms (Figure 4.1), the intricate differences between how the different variants are regulated are bound to have profound biological outcomes. Previous studies have shown us that *TP53BP2* is an E2F(1-3) target gene (Chen, 2005;

Fogal *et al.*, 2005) and in Chapter 3 we interrogated the ability of MYC to control ASPP2 expression. We predict that ΔN-ASPP2 expression is regulated by a separate internal promoter so by extension it would be interesting to explore the regulation of the *ΔN-ASPP2* transcript by these same transcription factors. As a preliminary step, we examined the regions proximal to the predicted TSS of ΔN-ASPP2 in intron 6 for E-box regulatory elements. Interestingly, there are several non-canonical MYC-binding sites upstream of our predicted ΔN-ASPP2 translation start site (intron 5), one downstream (exon 8), and a canonical E-box in exon 7. While the functionality and importance of these potential binding sites is still untested, based on the multifaceted nature of the *TP53BP2* locus and the different functions of each isoform we anticipate complex and context-dependent regulation of ΔN-ASPP2 expression.

The N-terminus of ASPP2 mediates tumor suppressive functions

Our discovery of an N-terminally truncated isoform of ASPP2 comes at a very exciting time in the ASPP2 field. Until recently studies have focused on the C-terminus of ASPP2 and the functional ramifications of its interaction with p53; however the focus has gradually shifted to one that encompasses the important interactions and functions mediated by its N-terminus as well. Through examination of these recent studies we can gain insight into how ΔN-ASPP2 may be functioning and generate hypotheses on which future studies will be built.

Summary and Discussion

Full-length ASPP2 is necessary to promote senescence

It has become increasingly clear that ASPP2 has far reaching functions within the cell and that its role as a tumor suppressor extends beyond its ability to induce apoptosis. One of the most interesting new avenues of study involves ASPP2's ability to promote RAS-induced senescence. RAS is a small GTPase that, through its binding of GTP, can quickly translate mitogenic (or anti-mitogenic) signaling into cellular function. It is an upstream regulator for the powerful MEK/ERK and AKT/PI3K signaling cascades that have broad reaching effects within the cell. For example, depending on the cell context, RAS signaling can drive proliferation, suppress apoptosis, and/or promote angiogenesis and invasion, making deregulation of RAS activity an attractive pathway for transformation (Campisi, 2007). Like E2F and MYC, however, the transformative properties of RAS are kept in check through its ability to initiate tumor suppressive pathways, like senescence. RAS activation levels appear to be important for its ability to induce senescence and understanding the mediators of this regulation remains a barrier to therapeutic intervention (Pylayeva-Gupta, 2011). Our data and others implicates ASPP2, and more specifically the N-terminus of ASPP2, as an important mediator in this process, by demonstrating that ASPP2, but not N-terminally truncated BBP, can potentiate RAS signaling and ultimately senescence (Wang, 2013; Wang, 2012a; Wang, 2012b). Mechanistically, ASPP2 enhances phosphorylation and activation of C-RAF, C-RAF/B-RAF dimerization, and a subsequent increase in flux through the MEK/ERK signaling cascade (Wang, 2012b). These findings have interesting

implications when taken together with our discovery of ΔN-ASPP2. Because the N-terminally truncated BBP does not stimulate RAS activity to the same extent as full-length ASPP2 (Wang, 2013; Wang, 2012a; Wang, 2012b), we anticipate a similar deficiency when testing ΔN-ASPP2 in the same system. Additionally, ASPP2 activation of RAS signaling is independent of p53 binding (Wang, 2012b) which compels us to look more broadly at how ΔN-ASPP2 may function in this network. Perhaps ΔN-ASPP2 regulation is needed to slow or turn off ASPP2-mediated RAS signaling, in which case ΔN-ASPP2 could act by directly binding and inhibiting ASPP2 or another component of the pathway.

The N-terminus of ASPP2 is vital for inhibition of autophagy

In addition to promoting senescence, ASPP2 is also being studied for its ability to inhibit autophagy. Autophagy is a catabolic process, often the result of nutrient starvation, through which cellular components are metabolized for re-purposing in other pathways. Like many cellular processes, our understanding of autophagy is incomplete and complex, as it appears to promote survival in some contexts and cell types but cell death in others (Kundu, 2008). ASPP2 was recently shown to inhibit autophagy by competing with the structurally similar ATG16 protein for binding of the integral autophagic complex ATG5/ATG12 and through this inhibition it relieves suppression of RAS-induced senescence (Wang, 2012a). Inhibition was mediated by the N-terminus of ASPP2 (specifically the first 130 amino acids), suggesting that ΔN-ASPP2 may not regulate autophagy in the same way. Interestingly, a similar process of autophagy masking the ability of an

oncogene to initiate tumor suppressive pathways has also been shown in a MYC-driven tumor model. Hart *et al.* demonstrated that pharmacological or genetic inhibition of autophagy in MYC-inducible or MYC-transformed MEFs promotes apoptosis and inhibits tumor growth *in vivo* (Hart, 2012). Given that ASPP2 can inhibit autophagy and that there appears to be an emerging role for autophagy levels dictating the cellular response to RAS and MYC signaling, exploring the extent to which ASPP2 can influence this paradigm becomes an exciting possibility. This is particularly true when taking into consideration the results presented here illustrating that ASPP2 loss has an impact on cell survival in response to MYC signaling (Figure 3.4).

Possible therapeutic ramifications

Both inhibition of autophagy and stimulation of senescence appear to depend on interactions with the N-terminus of ASPP2 (Wang, 2012a; Wang, 2012b). In light of our discovery of an ASPP2 isoform that lacks this N-terminus, along with its pro-survival functions (Chapter 2), future studies will explore the effects of ΔN-ASPP2 on senescence and apoptosis. Indeed, the N-terminally truncated isoform BBP cannot stimulate RAS signaling and senescence (Wang, 2013; Wang, 2012b) and the ASPP family member iASPP (which lacks N-terminal homology with ASPP2) cannot inhibit autophagy (Wang, 2012a)--making it reasonable to anticipate that without the important N-terminus, ΔN-ASPP2 will likewise not be capable of promoting senescence or inhibiting autophagy. Additionally, since the ability of ASPP2 to inhibit autophagy and promote senescence is based on the

structure of its N-terminus and since a peptide derived from the C-terminus of ASPP2 has previously been shown to restore the DNA binding function of the unstable I195T p53 mutant (Friedler, 2002), testing whether an N-terminally-derived peptide can restore the tumor suppressive functions of oncogenes like MYC and RAS becomes an intriguing prospect with therapeutic value. One may predict, however, that an N-terminal ASPP2 peptide therapeutic may have the unintended consequence of potentiating RAS-driven proliferation in addition to, or preferential to, RAS-induced senescence and thus drive tumor progression. The therapeutic benefit of such a peptide remains speculative and would need to be tested in the appropriate tumor contexts.

TP53BP2 is a MYC target gene with relevance in various tumor suppressive pathways

Recent ChIP-seq binding studies estimate that MYC binds ~22% of promoters following serum-stimulation in fibroblasts but that detectable regulation by MYC is only seen in a fraction of promoters bound, suggesting that though MYC may bind a large fraction of genes, it is only essential in regulating/amplifying the expression of a subset (Lin, 2012; Perna, 2012). Therefore it is crucial when identifying MYC target genes to verify and determine the functional importance of this regulation. In this dissertation we have presented evidence that *TP53BP2* has features of a MYC target gene and that MYC can promote transactivation of an E-box-containing luciferase reporter but not an E-box-deficient reporter

(Figure 3.1). We reason that this regulation is direct by demonstrating that MYC binds to E-box motifs in the *TP53BP2* promoter (Figure 3.3). Lastly, and importantly, we have shown that MYC regulation of *TP53BP2* has functional importance in regulating MYC-induced apoptosis (Figure 3.4). Examination of what is known about the pathways that both ASPP2 and MYC utilize to promote apoptosis reveals interesting overlap and provides a foundation for future studies.

The exact pathways through which ASPP2 mediates MYC-induced apoptosis remain unclear but we can speculate that ASPP2 may function directly with p53 to enhance transcription of its pro-apoptotic targets (Samuels-Lev *et al.*, 2001). Additionally, our discovery of the pro-survival isoform ΔN-ASPP2 (Figure 2.5 and 2.6) makes it possible that ASPP2 can promote cell death by inhibiting (directly or indirectly) the function of ΔN-ASPP2. Past studies also show that ASPP2 can stimulate the apoptotic abilities of both p63 and p73 (Bergamaschi *et al.*, 2004) and that BBP can induce apoptosis through the mitochondrial cell death pathway independent of p53 (Kobayashi, 2005). We can also speculate that the anti-apoptotic protein BCL-2 may provide a common link between ASPP2 and MYC. Repression of BCL-2 by MYC through the MIZ-1 pathway is essential for MYC-induced apoptosis in human fibroblasts (Patel, 2007). Expression of BCL-2 can block BBP-induced apoptosis, though the exact pathways involved remain unclear (Takahashi *et al.*, 2005). Interestingly both ASPP2 and BBP are known to bind BCL-2 through their C-terminal domains (Naumovski and Cleary, 1996; Rotem-Bamberger, 2013). It will be interesting to

explore the extent to which BCL-2 can inhibit ASPP2 and/or BBP and the extent to which repression of BCL-2 by MYC can free these proteins for other functions, such as promoting apoptosis.

ASPP2 has a multifaceted role in tumor prevention

Our results linking ASPP2 to MYC regulation and apoptosis, taken in combination with current knowledge about RAS and MYC activity, place ASPP2 at the heart of a novel tumor suppressive network whereby ASPP2 functions to inhibit tumorigenesis through multiple mechanisms (Figure 4.4). Activation of RAS promotes phosphorylation of the oncogene RB, which subsequently releases E2F from inhibition, and allows transcription of E2F targets necessary for cell cycle progression and apoptosis. E2F is then free to stimulate transcription of *TP53BP2,* where it can contribute to the lowering of the apoptotic threshold that accompanies proliferation. At the same time, activation of RAS leads to stabilization of MYC by promoting phosphorylation at S62 through ERK and other cyclin-dependent kinases. This stable MYC, whether in combination with E2F or not, can then engage the *TP53BP2* promoter and further sensitize the cell to apoptotic stimuli. In response to apoptotic stimuli, such as activated RAS or deregulated MYC, ASPP2 may directly stimulate apoptosis through p53-dependent or independent mechanisms. It may also prevent malignant transformation of normal cells by potentiating RAS-induced senescence through their direct interaction at the plasma membrane. Lastly, depending on the cell

type or context, ASPP2 may activate these tumor suppressive pathways indirectly by inhibiting a survival pathway like autophagy, thus exposing the tumor suppressive pathways mediated by RAS or MYC. Through inactivation of ASPP2, whether by promoter hypermethylation or another mechanism, an evolving tumor cell may be able to relieve tumor suppression in a variety of ways, making ASPP2 loss advantageous. It remains a possibility also that aberrant upregulation of ΔN-ASPP2 could function in an opposing way and antagonize these pathways by directly or indirectly functioning as a dominant negative against ASPP2 or p53.

After almost twenty years of study, our knowledge about ASPP2 has evolved from thinking of it primarily as a pro-apoptotic regulator of p53 to understanding that its contribution to the cell is much broader and includes roles in senescence, autophagy, development, and cell polarity. Upon reflection, it becomes clear that the findings outlined in this dissertation not only change the way we interpret prior findings about ASPP2 regulation and function but also how future studies should be designed and interpreted.

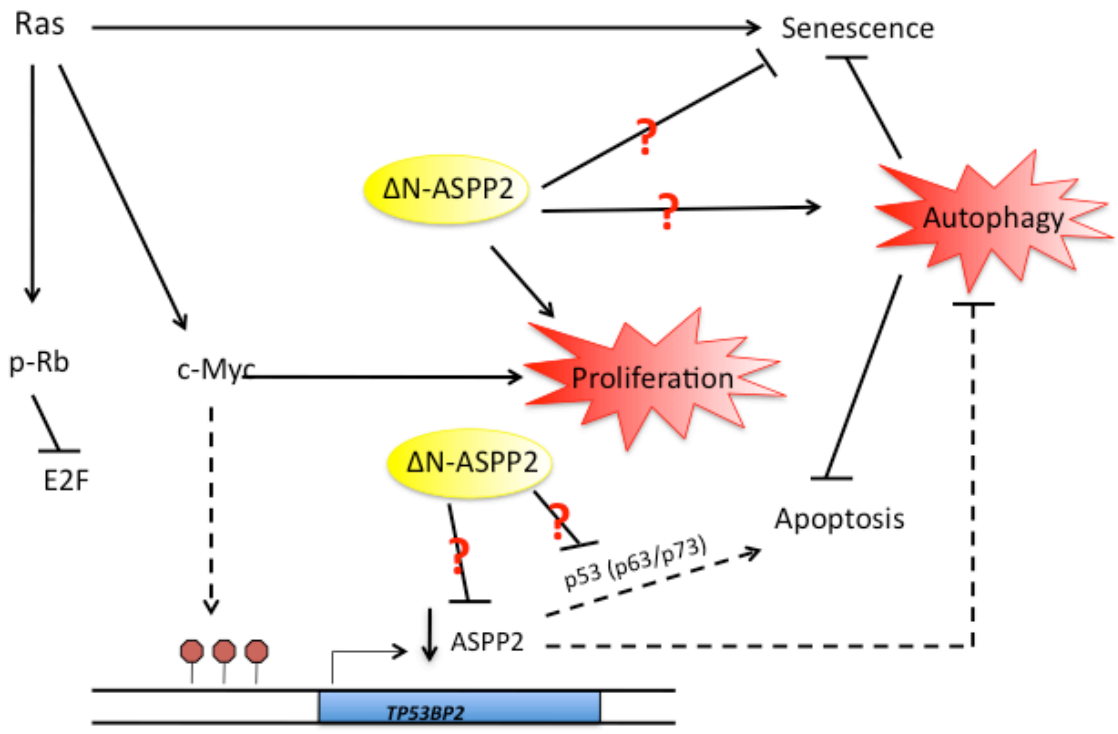

Figure 4.4. ASPP2 and ΔN-ASPP2 have a multifaceted role in tumor suppression. ASPP2 expression is regulated downstream of several signaling pathways. Activation of RAS leads to stabilization of MYC and activation of E2F leaving them free to regulate various target genes, like *TP53BP2.* Expression of ASPP2 can promote apoptosis or senescence directly or through inhibition of autophagy.

Chapter Five:

Materials and Methods

Materials and Methods

Plasmids

Construction of the pD40-His/V5-c-MYC, CMV-empty, CMV-ASPP2, and pRSV-β-galactosidase plasmids and reporter constructs *E2F2*-luciferase, *ASPP2*-luciferase (-1530→+276), and *ASPP2*-luciferase (-1080→+276) has been previously described (Chen, 2005; Sears *et al.*, 1997; Yeh *et al.*, 2004; Zhu, 2005). The p53 expression plasmid and the *p21*-luciferase reporter construct were generous gifts from Hua Lu, Tulane University. The V5-ΔN-ASPP2, FLAG-ΔN-ASPP2, FLAG-ASPP2, CMV-ΔN-ASPP2 and 5'UTR-ΔN-ASPP2 expression vectors were constructed by Zhiping Wang. The V5-ΔN-ASPP2 plasmid was generated by PCR amplifying ΔN-ASPP2 cDNA with restriction enzyme linking primers (*BamHI* 5' end and *XbaI* 3' end). The restriction digested PCR products were then cloned into V5pcDNA3.1. FLAG-ΔN-ASPP2 and FLAG-ASPP2 were generated by PCR amplifying either ΔN-ASPP2 or ASPP2 cDNA with restriction enzyme linking primers (FLAG-ΔN-ASPP2: *BamHI* 5' end and *XbaI* 3' end; FLAG-ASPP2: *XhoI* 5' end and *XbaI* 3' end). PCR products were cloned into 2XFLAGpcDNA3.1. CMV-ΔN-ASPP2 was generated by amplifying ΔN-ASPP2 cDNA with restriction enzyme linking primers (*BamHI* 5' end and *XbaI* 3' end). 5'UTR-ΔN-ASPP2 was generated by PCR amplifying the 5'UTR-containing ΔN-ASPP2 cDNA cloned from MCF7 cells with restriction enzyme linking primers (*BamHI* 5' end and *XbaI* 3' end). Both CMV-ΔN-ASPP2 and 5'UTR-ΔN-ASPP2

were cloned into pRcCMV. ASPP2, ΔN-ASPP2, and control siRNAs were designed as described in Appendix 1 and duplexes were purchased from Sigma-Aldrich (St. Louis, MO).

ΔN-ASPP2 Cloning

Full-length ΔN-ASPP2 was PCR amplified from a cDNA library created from the human breast cancer cell line MCF7. Total RNA was isolated as described in the *RNA preparation and RT-PCR* section (pg. 120). cDNA was generated using M-MLV Reverse Transcriptase (Invitrogen) according to manufacturers instructions using oligo-dT primers. Undiluted cDNA was PCR amplified with Platinum Taq polymerase (Invitrogen) according to manufacturers instructions. In accordance with Invitrogen suggested optimizing methods BSA and DMSO were added to reduce secondary structures, the annealing temperature was optimized to 72°C, and 35 cycles were run to achieve the desired product. Cycling conditions were as follows (98°C for 30 seconds, 98°C for 30 seconds, and 63°C for 30 seconds, 72°C for 1 minute with extension of the last cycle for 10 minutes at 72°C). Resulting PCR products were run on a 1% agarose gel. Products of the correct size were cut from the gel and purified using a Qiagen QIAquick Gel Extraction Kit according to manufacturer's instructions. Purified products were ligated into a TOPO TA Cloning Kit® from Invitrogen according to the provided instructions. Plasmids were transformed into the chemically competent One Shot® cells (Invitrogen) and resulting colonies were mini-prepped using a QIAprep Spin

Miniprep Kit (Qiagen) per included instructions. Purified products were sequenced with the following primers:

Primer name	**Sequence**
ForATG	*ATGAATAATTTGTTCCAGCAA*
T3	*ATTAACCCTCACTAAAGGGA*
T7	*TAATACGACTCACTATAGGG*
I6S1	*GTGTTGCAGTTAGGCTATTTTGAGC*
2735Rev	*AGACAAAGGAGCTTGGCCTGA*
2520Rev	*GTTCAGGAGAAGATGGGCATA*
2021Rev	*GAGAAGACTCGGTGAGCATGCG*
1521Rev	*CTAGAAGCCTTACGAAAG*
1020Rev	*CAGCCGAGAGTGCTGCTATCT*
517Rev	*GGCCGATGAAAATACAGACACTG*

Table 5.1. ΔN-ASPP2 sequencing primers

Cell lines, Primary Cells, and Transfections

Cell lines and primary cells

U2OS, H1299, 293T, HCTT116 and MCF7 cells were maintained in DMEM (Gibco®) supplemented with 10% fetal bovine serum (Hyclone) and 1% pen-strep (Gibco®). Tetracycline-regulatable FLAG-ASPP2 and FLAG-ΔN-ASPP2 cell lines were generated by transfection of cells with FLAG-ΔN-ASPP2 or FLAG-ASPP2 followed by Zeocin™ (Invitrogen) selection for two weeks at a concentration of 100 μg/mL. Resulting colonies were expanded, tested for expression by induction with 1 μg/mL doxycycline, and selected for use based on similar expression. The 293T-tr-HA-MYC cell line was a generous gift from Rosalie Sears. Both tetracycline-regulatable cell lines were maintained in media supplemented with 10% tetracycline-free serum (Hyclone) at all times. Mouse embryonic fibroblasts were maintained in DMEM (Gibco®) supplemented with 20% fetal bovine serum (Hyclone) and 1% pen-strep (Gibco®). All cells were maintained at 37°C with 5% CO_2.

HCC202 and DU4475 lysates were a generous gift from Trevor Levin and Joe Gray.

Transfections

H1299 cells were transfected with TransFectin™ Lipid Reagent (Bio-Rad) and U2OS cells were transfected with FuGENE® 6 (Roche) according to manufacturers' instructions. DNA:transfection reagent complexes were incubated

in Opti-MEM (Gibco®) or serum-free media before adding to cells. HCT116 cells were transfected with Lipofectamine™ 2000 (Invitrogen) in Opti-MEM (Gibco®) plus serum free media for 5 hours at which point serum was added to a final concentration of 10%. siRNAs were transfected using Mirus *Trans*IT-TKO® Transfection reagent from Mirus (Madison, WI) according to manufacturers' instructions.

Mice

Aspp2$^{+/+}$ and *Aspp2*$^{+/-}$ mice (C57BL/6) were generated at the Oregon Health and Science University Transgenic Core. Detail methods appear in (Kampa *et al.*, 2009a). RFS-c-Myc/*Lck*-Cre mice (C57BL/6) were a generous gift from Rosalie Sears, Oregon Health and Science University. The RFS-c-Myc mice are described in detail in (Wang, 2011) and the *Lck*-Cre mice in (Link, 2012). All animals were housed in the non-barrier facility at Oregon Health and Science University and maintained by breeding with C57BL/6 mice. To generate the RFS-c-Myc/*Lck*-Cre/*Aspp2*$^{+/+}$ and RFS-c-Myc/*Lck*-Cre/*Aspp2*$^{+/-}$ cohort RFS-c-Myc/*Lck*-Cre males were mated to *Aspp2*$^{+/-}$ females and resulting offspring (F1 generation) were genotyped using the primers described in Table 5.1. The F1 generations were all RFS-c-Myc$^{+/-}$ with a relatively Mendelian breakdown of *Lck*-Cre+ (~42%) and *Lck*-Cre- animals (~58%). *Aspp2*$^{+/+}$ (~30%) and *Aspp2*$^{+/-}$ (~70%) ratios were as expected given that *Aspp2*$^{-/-}$ are not viable. RFS-c-Myc$^{+/-}$/*Lck*-Cre+/*Aspp2*$^{+/-}$ and RFS-c-Myc$^{+/-}$/*Lck*-Cre-/*Aspp2*$^{+/-}$ (for controls) were subsequently crossed again and resulting RFS-c-Myc$^{+/+}$/*Lck*-Cre+/*Aspp2*$^{+/+}$, RFS-

c-Myc$^{+/+}$/*Lck*-Cre+/*Aspp2*$^{+/-}$, RFS-c-Myc$^{+/+}$/*Lck*-Cre-/*Aspp2*$^{+/+}$, and RFS-c-Myc$^{+/+}$/*Lck*-Cre-/*Aspp2*$^{+/-}$ were monitored for tumor formation for 2 years.

Animals with visible tumors were sacrificed before they exceeded the maximum size allowed by the Oregon Health and Science University Department of Comparative Medicine. Animals without visible tumors were sacrificed when they became moribund. Necropsies were performed and lymphoma was diagnosed based on tumor burdens located in the thymus, spleen, liver, and/or surrounding lymph nodes.

Genotyping was performed on tail biopsies collected from animals at weaning (~3 weeks of age). Tails were digested in lysis buffer (10 mM Tric-HCl ph 8..0, 25 mM EDTA, pH 8, 100 mM NaCl, 0.5% SDS) supplemented with 200 µg/mL of proteinase K (Invitrogen) and incubated in a water bath overnight at 37°C. DNA was isolated from tail samples by adding phenol:chloroform:isoamyl alcohol (25:24:1), transferring the aqueous phase to a new tube and precipitating with ethanol. Samples were genotyped using the primers in Table 5.1 and the following cycling parameters (95°C for 30 seconds, 50°C for 30 seconds, and 72°C for 30 seconds with extension of the last cycle for 10 minutes at 72°C).

Genotyping Primers	**Sequence**	**Type**
5’ Lck promoter	*CCTTGGTGGAGGAGGGTGGAATGAA*	traditional
3’ CRE coding	*AATGTTGCTGGATAGTTTTTACTGC*	traditional
pROSA884F	*AAAGTCGCTCTGAGTTGTTAT*	traditional
pROSA1447R	*GGAGCGGGAGAAATGGATATG*	traditional

pBigT86R	*GCGAAGAGTTTGTCCTCAACC*	traditional
Aspp2Neo (F)	*AGGTGAGATGACAGGAGATC*	traditional
Aspp2Neo (R)	*CTTGGGTGGAGAGGCTATTC*	traditional

Table 5.2: Genotyping primers

Antibodies and Chemicals

Antibodies

The N-terminal ASPP2 (ASPP2c) and MYC (Y69) antibodies were purchased from Abcam (Cambridge, UK). One of the C-terminal ASPP2 (ASPP2a) antibodies, α-tubulin, and FLAG (M2) antibodies were purchased from Sigma-Aldrich (St. Louis, MO). Another C-terminal ASPP2 antibody (ASPP2b) was purchased from BDBiosciences (San Jose, CA). Generation of another C-terminal ASPP2 antibody (ASPP2d) has been described previously (Naumovski and Cleary, 1996). The mouse immunoglobulin, rabbit immunoglobulin, rabbit polyclonal MYC (N262) and rabbit polyclonal p53 antibody were purchased from Santa Cruz Biotechnology (Santa Cruz, CA). The V5 antibody is commercially available through Invitrogen™ (Grand Island, NY). The mouse monoclonal p53 antibody (DO-1) was purchased from Calbiochem®. Goat α-mouse and goat α-rabbit horseradish peroxidase-conjugated secondary antibodies [AffiniPure Rabbit α-Mouse IgG (H+L)] used for immunoblotting and the rabbit α-mouse bridging antibody used for ChIP were purchased from Jackson ImmunoResearch Goat α-rabbit IgG-FITC and Goat α-mouse IgG-CY3 fluorescent secondary antibodies were purchased from Santa Cruz Biotechnology (Santa Cruz, CA).

Chemicals

Cisplatin (*cis*-diamineplatinum (II) dichloride, doxorubicin hydrochloride, and doxycycline were purchased from Sigma-Aldrich (St. Louis, MO). VectaShield mounting media with DAPI nuclear staining reagent was purchased from Vector Laboratories (Burlingame, CA).

Immunoblotting

Cells were lysed in RIPA buffer (150 mM sodium chloride, Triton X-100, 0.5% sodium deoxycholate, 0.1% SDS, 50 mM Tris, pH 8.0) supplemented with 1X protease inhibitor cocktail (Roche) and 1 mM PMSF. Protein extract concentrations were quantified in triplicate using an *RC DC*™ Protein Assay kit according to manufacturers instructions (Bio-Rad). 4X SDS sample buffer was added and protein lysates were boiled for five minutes. Samples were separated on an SDS-PAGE gel, transferred to Westran® Clear Signal polyvinylidene fluoride (PVDF) membrane (Sigma-Aldrich) and blocked with 1% non-fat dry millk in PBS. Membranes were then probed with indicated selected primary antibody in fish serum overnight (all primary antibody dilutions were 1:1000 unless otherwise noted), washed, and probed with either α-mouse or α-rabbit IgG horseradish peroxidase-conjugated secondary antibody in 1% non-fat dry milk (all secondary antibody dilutions were 1:15,000). Membranes were then developed with Western Lightning® enhanced luminol-based chemiluminescence substrate (Perkin-Elmer) or SuperSignal West Femto Chemiluminescent Subsrate (Thermo Scientific), exposed to Blue Ultra Autorad Film Double

Emulsion Blue (GeneMate) and developed using an SRX-101A X-OMAT (Konica Minolta).

RNA preparation and RT-PCR analysis

Total cellular RNA was isolated from whole cells using TRIzol® (Invitrogen) according to manufactuerers instructions. Samples were DNase treated for 30 minutes at 37°C to protect against genomic DNA contamination of RNA. cDNA was synthesized using the High Capacity cDNA Reverse Transcriptase Kit (Life Technologies) according to the provided protocol. Quantitative RT-PCR analysis was performed using indicated primers listed in Table 5.2. Human *GAPD (GAPDH)* Endogenous Control primer/probe set (Invitrogen) was used for Taqman normalization. Samples were run using either Taqman® Universal PCR Master Mix or SYBR® Green PCR Master Mix and run on the StepOne™ Real-Time PCR system (Applied Biosystems) according to manufacturer's instructions.

Quantitative RT-PCR primers	Sequence	Type
Taqman ASPP2 (F)	*ATGCGGTTCGGGTCCAAG*	quantitative
Taqman ASPP2 (R)	*CTTGGACCCGAACCGCAT*	quantitative
Taqman ASPP2 probe	*ATGTTTCTTACCGTGTATCTCATGATGCCG*	quantitative
ΔN-ASPP2 (F)	*GGCTATTTTGAGCTTAGTGGTGTACA*	quantitative
ΔN-ASPP2 (R)	*CGCTGATCTTGTTGTTTCAAAAAC*	quantitative
ΔN-ASPP2 (F) pair 1	*GTGTTGCAGTTAGGCTATTTTGAGC*	nested semi-quantitative
ΔN-ASPP2 (R) pair 1	*CAATTCAGGCCTTGAGGGCATCCGAG*	nested semi-quantitative
ΔN-ASPP2 (F) pair 1	*GTGGTGTACATACCTAAAATGACATAC*	nested semi-quantitative
ΔN-ASPP2 (R) pair 1	*GCATAGTAGATGACTGGATATAGGGA*	nested semi-quantitative
GAPDH SE1	*GAGCCACATCGCTCAGACAC*	semi-quantitative
GAPDH ASE6	*GGTGCAGGAGGCATTGCTGA*	semi-quantitative
ASPP2 Ebox1 (F)	*AGGCATGCGGCCACCAT*	quantitative ChIP
ASPP2 Ebox2 (R)	*GCAGTGGCTCACGCCTGTA*	quantitative ChIP
Negative control (F8)	*GCGGTTCTTACCATCACCTTTG*	quantitative ChIP
Negative control (R8.1)	*CTCCCAACATGCCTATCCTACTCT*	quantitative ChIP
E2F2 positive control (F)	*TCACCCCTCTGCCATTAAAGG*	quantitative ChIP
E2F2 positive control (R)	*AGCAGTGTATTCCCCAGGCC*	quantitative ChIP
Bax (F)	*TAATCCCAGCGCTTTGGAAG*	quantitative

		ChIP
Bax (R)	*TTGCTAGATCCAGGTCTCTGCA*	quantitative ChIP
Nucleolin (F)	*TTGCGACGCGTACGAGCTGG*	quantitative ChIP
Nucleolin (R)	*ACTCCGACTAGGGCCGATAC*	quantitative ChIP
p21 (F)	*GTGGCTCTGATTGGCTTTCTG*	quantitative ChIP
p21 (R)	*CTGAAAACAGGCAGCCCAAGG*	quantitative ChIP
p21 (F)	*CTGGACTGTTTTCTCTCGGCTC*	quantitative
p21 (R)	*TGTATATTCAGCATTGTGGGAG*	quantitative
GAPDH (F)	*ATGACCTTGCCCACAGCCT*	quantitative
GAPDH (R)	*CGGGGCTCTCCAGAACATC*	quantitative

Table 5.3: Semi-quantitative and quantitative RT-PCR primers/probes

Chromatin Immunoprecipitations and Immunopreciptiations

p53 ChIP

FLAG-ASPP2-tr-U2OS, FLAG-ΔN-ASPP2-tr-U2OS, 293-tr-HA-MYC^{WT}, cells were induced (or not) with doxycycline for 18 hrs. U2OS cells were then exposed to 20 μM cisplatin or 0.9% NaCl vehicle for 4 hours at which point paraformaldehyde was added to a final concentration of 1% and quenched 10 minutes later with glycine (0.125 final concentration). Cells were then collected, lysed in RIPA buffer supplemented with 1X protease inhibitor cocktail (Roche) and 1 mM PMSF. Lysates were sonicated for 5 rounds (30% duty, 3.5 output, 10 pulses) with at least one minute of rest on ice between rounds. Lysates were pre-cleared with bovine serum albumin-blocked recombinant Protein A Sepharose

beads (Repligen) and incubated with 2 µg α-p53 (DO-1) or α-mouse IgG overnight. Pre-blocked beads were added to lysates and rotated for one hour and thoroughly washed. Complexes were eluted from the beads by incubating in elution buffer (0.1 M $NaHCO_3$, 1% SDS) for 30 min. 5M NaCl was added to eluted complexes and cross-links were reversed by incubating samples at 65°C overnight. Bound DNA was isolated using a Qiagen QAIquick PCR kit according to manufacturers' instuctions and qRT-PCR was performed using indicated primers.

MYC ChIP

H1299 and 293T-tr-HA-MYC cells were processed as described above with the following changes: 293T-tr-HA-MYC cells were induced (or not) for 8 hours with 1 µg/mL dox. Two µg of the N262 MYC antibody or α-rabbit IgG were used for MYC ChIPs. Cells were washed three times with PBS and not quenched with glycine. After primary antibody incubation lysates were incubated with 1.5 times excess of a rabbit α-mouse bridging antibody. ChIP DNA was run on a 2% agarose gel.

Immuoprecipitations

IPs were performed as described above on lysates that had not been cross-linked or sonicated. Washed beads were boiled in 1X SDS loading buffer and run on a gel with 10% whole cell lysate inputs.

Luciferase Assays

Cells were transfected with indicated plasmids making sure to account for differences in vector concentrations. Cell were then collected and lysed in 0.1M K_2PO_4 buffer supplemented with 1 mM DTT in combination with 3 rounds of freeze-thaw lysis in liquid nitrogen. Glygly solution [(50 mM Glygly, 30 mM $MgSO_4$, pH 75.)+20 mM ATP +H_2O; 2:1:1 ratio respectively] was added to each sample (300µL) and 100 uL of 100 µM luciferin was added automatically while luminescence was measured using a Lumat LB9507 Luminometer (Berthold Technologies). Remaining lysate was assessed for β-galactosidase activity using ortho-nitrophenol-β-D-galactopyranoside substrate and measured at $\lambda_{570.}$

Immunofluorescence

HCT116 cells were grown on cover slips and transfected with equivalent amounts of FLAG-ΔN-ASPP2 or empty vector and incubated with 20 µM cisplatin or 0.9% NaCl as vehicle for 4 hours. Cells were then washed two times with PBS and fixed while rocking for 10 min with 10% formalin neutral buffered solution and washed again three times. Fixed cells were rocked and incubated with 1% Triton-X100 in PBS for 20 minutes then washed three times. A 2% BSA + 1% goat serum blocking buffer was used to block the cells for one hour. After washing two times in PBS cells were incubated overnight at room temperature in primary antibody (1:1000) diluted in blocking buffer. Cells were then washed three times and incubated in either goat α-mouse-CY3 or goat α-rabbit-FITC (1:500) diluted in blocking buffer and rocked in the dark for one hour. After washing three times

cover slips were placed on slides dotted with DAPI/mounting solution. Images were captured with a Nikon Eclipse 80i fluoresecence microscope.

Live Cell Imaging

Cells were plated at a density of 1,500 cells/well in a 96-well plate and treated as indicated. Twenty-four hours later plates were placed in the IncucyteZOOM (Essen) and phase image data was collected every 2 hours for 48 hours. Cell confluence percent was determined using customized phase-contrast software (Essen).

Cell Viability Assay

Cells were plated at a density of 1,500 cells/well in a 96-well plate and treated as indicated. Twenty-four hours later they were assessed using the MTS proliferation assay (Pierce) according to manufacturer's instructions and measured at λ_{490}.

RNAseq

RNA collected from BRCA cell lines were converted into cDNA library fragments. Sequencing adaptors were added to each cDNA fragment and paired end sequencing was done using Illumina GAII. The reads were then aligned to reference genome build hg19 using Tophat (Langmead B, 2009; Trapnell C, 2009), a splice junction aligner. Integrative Genomics Viewer (IGV) (Helga

Thorvaldsdóttir, 2012) was used to view aligned reads, which provided evidence for isoforms of ASPP2.

5'RACE

Total RNA collected from fresh mouse or rat brain tissue, or the human cell line HCT116 were used as template in the GeneRacer™ 5' RACE System (Invitrogen) along with *ASPP2*-specific reverse primers (See Table 5.4) in accordance with manufacturer's instructions.

Primer	Sequence 5'>3'	Type
hASPP2 5'RACE	*GTTTCTTAGCTGCAGCTCCTTATAG*	5'RACE
r/mASPP2 5'RACE	*CCGTGGCATAGTGGATGACTGGATG*	5'RACE
Rat f1	*GTGGAGGAAATTGAACAGATGAACAG*	RT-PCR
Rat f2	*CACCTGTGGTCATTCTCTTTGTTCT*	RT-PCR
Rat f3	*GCTTGATTGTCTGGGAAGTGATTC*	RT-PCR
Rat f4	*GGTATTTAGTGGTGTCTCGTTGATTTC*	RT-PCR
Rat f5	*TTGAAGTCAGGTTGGCGTAAGACGC*	RT-PCR
hExon 1 (F)	*ATGCGGTTCGGGTCCAA*	RT-PCR
hExon 4 (R)	*AATGTCCCTGCCAGGGGG*	RT-PCR
hExon 6 (R)	*GCCATTTCCTGAAGTTCAGC*	RT-PCR
mExon 1 (F)	*ATGCGGTTCGGGTCCAA*	RT-PCR
mExon 4 (F)	*GGTGAGCATCGGAGGAAGGAGAATG*	RT-PCR
mExon 5 (F)	*ACGCTTGCTGAACTCCAGGAAATGG*	RT-PCR
mExon 5 (F)	*CAGCAACAAATCTGGCTACTAAG*	RT-PCR
mExon 8 (R)	*GTTTGGCATTCTGCTCTTGGTTCAG*	RT-PCR
mExon 9 (R)	*CAGCCACACGACTTGGGGCTG*	RT-PCR

Table 5.4. 5'RACE and RT-PCR Primer sequences

Apoptosis Assay

U2OS cells were transfected with FLAG-ΔN-ASPP2 or empty vector control using Fuguene® 6 (Roche) according to manufacturers instructions Twenty-four after transfection cells were UV-irradiated harvested 18 hours later. Cells were detached with 0.25% trypsin (Gibco) and collected in 10% serum medium. Cells were then gently washed twice with 1X PBS and resuspended in 1X Annexin V Binding Buffer (BD Pharmingen™). APC Annexin V (BD Pharmingen™) and propidium iodide were added to transfected cells along with controls (propidium iodide alone, annexin alone, and unstained) and incubated for 20 minutes in the dark. Binding buffer (1X) was then added and cells were analyzed with a BD FACSCalibur flow cytormeter (BD Biosciences).

Appendix 1. ΔN-ASPP2 Methods Development

As discussed in Chapter 4, detection of ΔN-ASPP2 has proven challenging for a variety of reasons, not the least of which is the fact that there are no unique epitopes to distinguish it from full-length ASPP2, making targeted immunoblotting an impossibility. There is however a unique stretch of sequence in the *ΔN-ASPP2* 5'UTR that allows for distinction at the genetic level, specifically with targeted siRNAs and qPCR. While working to characterize ΔN-ASPP2 I developed and validated both of these tools for detection of this novel protein but was not able to utilize them for various reasons. Here I offer a brief overview of each.

ΔN-ASPP2 qRT-PCR SYBR® Green primers

Human ΔN-ASPP2 is generated from an alternative transcription start site in intron 6 of *TP53BP2* with a predicted translation start site in exon 8, leaving exon 7 and a portion of intron 6 untranslated. Since intron 6 is spliced out of both *ASPP2* and *BBP* transcripts the stretch of sequence downstream of the *ΔN-ASPP2* transcription start site (intron 6) and upstream of exon 7 of sequence is unique to the *ΔN-ASPP2* transcript. Indeed, sequence verification demonstrates that the *ΔN-ASPP2* transcript contains 77 unique base pairs upstream of its coding region. Using this region as a template in Primer Express® 3.0 (Applied Biosystems), I designed a series of SYBR® Green qRT-PCR primer pairs

predicted to specifically detect *ΔN-ASPP2*, based on the software design parameters.

Primer sets were chosen based on predicted compatibility (minimizing self-dimer capacity, hairpin structures, and cross-dimer capacity) and tested on cDNA from a panel of breast tumor cell lines, RNA template to ensure that genomic DNA was not detected, or water as a negative control. As shown in the representative melt curve in Figure A1.1A the set of primers chosen amplified a specific product (represented by a sharp peak in the cDNA template samples) as compared to no cDNA and no RT template samples. In subsequent qPCR runs fluorescence was set to be collected at 2°C below the peak melting temperature (73.8°C) to ensure maximal signal detection. These primers were successfully used to detect *ΔN-ASPP2* in a panel of breast cancer cell lines (Figure A1.1B) and will be a useful tool for studying *ΔN-ASPP2* in the future.

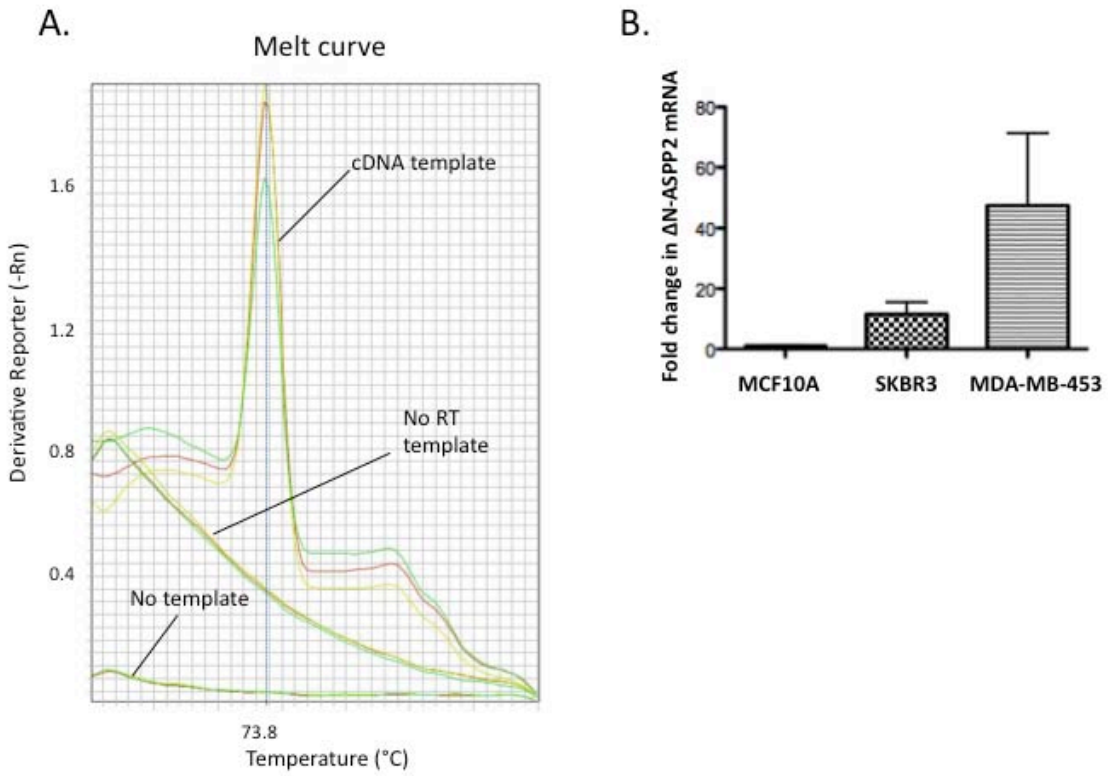

Figure A1.1 *ΔN-ASPP2* is specifically and quantitatively detected in cell lines. (A) Representative melt curve from a qPCR run using *ΔN-ASPP2*-specific primers with cDNA template, without template, and with RNA template (No RT). (B) Quantitation of *ΔN-ASPP2* mRNA in the non-malignant MCF10A cell line and the SKBR3 and MDA-MB-453 breast cancer cell lines. Values are normalized to *GAPDH* and error bars represent the positive and negative error of 3 technical replicates.

Appendix 1

ΔN-ASPP2-specific siRNA

The unique 77 base pairs located in the 5'UTR of *ΔN-ASPP2* were also used as a target sequence for siRNA design. This unique *ΔN-ASPP2* sequence (along with a sequence upstream of intron 6 chosen to specifically target *ASPP2*) was analyzed by Sigma's Rosetta design algorithm (Sigma-Aldrich) and potential siRNA sequences were ranked according to theoretical knockdown efficiency. Two *ΔN-ASPP2*-specific and two *ASPP2*-specific sequences were chosen for validation.

Again, as a result of our difficulty detecting ΔN-ASPP2 at the protein level, validation of these tools with immunoblotting has remained a challenge. However, when we quantified *ΔN-ASPP2* knockdown in SKBR3 cells 24 hours post transfection with siRNAs using the qPCR reagents described above, we see a significant reduction in *ΔN-ASPP2* message as compared to a control siRNA sample (Figure A1.2). It is of course important to monitor the off-target effects of siRNAs, specifically in our case any effects seen on full-length *ASPP2* detection. There is a reduction of *ASPP2* with our *ΔN-ASPP2*-specific siRNAs, a possible consequence of a reduction in a pool of pre-spliced *ASPP2*, however the fold change in *ΔN-ASPP2* knockdown is much more dramatic, suggesting a higher degree of specificity for this target. Nevertheless, these results will be important to consider when analyzing the functional consequences of *ΔN-ASPP2* knockdown in future experiments.

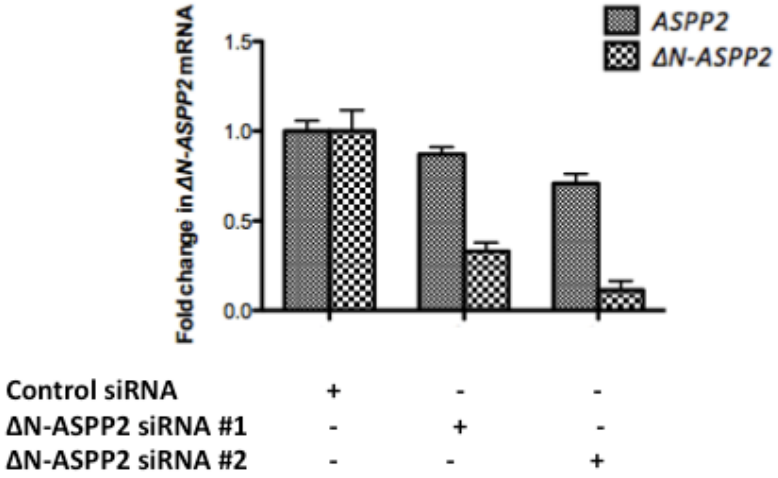

Figure A1.2 Validation of *ΔN-ASPP2* knockdown. SKBR3 cells were transfected with equivalent amounts of control siRNA or one of two *ΔN-ASPP2* siRNAs and harvested for total RNA 48 hours later. cDNA was prepared as described in *Methods* and samples were assayed using SYBR® Green reagents for *ΔN-ASPP2* expression and using Taqman® reagents for *ASPP2*. Error bars represent the positive and negative error of 3 technical replicates.

Appendix 2. Figure Contributions

Figure 2.1. 5'RACE (Figure 2.1A) was performed by Dexi Chen. Gel mapping of *ΔN-ASPP2* transcription start site was done by Zhiyi Zhu.

Figure 2.2. RT-PCR of both human (2.2A) and mouse (2.2B) was performed by Zhiyi Zhu.

Figure 2.3. The cloning PCR reaction (Figure 2.3A) was run by Casey Nold. Immunoblot (Figure 2.3E *left*) was performed by Charles Lopez and the RT-PCR (Figure 2.3E *right*) was performed by Dexi Chen.

Table 2.1. RNA-seq mining was performed by Pavana Anur

Figure 2.4. Immunoblot (Figure 2.4C *inset*) performed by Zhiping Wang.

Figure 2.6. Apoptosis assay (Figure 2.6A) and immunoblot (Figure 2.6B) were performed by Hun Joo Lee.

Figure 2.7. Semi-quantitative PCR performed by Dexi Chen (Figure 2.7A) and quantitative PCR performed by Hun Joo Lee (Figure 2.7B).

Figure 4.3. Immunopreciptiations and Immunoblots (Figure 4.3B and C) performed by Zhiping Wang

References

Allocati N, Di Ilio, C., De Laurenzi, V. (2012). p63/p73 in the control of cell cycle and cell death. *Exp Cell Res* **318:** 1285-90.

American Cancer Society (2013). Cancer Facts & Figures 2013. . *Atlanta: American Cancer Society* **2**.

Ao Y, Rohde LH, Naumovski L (2001). p53-Interacting Protein 53BP2 Inhibits Clonogenic Survival and Sensitizes Cells to Doxorubicin But Not Paclitaxel-Induced Apoptosis. *Oncogene* **20:** 2720-2725.

Ayer DE LQ, Eisenman RN (1995). Mad-Max transcriptional repression is mediated by ternary complex formation with mammalian homologs of yeast repressor Sin3. *Cell* **80:** 767-76.

Benasayag C, Montero, L., Colombie, N., Gallant, P., Cribbs, D., Morello, D. (2005). Human c-Myc isoforms differentially regulate cell growth and apoptosis in Drosophila melanogaster. *Mol Cell Biol* **25:** 9897-909.

Bergamaschi D, Samuels-Lev Y, Jin B, Duraaisingham S, Crook T, Lu X (2004). ASPP1 and ASPP2: Common Activators of p53 Family Members. *Molecular and Cellular Biology* **24:** 1341-1350.

Bergamaschi D, Samuels, Y., O'Neil, N. J., Trigiante, G., Crook, T., Hsieh, J., O'Connor, D. J., Zhong, S., Campargue, I., Tomlinson, M. L., Kuwabara, P. E., and Lu, X. (2003). iASPP Oncoprotein is a Key Inhibitor of p53 Conserved from Worm to Human. *Nature* **33:** 162-167.

Blackwell T, Kretzner, L., Blackwood, EM., Eisenman, RN., Weintraub, H. (1990). Sequence-specific DNA binding by the c-Myc protein. *Science* **250:** 1149-51.

Blackwood E, Eisenman, RN (1991). Max: a helix-loop-helix zipper protein that forms a sequence-specific DNA-binding complex with Myc. *Science* **251:** 1211-7.

Blanchard J, Piechaczyk, M., Dani, C., Chambard, JC., Franchi, A., Pouyssegur, J., Jeanteur, P. (1985). c-myc gene is transcribed at high rate in G0-arrested fibroblasts and is post-transcriptionally regulated in response to growth factors. *Nature* **317:** 443-5.

Bouchard C, Thieke, K., Maier, A., Saffrich, R., Hanley-Hyde, J., Ansorge, W., Reed, S., Sicinski, P., Bartek, J., Eilers, M. (1999). Direct induction of cyclin D2 by Myc contributes to cell cycle progression and sequestration of p27. *EMBO J* **18:** 5321-33.

References

Bunz F, Dutriaux A, Lengauer C, Waldman T, Zhou S, Brown J *et al* (1998). Requirement for p53 and p21 to Sustain G2 Arrest After DNA Damage. *Science* **282:** 1497-1501.

Campisi J, d'Adda di Fagagna, F. (2007). Cellular senescence: when bad things happen to good cells. *Nat Rev Mol Cell Biol* **8:** 729-40.

Chen D, Padiernos, E., Ding, F., Lossos, I.S., and Lopez, C. D. (2005). Apoptosis-stimulating protein of p53 (ASPP2/^{53BP2L}) is an E2F target gene. *Cell Death and Differentiation* **12:** 358-368.

Christophorou M, Ringshausen, I., Finch, AJ., Sigart, LB., Evan, GI. (2006). The pathological response to DNA damage does not contribute to p53-mediated tumour suppression. *Nature* **443:** 214-7.

Cobleigh M, Tabesh B, Bitterman P, Baker J, Cronin M, Liu M *et al* (2005). Tumor gene expression and prognosis in breast cancer patients with 10 or more positive lymph nodes. *Clinical Cancer Research* **11:** 8623-8631.

Collado M, Serrano, M (2010). Senescence in tumours: Evidence from mice and humans.
. *Nat Rev Cancer* **10:** 51-57.

Cong W, Hirose, T., Harita, Y., Yamashita, A., Mizuno, K., Hirano, H., Ohno, S. (2010). ASPP2 regulates epithelial cell polarity through the PAR complex. *Curr Biol* **20:** 1408-14.

Cowling VHaC, M. D. (2006). Mechanism of Transcriptional Activation by the Myc Oncoproteins. *Seminars in Cancer Biology* **16:** 242-252.

Dang C (2012). MYC on the path to cancer. *Cell* **149:** 22-35.

Dynlacht B (2005). E2F and p53 Make a Nice Couple: Converging Pathways in Apoptosis. *Cell Death and Differentiation* **12:** 313-314.

Efeyan A, Serrano M (2007). p53: Guardian of the Genome and Policeman of the Oncogenes. *Cell Cycle* **6:** 1006-1010.

Eilers M, Schirm S., Bishop, JM (1991). The MYC protein activates transcription of the alpha-prothymosin gene. *EMBO J.* **10:** 133-41.

Evan GI, Wyllie, A. H., Gilbert, C. S., Littlewood, T. D., Land, H., Brooks, M., Water, C. M., Penn, L J. Z., and Hancock, D. C. (1992). Induction of Apoptosis in Fibroblasts by c-Myc Protein. *Cell* **69:** 119-128.

References

Felsher DW, Bishop JM (1999). Reversible Tumorigenesis by MYC in Hematopoietic Lineages. *Molecular Cell* **4:** 199-207.

Fernandez P, Frank S, Wang L, Schroeder M, Liu M, Greene J *et al* (2003). Genomic Targets of the Human c-Myc Protein. *Genes and Development* **17:** 1115-1129.

Fesik SW (2005). Promoting Apoptosis as a Strategy for Cancer Drug Discovery. *Nature* **5:** 876-885.

Fogal V, Kartasheva N, Trigiante G, Llanos S, Yap D, Vousden K *et al* (2005). ASPP1 and ASPP2 are New Transcriptional Targets of E2F. *Cell Death and Differentiation* **12:** 369-376.

Frank S, Schroeder, M., Fernandez, P., Tauber, S., Amati, B. (2001). Binding of c-Myc to chromatin mediates mitogen-induced acetylation of histone H4 and gene activation. *Genes Dev* **15:** 2069-82.

Friedler A, Hansson, LO., Veprintsev, DB., Freund, SMV., Rippen, TM., Nikolova, PV., Proctor, MR., Rudiger, S., Fersht, AR. (2002). A peptide that binds and stabilizes p53 core domain: Chaperone strategy for rescue of oncogenic mutants. *Proceedings National Academy of Science* **99:** 937-42.

Fujita K, Mondul A, Horikawa I, Nguyen G, Kumamoto K, Sohn J *et al* (2009). p53 Isoforms delta133p53 and p53-beta are Endogenous Regulators of Replicative Cellular Senescence. *Nature Cell Biology* **11:** 1135-1142.

Gasco M, Shami S, Crook T (2002). The p53 Pathway in Breast Cancer. *Breast Cancer Res* **4:** 70-76.

Gomez-Roman N, Grandori, C., Eisenman, RN., White, RJ. (2003). Direct activation of RNA polymerase III transcription b c-Myc. *Nature* **421:** 290-4.

Gorina S, Pavletich N (1996). Structure of the p53 Tumor Suppressor Bound to the Ankyrin and SH3 Domains of 53BP2. *Science* **274:** 1001-1005.

Hanahan DaW, RA. (2011). Hallmarks of cancer: the next generation. *Cell* **144:** 646-74.

Hart L, Cunningham, JT., Datta, T., Dey, S., Tameire, F., Lehman, SL., Qiu, B., Zhang, H., Cerniglia, G., Bi, M., Li, Y., Gao, Y., Liu, H., Li, C., Maity, A., Thomas-Tikhonenko, A., Perl, AE., Koong, A., Fuchs, SY., Diehl, JA., Mills, IG., Ruggero, D., Koumenis C. (2012). ER stress-mediated autophagy promotes Myc-dependent transformation and tumor growth. . *J Clin Invest* **122:** 4621-34.

References

Hedenfalk M, Duggan D, Chen Y, Radmucher M, Bittner M, Simon R *et al* (2001). Gene-expression profiles in hereditary breast cancer. *New England Journal of Medicine* **344:** 539-548.

Helga Thorvaldsdóttir JTR, Jill P. Mesirov (2012). Integrative Genomics Viewer (IGV): high-performance genomics data visualization and exploration. *Brief Bioinformatics*.

Hershko T, Chaussepied M, Oren M, Ginsberg D (2005). Novel Link Between E2F and p53: Proapoptotic Cofactors of p53 are Transcriptionally Upregulated by E2F. *Cell Death and Differentiation* **12:** 377-383.

Hurlin P, Huang, J. (2006). The MAX-interacting transcription factor network. *Semin Cancer Biol* **16:** 265-74.

Iwabuchi K, Bartel PL, Li B, Marraccino R, Fields S (1994). Two Cellular Proteins that Bind to Wild-type but not Mutant p53. *Proceedings of the National Academy of Science USA* **91:** 6098-6102.

Iwabuchi K, Li B, Massa HF, Trask BJ, Takayasu D, Fields S (1998). Stimulation of p53-mediated Transcriptional Activation by the p53-binding Proteins, 53BP1 and 53BP2. *The Journal of Biological Chemistry* **273:** 26061-26068.

Jemal A, Simard, EP, Dorell, C, Noone, AM, Markowitz, LE, Kohler, B, Eheman, C, Saraiya, M, Bandi, P, Saslow, D, Cronin, KA, Watson, M, Schiffman, M, Henley, SJ, Schymura, MJ, Anderson, RN, Yankey, D, and Edwards, BK. (2013). Annual Report to the Nation on the Status of Cancer, 1975–2009, Featuring the Burden and Trends in HPV-Associated Cancers and HPV Vaccination Coverage Levels. . *Journal of the National Cancer Institute*.

Jiang X, Tsang, YH., Yu, Q. (2007). c-Myc overexpression sensitizes Bim-mediated Bax activation for apoptosis induced by histone deacetylase inhibitor suberoylanilide hydroxamic acid (SAHA) through regulating Bcl-2/Bcl-xL expression. *Int J Biochem Cell Biol* **39:** 1016-25.

Ju H, Lee K, Yang M, Kim H, Kang C, Sohn T *et al* (2005). TP53BP2 Locus is Associated with Gastric Cancer Susceptibility. *International Journal of Cancer* **117:** 957-960.

Juin P, Hunt, A., Littlewood, T., Griffiths, B., Swigart, LB., Korsmeyer, S., Evan, G. (2002). c-Myc functionally cooperates with Bax to induce apoptosis. *Mol Cell Biol* **22:** 6158-69.

Kampa K, Acoba J, Chen D, Gay J, Lee H-J, Beemer K *et al* (2009a). Apoptosis Stimulating Protein of p53 (ASPP2) Heterozygous Mice are Tumor Prone and

have Attenuated Cellular Damage-response Thresholds. *Proc Natl Acad Sci USA* **106:** 4390-4395.

Kampa K, Bonin M, Lopez CD (2009b). New Insights Into the Expanding Complexity of the Tumor Suppressor ASPP2. *Cell Cycle* **8:** 2871-2876.

Kampa-Schittenhelm K, Lopez, CD., Illing, B., Walter, M., Schittenhelm, MM. (2013). *Proceedings of the 104th Annual Meeting of the American Association of Cancer Research National Meeting*. AACR: Washington DC.

Khoury M, Bourdon J (2010). The Isoforms of the p53 Protein. *Cold Spring Harbor Perspectives in Biology* **2:** a000927.

Knudsen E (1999). Promoter2.0: for the Recognition of Pol II Promoter Sequences. *Bioinformatics* **15:** 356-361.

Kobayashi S, Kajino, S., Takahashi, N., Kanazawa, S., Imai, K., Hibi, Y., Ohara, H., Itoh, M., and Okamoto, T (2005). 53BP2 Induces Apoptosis Through the Mitochondrial Death Pathway. *Genes to Cells* **10:** 253-260.

Kundu MaT, CB. (2008). Autophagy: basic principles and relevance to disease. *Annu Rev Pathol* **3:** 427-55.

Langmead B TC, Pop M, Salzberg SL (2009). Ultrafast and memory-efficient alignment of short DNA sequences to the human genome. . *Genome Biology* **10**.

Leone G, Sears R, Huang E, Rempel R, Nuckolls F, Park C-H *et al* (2001). Myc Requires Distinct E2F Activities to Induce S Phase and Apoptosis. *Molecular Cell* **8:** 105-113.

Leung J, Ehmann G, Giangrande P, Nevins J (2008). A Role for Myc in Facilitating Transcription Activation by E2F1. *Oncogene* **27:** 4172-4179.

Li L, Nerlov, C., Prendergast, G., MacGregor, D., and Ziff, EB. (1994). c-Myc represses transcription in vivo by a novel mechanism dependent on the initiator element and Myc box II. *EMBO J* **13:** 4070-79.

Li S, Shi, G., Yuan, H., Zhou, T., Zhang, Q., Zhu, H., Wang, X. (2012). Abnormal expression patter of the ASPP family of proteins in human non-small cell lung cancer and regulatory functions on apoptosis through p53 by iASPP. *Oncol Rep* **28:** 133-40.

Lin C, Loven, J., Rahl, PB., Paranal, RM., Burge, CB., Bradner, JE., Lee, TI., and Young, RA (2012). Transcriptional amplification in tumor cells with elevated c-Myc. *Cell* **151:** 56-67.

References

Link J, Ota, S., Zhou, ZQ., Daniel, CJ., Sears, RC., Hurlin, PJ. (2012). A critical role for Mnt in Myc-driven T-cell proliferation and oncogenesis. *Proceedings National Academy of Science* **109:** 19685-90.

Liu C, Lv X, Li T, Xu Y, Zhou X, Zhao S *et al* (2011). PP1 Cooperates with ASPP2 to Dephosphoryate and Activate TAZ. *Journal of Biological Chemistry* **18:** 5558-5566.

Liu W, Jiang, XY., Ren, JK., and Zhang, ZX. (2010). Expression pattern of the ASPP family members in endometrial endometrioid adenocarcinoma. *Onkologie* **33:** 500-3.

Liu Z, Lu, X., Zhang, Y., Zhong, S., Gu, S., Zhang, X., Yang, X., and Xin, H. (2005). Downregulated mRNA Expression of ASPP and the Hypermethylation of the 5'-untranslated Region in Cancer Cell Lines Retaining Wild-type p53. *Federation of Biochemical Societies* **579:** 1587-1590.

Lopez CD, Ao, Y., Rohde, L. H., Perez, T. D., O'Connor, D. J., Lu, X., Ford, J. M., and Naumovski L. (2000). Proapoptotic p53-interacting protien 53BP2 is induced by UV irradiation but suppressed by p53. *Molecular and Cellular Biology* **20:** 8018-8025.

Lossos I, Czerwinski D, Alizadeh A, Wechser M, Tibshirani R, Bostein D *et al* (2004). Prediction of Survival in Diffuse Large-B-Cell Lymphoma Based on the Expression of Six Genes. *New England Journal of Medicine* **350:** 1828-1837.

Lossos I, Natkunam Y, Levy R, Lopez CD (2002). Apoptosis Stimulating Protein of p53 (ASPP2) Expression Differs in Diffuse Large B-Cell and Follicular Center Lymphoma: Correlation with Clinical Outcome. *Leukemia and Lymphoma* **43:** 2309-2317.

McMahon SB, Van Buskirk, H. A., Dugan, K. A., Copeland, T. D., and Cole M. D. (1998). The novel ATM-related protein TRRAP is an essential cofactor for the c-Myc and E2F oncoproteins. *Cell* **94:** 363-374.

Meek D (2009). Tumor Suppression by p53: a Role for the DNA Damage Response? *Nature Reviews Cancer* **9:** 714-723.

Meng W, Chu, RX., Wang, BZ., Wang, LP., Ma, LL., and Wang, LX. (2013). Heliobacter pylori infection and expression of apoptosis-related proteins p53, ASPP2, and iASPP in gastric cancer and precancerous lesions. *Pathol Biol*.

Meyer N, Penn L (2008). Reflecting on 25 Years with MYC. *Nature Reviews Cancer* **8:** 976-990.

References

Mori T, Okamoto H, Takahashi N, Ueda R, Okamoto T (2000). Aberrant Overexpression of 53BP2 mRNA in Lung Cancer Cell Lines. *FEBS Letters* **465:** 124-128.

Murphy D, Juntilla M, Pouyet L, Karnezis A, Shchors K, Bui D *et al* (2008). Distinct Thresholds Govern Myc's Biological Output In Vivo. *Cancer Cell* **14:** 447-457.

Naumovski L, Cleary M (1994). Bcl2 Inhibits Apoptosis Associated with Terminal Differentiation of HL-60 Myeloid Leukemia Cells. *Blood* **83:** 2261-2267.

Naumovski L, Cleary ML (1996). The p53-Binding Protein 53BP2 Also Interacts with Bcl2 and Impedes Cell Cycle Progression at G2/M. *Molecular and Cellular Biology* **16:** 3884-3892.

Nesbit C, Tersak, JM., Prochownik, EV (1999). MYC oncogenes and human neoplastic disease. *Oncogene* **18:** 3004-16.

Nilsson JA, and Cleveland J. L. (2003). Myc Pathways Provoking Cell Suicide and Cancer. *Oncogene* **22:** 9007-9021.

Park S, An C, Kim S, Yoo N, Lee S (2010). Mutational Analysis of ASPP1 and ASPP2 Genes, a p53-related Gene, in Gastric and Colorectal Cancers with Microsatellite Instabillity. *Gut and Liver* **4:** 292-293.

Patel J, Loboda, AP., Showe, MK., Showe, LC., McMahon, SB. (2004). Analysis of genomic targets reveals complex function of MYC. *Nat Rev Cancer* **4:** 562-8.

Patel J, McMahon, SB. (2007). BCL2 is a downstream effector of MIZ-1 essential for blocking c-Myc-induced apoptosis. *J Biol Chem* **282:** 5-13.

Perna D, Faga, G., Verrecchia, A., Gorski, MM., Barozzi, I., Narang, V., Khng, J., Lim, KC., Sung, W-K., Sanges, R., Stupka, E., Oskarsson, T., Trumpp, A., Wei, C-L., Muller, H., Amati, B. (2012). Genome-wide mapping of Myc binidn and gene regulation in serum-stimulated fibroblasts. *Oncogene* **31:** 1695-1709.

Pietsch E, Sykes S, McMahon S, Murphy M (2008). The p53 family and Programmed Cell Death. *Oncogene* **27:** 6507-6521.

Pomeroy S, Tamayo P, Gaasenbeek M, Sturia LM, Angelo M, McLaughlin M *et al* (2002). Prediction of Central Nervous System Embryonal Tumour Outcome Based on Gene Expression. *Nature* **415:** 436-442.

Prendergast G, Ziff, EB. (1991). Methylation-sensitive sequence-specific DNA binding by the c-Myc basic region. *Science* **251:** 186-9.

References

Pylayeva-Gupta Y, Grabocka, E., Bar-Sagi, D. (2011). RAS oncogenes: weaving a tumorigenic web. *Nat Rev Cancer* **11:** 761-74.

Rotem S, Katz C, Benyamini H, Lebendiker M, Veprintsev D, Rudiger S *et al* (2008). The Structure and Interactions of the Proline-rich Domain of ASPP2. *Journal of Biological Chemistry* **283:** 18990-18999.

Rotem S, Katz C, Friedler A (2007). Insights into the Structure and Protein-protein Interactions of the Pro-apoptotic Protein ASPP2. *Biochemical Society Transactions* **35:** 966-969.

Rotem-Bamberger S, Katz, C., Friedler A. (2013). Regulation of ASPP2 interaction with p53 core domain by and intramolecular autoinhibitory mechanism. *PLos One* **8**.

Samuels-Lev Y, O'Connor D, Bergamaschi D, Trigiante G, Campargue I, Naumovski L *et al* (2001). ASPP Proteins Specifically Stimulate the Apoptotic Function of p53. *Molecular Cell* **8:** 781-794.

Sarraf A, Stancheva I (2004). Methyl-CpG Binding Protein MBD1 Couples Histone H3 Methylation at Lysine 9 by SETDB1 to DNA Replication and Chromatin Assembly. *Molecular Cell* **15:** 595-605.

Sears R, Leone, G., DeGregori, J., Nevins, JR. (1999). Ras enhances Myc protein stability. *Mol Cell* **3:** 169-79.

Sears R, Ohtani K, Nevins J (1997). Identification of Positively and Negatively Acting Elements Regulating Expression of the E2F2 Gene in Response to Cell Growth Signals. *Molecular and Cellular Biology* **17:** 5227-5235.

Seoane J, Le H, Massague J (2002). Myc Suppresssion of the p21(Cip1) Cdk Inhibitor Influences the Outcome fo the p53 Response to DNA Damage. *Nature* **419:** 729-734.

Sgroi DC, Teng, S., Robinson, G., LeVangie, R., Hudson Jr., J. R., and Elkahloun A. G. (1999). *In Vivo* Gene Expression Profile Analysis of Human Breast Cancer Progression. *Cancer Research***:** 5656-5661.

Sherr CaM, F. (2002). The Rb and p53 Pathways in Cancer. *Cancer Cell* **2:** 103-112.

Skene-Arnold T, Luu, HA., Uhrig, RG., De Wever, V., Nimick, M., Maynes, J., Fong, A., James, MN., Trinkle-Mulcahy, L., Moorhead, GB., and Holmes, CF. (2013). Molecular mechanisms underlying the interaction of protein phosphatase-1c with ASPP proteins. *Biochem J* **1:** 649-59.

References

Sottocornola R, Royer C, Vives V, Tordella L, Zhong S, Wang Y *et al* (2010). ASPP2 Binds Par-3 and Controls the Polarity and Proliferation of Neural Progenitors During CNS Development. *Developmental Cell* **19:** 126-137.

Takahashi N, Kobayashi S, Jiang X, Kitagori K, Imai K, Hibi Y *et al* (2004). Expression of 53BP2 and ASPP2 Proteins from TP53BP2 Gene by Alternative Splicing. *Biochemical and Biophysical Research Communications* **315:** 434-438.

Takahashi N, Kobayashi S, Kajino S, Imai K, Tomoda K, Shimizu S *et al* (2005). Inhibition of the 53BP2S-mediated Apoptosis by Nuclear Factor kappaB and Bcl-2 Family Proteins. *Genes to Cells* **10:** 803-811.

Thukral S, Blain G, Chang K, Fields S (1994). Distinct Residues of Human p53 Implicated in Binding to DNA, Simian Virus 40 Large T Antigen, 53BP1 and 53BP2. *Molecular and Cellular Biology* **14:** 8315-8321.

Tidow H, Andreeva, A., Rutherford, T. J., and Fersht, A. R. (2007). Solution Structure of ASPP2 N-terminal Domain (N-ASPP2) Reveals a Ubiquitin-like Fold. *Journal of Molecular Biology* **371:** 948-958.

Trapnell C PL, Salzberg SL (2009). TopHat: discovering splice junctions with RNA-seq. *Bioinformatics* **25**.

Vives V, Su, J., Zhong S., Ratnayaka, I., Slee, E., Goldin, R., and Lu, X. (2006). ASPP2 is a haploinsufficient tumor suppressor that cooperates with p53 to suppress tumor growth. *Genes and Development* **20:** 1262-1267.

Vousden K, Prives C (2009). Blinded by the Light: the Growing Complexity of p53. *Cell* **137:** 413-431.

Wang X, Cunningham, M., Zhang, X., Tokarz, S., Laraway, B., Troxell, M., Sears, R. (2011). Phosphorylation regulates c-Myc's oncogenic activity in the mammary gland. *Cancer Res* **71:** 925-36.

Wang X, Lapi E, Sullivan A, Ratnayaka I, Goldfin R, Hay R *et al* (2010). SUMO-modified Nuclear Cyclin D1 Bypasses Ras-induced Senescence. *Cell Death and Differentiation*.

Wang Y, Godin-Heymann, N., Dan Wang, X., Bergamaschi, D., Llanos, S., and Lu, X. (2013). ASPP1 and ASPP2 bind active RAS, potentiate RAS signalling and enhance p53 activity in cancer cells. . *Cell Death and Differentiation*.

Wang Y, Wang, XD., Lapi, E., Sullivan, A., Jia, W., He, YW., Ratnayaka, I., Zhong, S., Goldin, RD., Goemans, CG., Tolkovsky, AM., Lu, X. (2012a). Autophagic activity dictates the cellular response to oncogenic RAS. *Proceedings National Academy of Science* **109:** 13325-30.

References

Wang Y. G-HN, Dan Wang X., Bergamaschi D., Llanos S., and Lu X. (2013). ASPP1 and ASPP2 bind active RAS, potentiate RAS signalling and enhance p53 activity in cancer cells. . *Cell Death and Differentiation*.

Wang Z, Liu, Y., Takahashi, M., Van Hook, K., Kampa-Schittenhelm, KM., Sheppard, BC., Sears, R., Stork, PJ., Lopez, CD. (2012b). The N-terminus of the ASPP2 tumor suppressor binds to Ras and enhances Ras/Raf/MEK/ERK activation to promote oncogene-induced cellular senescence. *Proceedings National Academy of Science* **1:** 312-317.

Wierstra I, Alves, J. (2008). The c-Myc promoter: still MyterY and challenge. *Adv Cancer Res* **99**.

Wu S, Cetinkaya, C., Munoz-Alonso, MJ., von der Lehr, N., Bahram, F., Beuger, V., Eilers, M., Leon, J., Larsson, LG. (2003). Myc represses differentiation-induced p21CIP1 expression via Miz-1-dependent interation with the p21core promoter. *Oncogene* **22:** 351-60.

Yang J, Hori, M., Takahashi, N., Kawabe, T., Kato, H., and Okamoto, T. (1999). NF-κB Subunit p65 Binds to 53BP2 and Inhibits Cell Death Induced by 53BP2. *Oncogene* **18:** 5177-5186.

Yang J, Ono T, Sonta S, Kawabe T, Okamoto T (1997). Assignment of p53 Binding Protein (TP53BP2) to Human Chromosome Band 1q42.1 by In Situ Hybridization. *Cytogenetics and Cell Genetics* **78:** 61-62.

Yang S, Wang, X., Contino, G., Liesa, M., Sahin, E., Ying, H., Bause, A., Li, Y., Stommel, JM., Dell'antonio G., Mautner, J., Tonon, G., Haigis, M., Shirihai, OS., Doglioni, C., Bardeesy, N., Kimmelman, AC. (2011). Pancreatic cancers require autophagy for tumor growth. *Genes Dev* **25:** 717-29.

Yeh E, Cunningham M, Arnold H, Chasse D, Monteith T, Ivaldi G *et al* (2004). A Signalling Pathway Controlling c-Myc Degradation That Impacts Oncogenic Transformation of Human Cells. *Nature Cell Biology* **6:** 308-318.

Zhao J, Wu G, Bu F, Lu B, Liang A, Cao L *et al* (2010). Epigenetic Silence of Ankyrin-Repeat-Containing, SH3-Domain-Containing, and Proline-Rich-Region-Containing Protein 1 (ASPP1) and ASPP2 Genes Promotes Tumor Growth in Hepatitis B Virus-Positive Hepatocellular Carcinoma. *Hepatology* **51:** 142-153.

Zhu Z, Ramos, J., Kampa, K., Adimoolam, S., Sirisawad, M., Yu, Z., Chen, D., Naumovski, L., and Lopez, C. D. (2005). Control of ASPP2/(53BP2L) protein levels by proteosomal degradation modulates p53 apoptotic function. *Journal of Biological Chemistry* **280:** 34473-34480.

References

Zindy F, Eischen C, Randle D, Kamijo T, Cleveland J, Sherr C *et al* (1998). Myc Signaling Via the ARF Tumor Suppressor Regulates p53-dependent Apoptosis and Immortalization. *Genes and Development* **12:** 2424-2433.